Optimization of Struvite Recovery Utilizing Magnesium Oxide

Sydney Marie Goy

Thesis submitted to the faculty of the Virginia Polytechnic Institute and State University in partial fulfillment of the requirements for the degree of

Master of Science
In
Environmental Engineering

Charles B. Bott
Andrea M. Dietrich
William R. Knocke

November 20, 2020
Blacksburg, VA

Keywords:
Struvite Precipitation, Magnesium Oxide, Nutrient Recovery, Hydration, Magnesium Oxide Activity, Magnesium Oxide Suspension, Phosphorus, MgO

Optimization of Struvite Recovery Utilizing Magnesium Oxide

Sydney Goy

Abstract

Magnesium oxide (MgO) is a cost-effective and environmentally sustainable alternative to magnesium chloride ($MgCl_2$) and sodium hydroxide (NaOH) used for sidestream struvite recovery from anaerobically digested supernatant (centrate) through the Pearl® process. MgO is produced from magnesite ($MgCO_3$) calcination, and different calcination conditions can alter the quality and characteristics of the MgO product. It was hypothesized that the insolubility of MgO could provide a "slowly available" form of Mg^{2+} in the reactor and consequently allow the reactor to be operated beyond design phosphorus (P) reactor loading. MgO has been utilized in other P recovery technologies, e.g. the Phospaq™ Process, but operation and performance of MgO using a full-scale Pearl® 500 fluidized bed reactor was investigated. Performance at rated reactor loading utilizing MgO was initially comparable to baseline conventional $MgCl_2$ reactor operation, ≥50% struvite yield (P recovered/theoretical P recovery) and ≥70% total phosphorus (TP) removal. However, the pilot reactor operated at 2X reactor loading showed comparable results to baseline performance at 1.5X reactor loading. During the full-scale pilot, optimization of the reactor utilizing MgO was limited by the struvite product size that the struvite post-processing equipment could effectively harvest. Additionally, the MgO characteristics due to calcination conditions were hypothesized to affect struvite precipitation kinetics. In struvite precipitation jar testing, MgO products were used to analyze the saturation index, measure precipitation kinetics, and understand the effect that MgO hydration and reactivity had on struvite precipitation. Jar testing showed that initial P removal increased with increasing MgO product reactivity. The most reactive MgO used, Timab AK98, showed 1-40% P removal and substantial decrease in solution saturation index immediately after dosing MgO to centrate. The slower P removal and decrease in saturation index observed with the less reactive material suggests that MgO can provide a "slowly available" Mg^{2+} reserve throughout the struvite precipitation reaction.

Optimization of Struvite Recovery Utilizing Magnesium Oxide

Sydney Goy

General Audience Abstract

Phosphorus is an essential element for human, plant and animal health. Necessary bodily functions cannot be performed without inputting phosphorus to cell metabolic pathways, such as cell repair and formation of nucleic acids, bone mineral and stored energy. Phosphates are the most common form of phosphorus found in the environment and are a component of many common substances, such as detergents, fertilizers, food and urine. Due to the increasing population and food demand the need for phosphorus-based fertilizers has soared since the 1940s. In 2018, 240 megatons of phosphate rock were mined, and 17 megatons of phosphorus were extracted from mined ore. 15 megatons of the extracted phosphorus were used in fertilizer production. Because of phosphorus loss from the soil and inefficient agro-practices, only 20% of the extracted phosphorus is consumed by humans and animals from food and little is then recycled from our waste systems. There is a major gap in the agricultural phosphorus cycle that is necessary to address with sustainable practices (Oster, M. et al. 2018). Phosphorus can be recovered from wastewater in the form of struvite, which is a mineral that can be utilized a slow-release fertilizer. Conventional methods of phosphorus recovery from wastewater have the potential to be costly. By utilizing an alternative chemical, struvite recovery can be more cost-effective and environmentally sustainable.

Table of Contents

List of Tables

List of Figures

List of Abbreviations

HRSD – Hampton Roads Sanitation District

SRF – Struvite Recovery Facility

WWTP – Wastewater Treatment Plant

EBPR – Enhanced Biological Phosphorus Removal

PAO – Phosphorus Accumulating Organism

R1 – Reactor 1

R2 – Reactor 2

R3 – Reactor 3

MgO – Magnesium Oxide, Magnesia

$MgCl_2$ – Magnesium Chloride

$MgCO_3$ – Magnesium Carbonate, Magnesite

$Mg(OH)_2$ – Magnesium Hydroxide

P – Phosphorus

N – Nitrogen

Mg - Magnesium

Mg^{2+} - Magnesium Ion

NH_4^+ - Ammonium Ion

PO_4^{3-} - Phosphate Ion

γ = Activity

OP – Orthophosphate

TP – Total Phosphorus

PO4-P – Phosphate as Phosphorus

NH3-N – Ammonia as Nitrogen

SI = Saturation Index

SSR = Supersaturation Ratio

S_a = supersaturation

mg/L – Milligram per Liter

kg P/day – Kilogram Phosphorus per Day

m/m – Mass per Mass Fraction

ρ = Density

mm = Millimeter

SGN – Standard Guide Number (mm x 100)

H_2SO_4 – Sulfuric Acid

L/min – Liter per Minute

Hz – Hertz

lbs./min – Pounds per Minute

1. Introduction

Phosphorus is an essential element for human, plant and animal health. Necessary bodily functions cannot be performed without inputting phosphorus to cell metabolic pathways, such as cell repair and formation of nucleic acids, bone mineral and stored energy. Phosphates are the most common form of phosphorus found in the environment and are a component of many common substances, such as detergents, fertilizers, food and urine. Due to the increasing population and food demand the need for phosphorus-based fertilizers has soared since the 1940s. In 2018, 240 megatons of phosphate rock were mined, and 17 megatons of phosphorus were extracted from mined ore. 15 megatons of the extracted phosphorus were used in fertilizer production. Because of phosphorus loss from the soil and inefficient agro-practices, only 20% of the extracted phosphorus is consumed by humans and animals from food and little is then recycled from our waste systems. There is a major gap in the agricultural phosphorus cycle that is necessary to address with sustainable practices (Oster, M. et al. 2018).

A wastewater treatment plant (WWTP) can experience phosphorus loads from municipal human sewage sources and/or industrial sources, such as livestock and food processing plants (Driver, J. 1999; Yuan, et al. 2012). In wastewater, phosphorus is found in the form of phosphates, polyphosphates or phosphorus-containing organic compounds (Ruzhitskaya et al. 2016). Typically, phosphorus is removed from wastewater streams by biological or chemical processes prior to discharging treated effluent to a waterway. A chemical method commonly used is dosing a metal salt and removing phosphorus as a metal coprecipitate. Biological nutrient removal (BNR) processes can allow for uptake of phosphorus by activated sludge which can then be diverted to waste and be disposed of. These methods of removal are efficient and enable a WWTP to meet discharge regulations and minimize the potential for eutrophication in waterways. However, phosphorus can accumulate in sludge, increase sludge volumes by chemical phosphorus removal, and cause a nuisance when uncontrolled in the presence of ammonium and magnesium ions in solids handling waste streams in the form of precipitated struvite ($MgNH_4PO_4 \cdot 6H_2O$) (Le Corre, K.S. et al. 2009). Side stream recovery of struvite can divert high phosphorus concentrations to be further treated and reduce sludge volumes by 10-20% when comparing to phosphorus removal performed by dosing a metal salt (Edge, D., 2000).

Struvite, or magnesium ammonium phosphate hexahydrate, is a crystal that can spontaneously occur in biological material where struvite constituent concentrations surpass the solubility product (Le Corre, K.S., 2009). Struvite is especially a common occurrence when an enhanced biological phosphorus removal (EBPR) treatment process is coupled with anaerobic digestion in a WWTP. EBPR can achieve phosphorus uptake from phosphorus accumulating organisms (PAOs) and thus low effluent phosphorus concentrations sent to the waterways. Anaerobic digestion following EBPR causes release of ammonium and phosphorus accumulated in the waste sludge which leads to an abundance of phosphate and ammonium ions present in post-digestion solids handling streams leading to struvite scale and maintenance issues over time. This can occur even when

minimal magnesium ion concentrations are present. Struvite precipitation can be controlled to allow for a valuable product to be recovered and reused unlike common biological and chemical methods for phosphorus removal. Recovering struvite from wastewater not only creates a sustainable phosphorus-based fertilizer but helps to close the gap in the agricultural phosphorus cycle.

Struvite precipitation is commonly applied using anaerobically digested supernatant, obtained from dewatering digested sludge, due to the abundance of phosphate and ammonium ions (Münch, E., et al. 2000). To take advantage of the struvite precipitation potential in wastewater sidestreams, it is important to operate at a magnesium (Mg^{2+}): ammonium (NH_4^+): phosphate (PO_4^{3-}) ion molar ratio of at least 1:1:1 as struvite is composed of equimolar parts of each ion (Kiani, D., et al. 2018). The limiting reagent is magnesium (Mg) and an additional external Mg source is required to recover as much phosphorus as possible. Effective sources of Mg are water-soluble Mg salts; e.g. magnesium chloride ($MgCl_2$) or magnesium sulfate ($MgSO_4$), which are uncommon in nature and are commonly made with seawater and the use of costly separation processes. Because of this, Mg salts comprise 75% of the operational costs to recover struvite (Kiani, D., et al. 2018). High operational costs can make struvite recovery inaccessible or undesirable , however operational costs can be minimized by utilizing alternative and naturally abundant forms of magnesium.

Magnesium oxide (Periclase, Magnesia, MgO), magnesium hydroxide (brucite, $Mg(OH)_2$), and magnesium carbonate (Magnesite, $MgCO_3$) are naturally occurring, slightly soluble minerals that can be used as a magnesium source for struvite recovery (Kirinovic, E., et al. 2017). The worldwide mineral commodity assessment conducted by the United States Geological Survey estimated 12 billion tons of magnesite reserve in 2017 (USGS, 2017; Kiani, D., et al. 2018).

It is hypothesized here that a more accessible and naturally abundant Mg compound can decrease struvite recovery operational costs and create an attractive phosphorus recovery method. MgO is a naturally occurring mineral and can also be created from the calcination of magnesite (Birchal, V.S.S., et al. 2000). Calcination is defined as the thermal treatment of ores causing a release of carbon dioxide. In addition, the treatment can also remove impurities and moisture. Depending on calcination conditions and previous magnesite quality, MgO can vary in particle size, reactivity, and porosity (Birchal, V.S.S., et al. 2000). MgO is capable of undergoing a hydration/dissolution (commonly known as slaking) reaction with water to produce $Mg(OH)_2$ (Kiani, D. et al. 2018). This hydration reaction of MgO to $Mg(OH)_2$ is strongly influenced by the physical properties of MgO which are determined by the calcination conditions of magnesite (Birchal, V.S., et al. 2001). The method of adding MgO into the struvite precipitation process has been shown to affect process operation and optimization. The solid nature of MgO is hypothesized to provide a "slowly available" Mg^{2+} reserve attributed to the MgO dissolution during hydration. The variability of MgO product quality and hydration reaction along with the observed successful struvite precipitation and cost effectiveness all represent good reasoning for further investigating MgO.

1.1. Research Motivation

Phosphorus recovery as struvite can capture a valuable product from wastewater that would otherwise most likely be disposed. As world population and food demands increase, the natural phosphorus deposits can become depleted and cause issues for agriculture and the subsequent consumers all around the world. It is necessary to recover phosphorus in a feasible and cost-effective manner. WWTPs and industrial sites can contain enriched nutrient streams that possess struvite recovery potential and incorporate recovered fertilizer into the agricultural phosphorus cycle. Current methods of struvite precipitation utilizing Mg salts have the potential to be costly given the initial capital costs and continuous operational costs. A full-scale process that does utilize MgO for Mg addition is the Phospaq™ process. Phospaq is a sidestream process utilizing aeration for biological treatment and MgO for chemical removal as struvite (Metcalf & Eddy, 2014). However, product obtained from this process is not always used as slow-release fertilizer and is course material with an average diameter of 0.7 mm (Ovivo Inc, 2017). Research conducted with different magnesium compounds for struvite precipitation sheds light on the opportunity to minimize operational costs and enable nutrient recovery technologies to be more appealing and become a more common practice.

Struvite recovery utilizing the Ostara Nutrient Recovery Technologies (Vancouver, BC, Canada) process has been deployed at the Hampton Roads Sanitation District's (HRSD) Nansemond Treatment Plant in Suffolk, VA for over 10 years. At HRSD's Struvite Recovery Facility (SRF), Ostara Pearl® 500 reactors are utilized to create Crystal Green®, a phosphorus-based fertilizer that is effectively pure struvite. A Pearl® reactor is a fluidized bed reactor (FBR) that utilizes an internal recycle of treated effluent to provide the necessary upward flow velocity to suspend struvite product. The recycle provides a moderate supersaturation to promote struvite crystal growth. Increasing radii up the height of the reactor decreases upward flow velocity experienced at higher portions of the reactor and allows for product size classification and sizeable product harvesting.

Since 2018, HRSD has been piloting MgO products for struvite precipitation in a designated Pearl® reactor. The transition from a soluble Mg salt to a slightly soluble Mg powder has brought an array of challenges but has been informative. Throughout the MgO trial at HRSD it was noticeable that MgO acts differently than the liquid $MgCl_2$ salt in use full-scale for 10 years. It was necessary to develop modified controls and alternative MgO feeding strategies that allowed for high phosphorus removal and recovery as well as manageable daily operations at the SRF.

Chapter 3 discusses baseline $MgCl_2$ reactor operation and different modes of control that were used on the MgO pilot reactor and the results from each trial. There are many operating parameters that are important for struvite precipitation, such as pH, alkalinity, supersaturation of solution, mixing, etc. MgO behaves differently than soluble Mg salt as it provides additional alkalinity and solid surfaces to the process as it adds a magnesium source. Because MgO is distinctly different, it altered typical operation and maintenance of the reactor and became important to ensure optimization of the SRF could be achieved and considered a success while using MgO. Pilot

operation and analysis are recorded in this chapter and compared to previous conventional MgCl2 reactor baseline operation and performance. Distinct improvements in pilot performance, specifically struvite yield, were documented in September 2019 and this prompted further investigation of conventional $MgCl_2$ reactor performance. An improvement in reactor performance was also observed for the MgCl2 reactors. This chapter goes into detail of this sudden improvement in performance and the hypothesis that explains this phenomenon.

Chapter 4 explores the slaking, slurry concentration, and product quality of the MgO and the effect it has on struvite precipitation. These trials were focused on the MgO activity and hydration reaction that occurs prior to dosing MgO suspension (slurry) to the reactor to recover struvite and if the variation in hydration of MgO and product reactivity affects struvite precipitation. Investigation of these qualities of MgO were done by bench-scale jar testing and full-scale reactor operation. It was important to understand if the pretreatment of the MgO product could impact the operation of the pilot reactor and if it could be utilized to potentially deliver optimal operating conditions.

2. Literature Review

2.1. Phosphorus Recovery from Wastewater as Struvite

2.2. Struvite Precipitation

Struvite is a mineral that contains equimolar concentrations of magnesium, ammonium and phosphate. Struvite has an orthorhombic crystal structure and a white appearance (Figure 1). The molecular weight is 245.41 g/mol and the density is 1.7 g/cm^3.

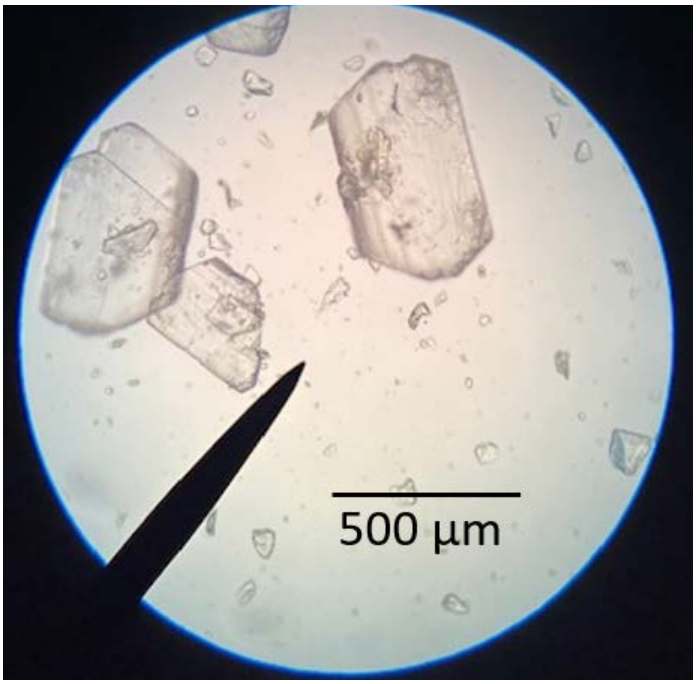

Figure 1: 100X Magnification of Struvite Crystals

Struvite's low solubility is represented by a water solubility around 160 mg/L (at a pH of 7 and temperature of 25 °C) and a thermodynamic solubility product (K_{sp}) experimentally determined between 10^{-10} to $10^{-13.3}$ under various experimental conditions (Adnan, A., et al. II, 2003, Harrison, M.L., et al. 2011). Struvite crystals can spontaneously precipitate out of solution when supersaturated conditions exist– the product of magnesium, ammonium, and phosphate ions in solution exceed the K_{sp} (Ohlinger, K.N., et al. 1998). Struvite, or $MgNH_4PO_4 \cdot 6H_2O$, precipitation reaction is reported as:

$$Mg^{2+} + NH_4^+ + H_nPO_4^{n-3} + 6H_2O \leftrightarrow MgNH_4PO_4 \cdot 6H_2O + nH^+ \quad (1)$$

This chemical equation represents struvite crystal formation from solution, also called nucleation. The release of protons (H^+) through struvite precipitation demonstrates this reaction's ability to consume alkalinity and the necessary alkalinity requirement to continue precipitation of struvite throughout time. An external Mg source is required to achieve an Mg:N:P of at least 1:1:1. Adding Mg can cause the limiting reagent to become phosphorus and increase the phosphorus removal achieved from solution, as is commonly the case in digester supernatant treatment. Table 1 below specifies the chemical composition of pure struvite; a drastic deviation from these percentages can deduce there is an impurity in the collected product.

Table 1: Struvite Chemical Composition of Phosphorus (P), Magnesium (Mg) and Nitrogen (N)

	% P	**% Mg**	**% N**
Struvite	12.6	9.9	5.7

Several operating parameters affect the precipitation of struvite such as pH, temperature, supersaturation, turbulence and the presence of other ions (Le Corre, K.S., et al. 2009; Metcalf & Eddy, 2014; Shaddel, S., et al. 2019). Supersaturation of the solution is the main control parameter for struvite precipitation and increases with an increase in pH between 6-10 (Bouropoulos, N.C. and Koutsoukos, P.G., 2000; Adnan, A., et al. II, 2003; Britton, A. et al., 2005, Mehta, C.M., et al. 2013). Supersaturation is necessary for crystallization to occur as either crystal nucleation or crystal growth. Crystallization in the form of nucleation will not occur when the solution is undersaturated. The driving force of nucleation is the difference in chemical potential between supersaturated solution (μ_s) and equilibrium in the solid state (μ_∞) (Bouropoulos, N.C. and Koutsoukos, P.G., 2000, Ohlinger, K.N., et al. 1999):

$$\Delta\mu = \mu_s - \mu_\infty \quad (2)$$

When incorporating the definition of chemical potential, μ, this becomes:

$$\Delta\mu = \left(\mu_\infty^0 + kTln\left(\alpha_{Mg^{2+}} \cdot \alpha_{PO_4^{3-}} \cdot \alpha_{NH_4^+}\right)_\infty^{1/3}\right) - \left(\mu_s^0 + kTln\left(\alpha_{Mg^{2+}} \cdot \alpha_{PO_4^{3-}} \cdot \alpha_{NH_4^+}\right)_s^{1/3}\right) \quad (3)$$

where k is Boltzmann's constant, T is absolute temperature and α is the activity. The difference in chemical potential provides the framework for understanding how supersaturation of solution causes precipitation (Bouropoulos, N.C. and Koutsoukos, P.G., 2000).

In literature, a simple method for calculating the supersaturation of solution uses the concept of conditional solubility and ignores anion and cation side reactions (Snoeyink, V., et al. 1980, Adnan, A., et al. II, 2003). The conditional solubility (P_S) is defined as the product of the molar concentrations of struvite constituents in solution– dissolved magnesium, ammonia/ ammonium and orthophosphate ions (Adnan, A., et al. II, 2003; Stumm, W. and Morgan, J., 1981).

$$P_S = [Mg^{2+}]_{Total} \cdot [NH_3 + NH_4^+]_{Total} \cdot [PO_4]_{Total} \quad (4)$$

The struvite equilibrium conditional solubility product (P_{Seq}) is defined as:

$$P_{Seq} = \frac{K_{SP}}{\alpha Mg^{2+}\alpha NH_4^+\alpha PO_4^{3-}\gamma Mg^{2+}\gamma NH_4^+\gamma PO_4^{3-}} \quad (5)$$

P_{Seq} is the solubility product of struvite once equilibrium is reached for the given experimental conditions where α is the ionization fraction and γ is the activity coefficient for the respective struvite constituent ions (Stumm, W. and Morgan, J., 1981). The activity coefficient used when determining the SSR is dependent on the ionic strength (I) of solution and the valency (Z) of the element or compound (i):

$$-\log \gamma_i = AZ_i^2 \left(\left[\frac{\sqrt{I}}{1+\sqrt{I}}\right] - 0.31\right) \quad (6)$$

$$I = 0.5 \sum [i] Z_i^2 \quad (7)$$

The activity coefficient equation (Equation 7) is defined as the Davies equation and is best used on solution of high ionic strength, but not more than 0.5 M ionic strength. The Deybe-Hückel constant (A) is a value of 0.509 at 25 °C. From the conditional solubility and the equilibrium solubility product the supersaturation ratio can be solved. The supersaturation ratio (SSR) defines the potential for struvite to precipitate out of solution until equilibrium is satisfied and is determined by the ratio at which P_S exceeds P_{Seq} (Snoeynik, V. and Jenkins, D., 1980). If the SSR = 1 than the system is at equilibrium, if SSR >1 than supersaturated conditions exist in solution, and lastly if SSR < 1 the solution is undersaturated with struvite constituents. The SSR equation is defined in terms of P_S and P_{Seq} :

$$SSR = \frac{P_S}{P_{Seq}} = \frac{IAP}{K_{SP}} = \frac{\gamma Mg^{2+}[Mg^{2+}] \cdot \gamma NH_4^+[NH_4^+] \cdot \gamma PO_4^{3-}[PO_4^{3-}]}{K_{SP}} \quad (8)$$

P_S normalized by PSeq is equivalent to the ion activity product (IAP) divided by K_{SP}. Saturation index (SI) is also commonly used (Stolenburg, P. et al., 2015) and can be defined in terms of the previously defined SSR:

$$SI = \log_{10}(SSR) \quad (9)$$

Supersaturation (Sa) has also been observed in literature and is defined as (Mullin, J.W., 2001):

$$S_a = \left(\frac{IAP}{K_{SP}}\right)^{1/3} \quad (10)$$

A supersaturated solution (SSR>1, SI>0, S_a>1)will precipitate struvite crystals until equilibrium is achieved by either nucleation or crystal growth. Supersaturated solutions can eventually reach a metastable zone where nucleation is not spontaneous and crystal growth is favored (Adnan, A., et al. II, 2003). Spontaneous nucleation from solution only occurs under supersaturated conditions, and the saturation index can significantly affect the performance of the struvite recovery process, i.e. phosphorus removal and struvite recovery.

Struvite recovery can also be referred to as the yield or process efficiency, the percent of theoretical production that is recovered. Struvite yield and phosphorus removal increase at higher Mg:N:P molar ratios and pH, which drives up the supersaturation of the solution. Literature shows better phosphorus removal and struvite yields are achieved at a pH of 9.5 rather than a pH of 7.5. Low Mg:N:P, experiments, e.g. 1:2:1, were only able to achieve high removal and yields when operated at a higher pH of 8.5 or 9.5 (Shaddel, S., et al. 2019). This demonstrates that Mg can also be a controlling parameter when optimizing struvite precipitation (Adnan, A., et al. II, 2003). The combination of a high Mg:N:P (1.67:12:1) and a high pH (9.5) were able to demonstrate essentially 100% phosphorus removal and struvite yield from the initial solution (Shaddel, S., et al. 2019). However, when the degree of supersaturation is high, small struvite crystal nuclei will spontaneously precipitate from solution, defined as homogeneous nucleation and these small struvite crystals, called fines, can be washed out in the effluent leading to lower TP removal (Adnan, A., et al. I, 2003).

Controlling the degree of supersaturation in the solution can optimize phosphorus removal and recovery but it can also impact the precipitation kinetics observed in the system. As the degree of supersaturation is reduced, struvite crystal nuclei can begin to grow by heterogeneous nucleation–formation of nuclei utilizing existing struvite or foreign object surface area as a precipitation foundation. Particles in solution function catalytically as a foundation for struvite precipitation to occur and overcome higher activation energies associated with a slight SSR in solution (Ohlinger, K.N., et al., 1999; Adnan, A., et al. II, 2003; Rahman, M.M., et al. 2013). This inverse relationship between degree of supersaturation and struvite product size is an important aspect of the struvite crystallization process optimization (Adnan, A., et al. II, 2003).

When precipitating struvite under Mg:P molar ratios of 0.5, 0.75 and 1 it is observed that the lower supersaturation utilizing a 0.5 Mg:P had the largest volume-weighted % is greater than 100 μm particle size. The higher supersaturated solution created from an Mg:P of 1 generated the largest volume-weighted % is around 20 μm. Struvite precipitation under an Mg:P of 0.75 had the highest weighted-volume % around 75 μm (Stolzenburg, P., et al. 2015). Altering the supersaturation conditions can also impact struvite properties, such as morphology, settleability, and size distributions.

2.2.1. Struvite Crystal Properties

Nucleation and crystal growth kinetics of struvite are dependent on the supersaturation of solution. It has been observed that the most basic orthorhombic struvite morphology is present at lower supersaturation conditions. As the supersaturation ratio is increased over the value of 3 by increasing struvite constituent ion concentrations or the pH, the crystal tends to change to a hopper, or butterfly, crystal morphology. Increasing the pH can elongate the crystal and increasing the ammonium concentration can trigger sharp faces on the crystal to form. Dendritic crystals begin to form when supersaturation ratios are increased above a value of 5 and the branching of the crystals amplify as ammonium concentrations are increased (Shaddel, S., et al. 2019). Figure 2 demonstrates the specific struvite morphology described in literature.

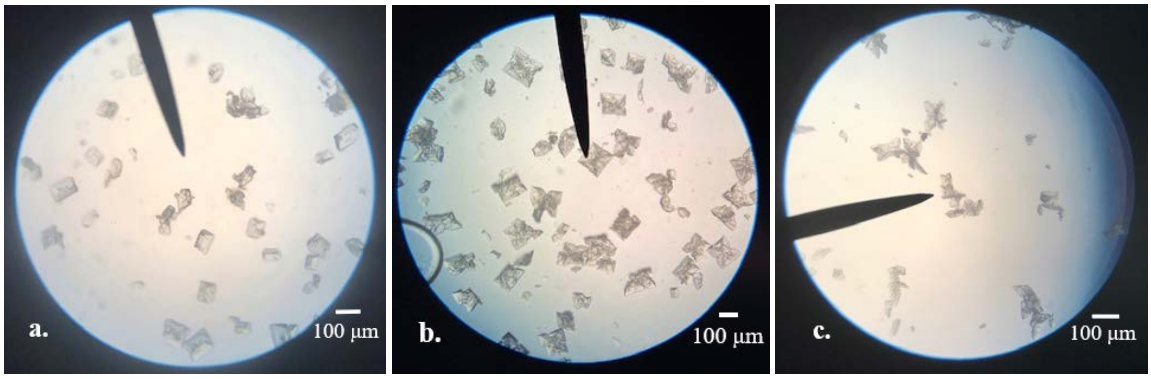

Figure 2: Struvite Morphology, a. Orthorhombic, b. Hopper, c. Dendritic

Different crystal size and shape can affect settleability, and the post-processing, i.e. filtering and drying. Dendritic struvite crystals tend to have the lowest settling velocity, complicating the removal of the crystals. The orthorhombic crystal structure had the highest settling velocity and are observed under lower supersaturation (<3). Low supersaturation can allow for a homogeneous particle size distribution and high supersaturation can cause an increase in fine particles. High supersaturation also causes a larger number of particles. This is due to a high supersaturation causing a high nucleation rate and depleting the Sa that could have been utilized for aggregation and crystal growth (Shaddel, S., et al. 2019). Struvite particles possess a higher zeta potential at a higher supersaturation and pH interfering with the aggregation of struvite particles due to the repulsive forces (Shaddel, S., et al. 2019). In literature it has also been specified that heterogeneous nucleation of struvite has been defined as the faster nucleation reaction in lower saturation conditions, observed to be below 15 minutes. Time needed for struvite precipitation increased to 20 – 45 minutes, depending on temperature, for homogeneous nucleation to occur in a low saturation solution with no seed material present (Crutchik, D., et al., 2016).

2.3. Struvite Recovery Utilizing a Fluidized Bed Reactor

Struvite is commonly recovered in a fluidized bed reactor (FBR) or stirred tank reactor. FBRs pump a large portion of the treated effluent, called the recycle flow, down from the clarifier to provide the necessary upward flow velocity (upflow velocity) to the bottom of the reactor to fluidize the struvite particles. Below, Equations 11 and 12 define the total upflow stream (Q_{up}) and the recycle flow (Q_r), where v_{up} is the upflow velocity, R is the radius of the harvest zone and RR is the recycle ratio (%) (Ye, X., et al., 2016):

$$Q_{up} = v_{up} \cdot \pi R^2 \tag{11}$$

$$Q_r = \frac{RR \cdot Q_{up}}{100} \tag{12}$$

Fluidized bed reactors are better suited for creating large-sized, uniform product by providing moderately supersaturated conditions influenced by the recycle flow portion containing low phosphorus concentration (Rahaman, M.S., et al. 2014). The radius of the reactor increases incrementally up the height of the reactor which decreases the upflow velocity experienced in the upper reactor portions. These increasing reactor radius increments can allow for turbulence created at the radius transitions and particle size classification up the reactor with the decreasing upward flow velocity (Bhuiyan, M.I.H., et al. 2007; Britton, A., et al. 2005). Struvite particles remain fluidized in a specific region in the reactor where the upward flow velocity is in equilibrium with the particle's settling velocity. This is how the reactor can separate struvite where larger particles are in the lower portion, with higher upflow velocities, and smaller struvite particles are in the upper portion, with lower upflow velocities. The top portion of the FBR is a clarifier which helps trap or recycle the fines that cannot withstand the upflow velocities and wash out of the reactor (Britton, A., et al. 2005).

Struvite precipitation in a fluidized bed reactor requires a nutrient rich influent, such as anaerobic digested supernatant at a WWTP, an Mg source and pH/alkalinity addition, typically as NaOH, at the bottom of the reactor. Since pH has been observed to act as a surrogate for the complex supersaturation measurement given a relatively constant nutrient concentration of the influent, the reactor is pH controlled. Influent centrate, Mg salt, $MgCl_2$ and NaOH are all incorporated with the recycle flow at the bottom of the reactor in a section called the injection port. The combination of highly concentrated influent centrate with the recycled effluent of lower phosphorus concentrations is responsible for the moderate supersaturation experienced in the bottom of the fluidized bed reactor. The high upflow velocity in the lower portion of the reactor where the larger particles are fluidized causes high relative velocities between the struvite particles and solution which can promote crystal growth by faster mass transfer rates (Bhuiyan, M.I.H., et al., 2007). The fluidized bed reactor technology is a seeded process where uniform crystal sizes can be added during reactor startup and throughout operation to help maintain a steady state condition of crystal growth in the reactor (Rahaman, M.S., et al. 2013). Struvite is harvested in the lower reactor (reactor radius = R) above the injection port through a harvest leg. Harvesting from the bottom removes the larger struvite product from the reactor

for post-processing which includes dewatering, drying and classifying the material. Figure 3 displays how a fluidized bed reactor is designed and operates.

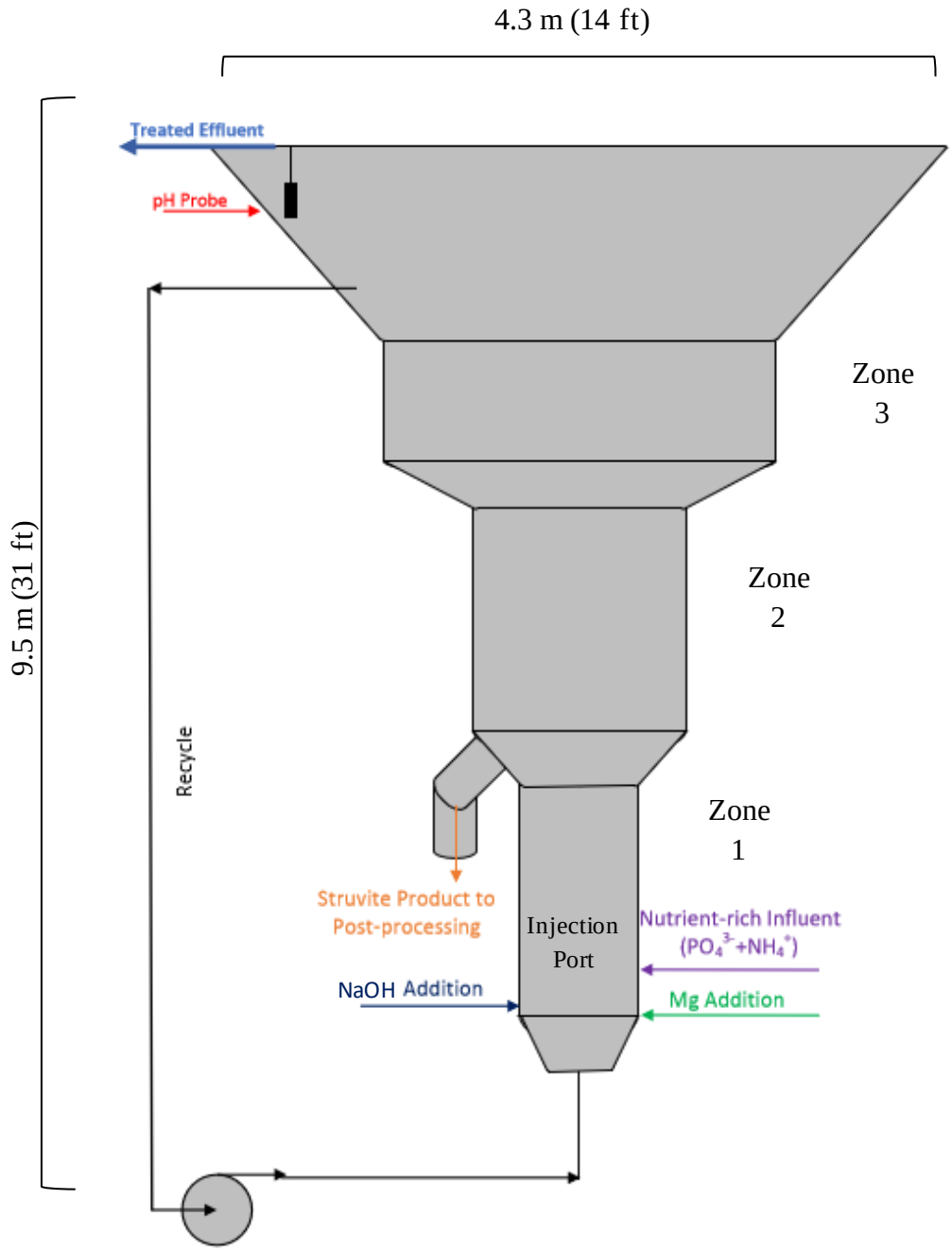

Figure 3:Fluidized Bed Reactor Schematic

Ostara Nutrient Recovery Technologies utilizes a fluidized bed reactor for struvite precipitation. Ostara has 3 different Pearl reactors of different sizes and production capacity – Pearl 500, Pearl 2K and Pearl 10K from smallest to largest. The idea of the fluidized bed reactor

is that the internal recycle controls effluent fines washout and initial supersaturation of solution to optimize crystal growth and nucleation kinetics at the injection port.

2.4. Magnesium Sources for Struvite Precipitation

As mentioned previously, 75% of struvite recovery chemical costs can be attributed to Mg addition, $MgCl_2$ can cost $350-700/ton. The necessity for pH adjustment adds $500-600/ton NaOH to conventional Pearl operation costs (Verigin, M., et al., WEFTEC 2020) The key to keeping nutrient recovery costs low is the nature of the Mg source. $MgCO_3$ and MgO are naturally abundant Mg sources that have low solubility in water. MgO product manufacturing is also more energy efficient. MgO production which includes milling and calcining the product has a carbon footprint of 3 tons of carbon dioxide (CO_2)/ ton Mg produced. Meanwhile, $MgCl_2$ production has a carbon footprint of 12.9 tons of CO_2/ ton Mg produced (Kiani, D., et al. 2018). Studies have shown successful struvite precipitation when using MgO and $MgCO_3$ in replacement of $MgCl_2$. MgO has also been shown to be an effective addition as a suspension in water to precipitate struvite (Capdevielle, A., et al. 2013).

2.5. Magnesium Oxide

Magnesium oxide (MgO) is a hygroscopic white metal oxide that can naturally occur or be produced. MgO has a density of 3.58 g/cm^3 and is slightly soluble in water. Magnesium oxide has the ability to undergo a hydration/slaking reaction with water to create magnesium hydroxide ($Mg(OH)_2$), and the mechanisms of this hydration reaction have been studied since the 1960s (Smithson, G.L., et al., 1969). MgO can be obtained by calcination of magnesite ($MgCO_3$) which is a thermal treatment conducted in a furnace or kiln that releases carbon dioxide (Zhang, X., et al. 2015; Birchal, V.S.S., et al. 2000). Depending on conditions of calcination, such as temperature and retention time, different properties of the MgO final product can be achieved. Different industries take advantage of MgO product quality for specific applications.

2.5.1. Magnesium Oxide Production

Caustic magnesia (light-burned MgO) or dead-burned magnesia (hard-burned MgO) are possible products of the calcination that can each be beneficial for different industrial applications. Caustic MgO is obtained from calcination at lower temperatures (<900 °C) which cause the material to be more porous and thus more reactive. Caustic MgO can be used in agriculture, cattle feed, environmental control, and the manufacturing of special cements. Dead-burned MgO is produced at high calcination temperatures (>1200 °C) which result in a low porosity and low reactivity/unreactive product that is beneficial to the refractory industry (Birchal, V.S.S., et al., 2000; Birchal, V.S., et al. 2001). It is necessary for industries that use MgO to understand what type of product it is and how fast and to what extent it hydrates. Hydration is undesirable for the refractory industry in order to produce strong products that can be effective for a long time. Hydration is favored when the goal of an industry is to achieve $Mg(OH)_2$, such as when producing $Mg(OH)_2$ as a flame

retardant (Birchal, V.S.S., et al. 2000, Aphane, M.E., et al. 2009). As the temperature increases the crystal size increases and the surface area decreases. The higher temperatures associated with dead-burned MgO calcination cause sintering of the MgO product which leads to less porous and thus less reactive material (Birchal, V.S.S., et al. 2000; Birchal, V.S., et al. 2001, Canteford, J.H. 1985). Development of porosity is correlated to the pseudo-morphic transformation of $MgCO_3$ to MgO (Liati, M. 1987; Nan, L 1989). It is discussed in literature that 90% of the specific surface area of an MgO particle occurs within the pores (Smithson, G.L. and Bakhshi, N.N, 1969). Magnesite calcination experiments at temperatures of 850, 900, 950, and 1000 ℃ with different retention times (90, 180 and 240 minutes) showed that temperature impacted the final MgO product more than the calcination retention time. Specific surface area of the MgO product was larger for the lower temperature calcinations and the specific surface area decreased with increasing temperature from 850 to 1000 ℃ (Birchal, V.S.S., et al 2000, Tang, X., et al. 2014).

2.5.2. Magnesium Oxide Activity

The activity of magnesium oxide is determined operationally using time-based measurement that can indicate how reactive an MgO product is relative to other MgO product activity values. An activity test is the time required for MgO to neutralize an acid–acetic acid or citric acid activity tests are common (Birchal, V.S.S, et al. 2000, Tang, X., et al. 2014). Highly reactive/light-burned MgO have activities < 60 seconds, medium reactivity is represented by an activity value between 180 – 300 seconds and low reactivity/hard-burned have activities > 600 seconds (Romero-Güiza, M.S., et al. 2015). The larger the activity, the less reactive an MgO product is (Birchal, V.S.S., et al. 2000). As the calcination temperature decreases the specific surface area increases and activity time decreases which indicates that an MgO product with a larger specific surface area is more reactive (Birchal, V.S.S., et al. 2000). An activity test can provide information about the MgO product production, quality, how it compares to other MgO products and possibly how it hydrates from MgO to $Mg(OH)_2$. In terms of utilizing MgO for struvite precipitation, it is important to understand the reactivity of a slightly soluble Mg product, such as MgO, as it influences the efficiency of phosphorus removal in the system (Salutsky, M.L., et al., 1972).

2.5.3. Magnesium Oxide Hydration

The magnesium oxide hydration reaction can be defined as the following equation:

$$MgO_{(s)} + H_2O_{(l)} \rightarrow Mg(OH)_{2\,(s)} \tag{13}$$

MgO hydration is a dissolution/precipitation reaction which involves the dissolution of MgO followed by the precipitation of $Mg(OH)_2$ on the MgO surface. The initial proposed model for MgO hydration was the shrinking core model with the rate limiting step determined by the removal of $Mg(OH)_2$ from the MgO particle surface (Smithson, G.L.

and Bakhshi, N.N. 1969, Matabola, K.P., et al., 2010). However, it was later determined that the rate determining step is the initial dissolution of MgO into solution and the hydration reaction could be kinetically modelled by assuming particle porosity changes with time as $Mg(OH)_2$ precipitates on the MgO surface (Birchal, V.S., et al. 2001). The hydration of MgO is not a simple reaction, it occurs in four distinct steps.

1. The water diffuses into the pores of the MgO particles and reacts with the MgO surface. This is the surface hydroxylation and dissolution of MgO, Mg^{2+} and hydroxide (OH^-) ions are released into solution and as a result the pH increases. This is the rate determining step for the MgO hydration reaction (Birchal, V.S.S., et al., 2000; Rocha, S.D.F., et al., 2004; Smithson, G.L. and Bakhshi, N.N., 1969).

$$MgO_{(s)} + H_2O_{(l)} \rightarrow MgOH^+_{(surface)} + OH^- \rightarrow Mg^{2+} + 2OH^- \quad (14)$$

2. The solution becomes supersaturated with Mg^{2+} and OH^- ions and magnesium hydroxide ($Mg(OH)_2$) precipitates on the surface and in the pores of the MgO particle once the K_{sp} is exceeded. MgO particle porosity changes and a rapid decrease in Mg^{2+} and OH^- ions in solution and pH are observed. MgO dissolution is still occurring and the Mg^{2+} ion concentration is low and remains in a quasi-equilibrium state as dissolution of MgO and precipitation of $Mg(OH)_2$ happen.

$$Mg^{2+} + 2OH^- \rightarrow Mg(OH)_{2\,(s)} \quad (15)$$

3. The $Mg(OH)_2$ precipitation continues to cover any free MgO surface until diffusion of water into pores and surface hydroxylation can no longer occur which cause the rate to slow and pH to stabilize.
4. A $Mg(OH)_2$ layer forms on the MgO surface which inhibits further dissolution of water into the MgO pores and prevents the hydroxylation of the surface. Precipitation of $Mg(OH)_2$ continues until local supersaturation of Mg^{2+} and OH^- in solution around the particle is removed and equilibrium is achieved.

As MgO is hydrated the Mg^{2+} ion concentration peaks shortly during dissolution and then decreases rapidly as it reaches equilibrium with MgO and $Mg(OH)_2$. MgO hydrated under no external force forms a $Mg(OH)_2$ layer enveloped around MgO. MgO hydrated under ultrasonic irradiation eliminates the in-situ precipitation of $Mg(OH)_2$ on the MgO surface and achieve a slightly higher conversion to $Mg(OH)_2$ (Tang, X., et al., 2017; Xing, Z., et al., 2018). A quantitative measurement of MgO conversion to $Mg(OH)_2$, or hydration extent, can be determined as a variation of solid weight (Smithson, G.L. and Bakhshi, N.N. 1969; Birchal, V.S.S., et al. 2000). Even though MgO is only slightly soluble in water, the high degree of solid-liquid interface in the MgO particle pores allows for the dissolution and high conversion of MgO to $Mg(OH)_2$. Figure 4 shows micrographs of particles before and after hydrating MgO in a slurry. More agglomeration, of what is thought to be $Mg(OH)_2$, can be observed around the brown/yellow MgO particle.

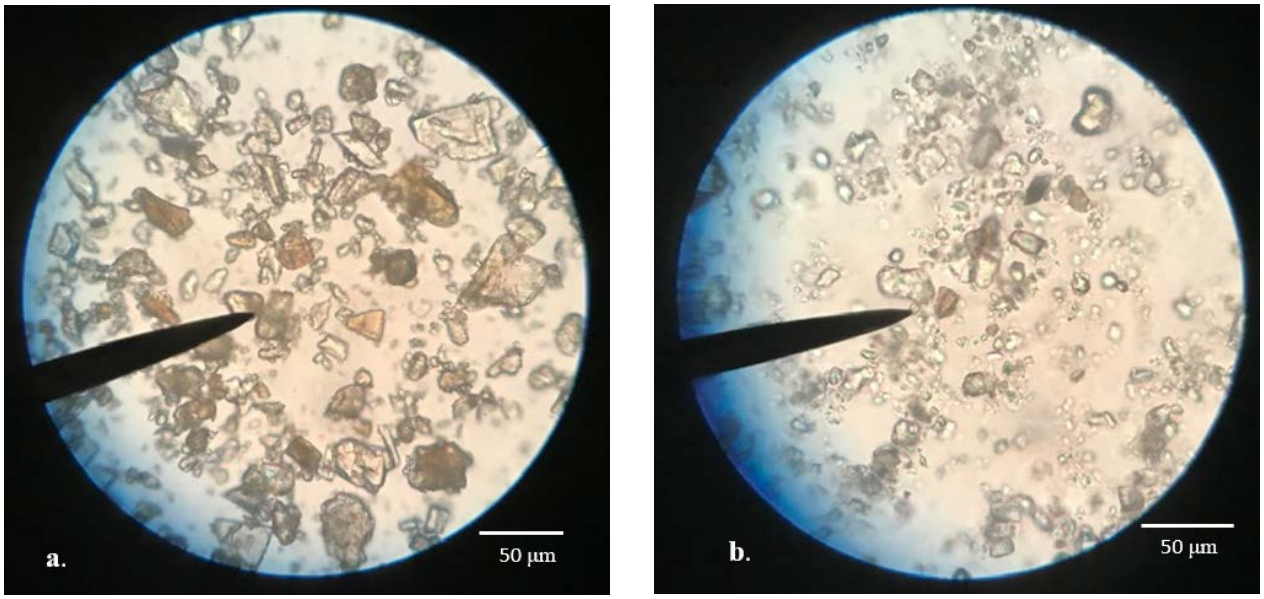

Figure 4:a. MgO Particles Before MgO Hydration, b. MgO Particles after MgO Hydration

The larger the surface area, the more reactive the sample will be which can infer that more MgO will be converted to $Mg(OH)_2$ within a hydration time period (Birchal, V.S., et al 2001). No matter the reactivity of the MgO product, determined by calcination conditions, the maximum degree of hydration or hydration extent is the same for MgO whether calcined at 650 °C or 1000 °C (Aphane, M.E., et al. 2009). However, hydrating dead burned MgO to the maximum hydration extent will take longer than when hydrating caustic MgO. Therefore, the rate of hydration changes given initial MgO product calcination conditions. It was demonstrated that the hydration extent of an MgO product could be influenced by the hydrating agent. Hydrating MgO in a magnesium acetate solution instead of water could alter the hydration extent achieved within a specific timeframe. The hydration extent of MgO in water levelled off at 65% after 800 minutes while the hydration extent of MgO in magnesium acetate solution levelled off at 85% after 500 minutes (Aphane, M.E., et al. 2009). It is thought that the additional Mg ions in a magnesium acetate solution allow for more precipitation of $Mg(OH)_2$ to occur and occur faster (Van der Merwe, E.M., et al. 2004, Castro, S.R., et al. 2015). The use of sodium chloride (NaCl) as a hydrating agent did not seem to influence the MgO hydration as the hydration rate and extent were relatively similar to that of water (Castro, S.R., et al. 2015).

Temperature also effects the hydration extent observed of MgO product. During 30-minute hydration reaction tests, it was noticed that the MgO hydration in an 80 °C water bath achieved the highest conversion to $Mg(OH)_2$. Hydration tests were done within the temperature range of 30 – 80 °C and utilized different hydrating agents to determine which combination saw the largest conversion of MgO to $Mg(OH)_2$. Hydrating agents used during these tests done by Matabola, K.P, et al. (2010) are listed in Table 2 below.

Table 2: Hydrating Agents used by Matabola, K.P., et al. (2010)

Compounds used as Hydrating Agents
Ammonium Chloride (NH_4Cl)
Magnesium Acetate Solution ($Mg(CH_3COO)_2 \cdot 4H_2O$)
Magnesium Nitrate ($MgNO_3$)
Acetic Acid (CH_3COOH)
Water (H_2O)
Magnesium Chloride Solution ($MgCl2 \cdot 6H2O$)
Sodium Acetate ($NaCH_3COO$)
Hydrochloric Acid (HCl)

Testing by Matabola, K.P., et al. (2010) resulted in the largest conversion to $Mg(OH)_2$ when hydrating MgO at a temperature of 80 °C and using magnesium acetate solution as a hydrating agent. The least successful hydrating agent was $NaCH_3COO$ and had the lowest conversion of MgO to $Mg(OH)_2$ when heated to 30 °C (Matabola, K.P, et al. 2010).

2.6. Magnesium Oxide Utilized for Struvite Precipitation

Recent studies have been conducted to examine struvite precipitation utilizing magnesium oxide as a Mg source due to its low cost (Huang, H., et al. 2016). The literature reveals that the price of struvite precipitation can potentially be decreased from 4000 €/metric ton of P to 350 €/metric ton of P when switching from $MgCl_2$ and NaOH to MgO slurry (Crutchik, D., et al. 2018). Magnesium oxide byproducts, or low-grade MgO, of the calcination process have also been investigated. MgO byproducts are from the cyclone residue of exhausted gases from $MgCO_3$ calcination (Quintana, M., et al., 2007). These low-grade MgO products have the potential to contain more metal oxide impurities, lower purity % of MgO, but can be 8 to 10 times cheaper than $Mg(OH)_2$ when used in suspension to undergo a hydration reaction (Castro, S.R., et al. 2015). An X-ray Diffraction (XRD) of MgO production by-product revealed 58% of the sample was MgO while 25% was $MgCO_3$ and 7% was dolomite ($CaMg(CO_3)_2$). This MgO production byproduct was utilized to precipitate struvite and was observed perform better, achieving ~90% P recovery after 4 hours, when sieved or ground <0.04 mm prior to dosing. MgO byproduct >0.04 mm achieved the lowest P recovery at 75% after 4 hours. The higher efficiency of the sieved <0.04 mm MgO byproduct relative to final struvite product purity was also observed in the composition of struvite product obtaining an Mg:P of 1.62 in struvite product. Unsieved MgO byproduct utilized for struvite precipitation showed Mg:P of 2.5 and 3 in final product and demonstrated the product composition contained MgO or $MgCO_3$ (Quintana, M., et al., 2004).

High-grade MgO can have very minimal metal oxide impurities in the product. It has been observed that dosing a concentrated MgO slurry is more advantageous than dosing bulk MgO powder material due to better dispersion and initial reaction of slurry (Stolzenburg, P., et al. 2015, Capdevielle, A., et al. 2013). Utilization of an MgO byproduct in suspension showed to decrease reaction time and increase quantity and quality of product when precipitating struvite

in comparison to bulk MgO dosing (Quintana, M., et al. 2007). Compared to soluble Mg salt, MgO use for struvite precipitation possesses a few obstacles such as the preceding complex hydration reaction that occurs during slurry preparation and its low solubility in aqueous solutions (Stolzenburg, P., et al. 2015).

Stolzenburg, P., et al. conducted struvite precipitation experiments with the use of a simulated wastewater nutrient solution and an MgO slurry dosed at Mg:P ratios of 0.5, 0.75 and 1. An Mg:P ratio is the molar concentration of Mg that is dosed to a system relative to the molar concentration of phosphorus present or dosed. Slurry preparation was specified as 80 gL^{-1} MgO slurry used in this experiment, which is about 7.4 % MgO mass/total slurry mass. The MgO used was light-burned MgO with a purity of 98% mass MgO/mass product. MgO slurry was used for struvite precipitation after mixing 8-16 hours when the slurry reached 99% hydration extent relative to product purity and a quasi-equilibrium state shown by a stable pH, which was reproducible for multiple trials. After 16 hours there was a pH decrease in the slurry that was linked to adsorption of CO_2 from the atmosphere.

Results from Stolzenburg, P., et al. (2015) study show that MgO slurry is an effective reagent for precipitating struvite and can achieve better results than that of $MgCl_2$ addition at all corresponding Mg:P dosages tested. MgO addition at an Mg:P of 1 achieved >90% recovery of phosphorus while $MgCl_2$ addition at an Mg:P of 1 achieved around 85% . This study also shows that while MgO addition caused struvite particles to be smaller than $MgCl_2$ addition for struvite precipitation, particles did increase in size as the Mg:P was decreased. Batch experiments were run to achieve the same final pH when using MgO and $MgCl_2$. Supersaturation ratios were higher for all Mg:P ratios when dosing MgO instead of $MgCl_2$. MgO slurry introduced to the batch system causes a pH increase that is associated with MgO and $Mg(OH)_2$ dissolution. The dissolution of the $Mg(OH)_2$ surface layer is encouraged by the solution's initial low pH and high phosphorus concentration that can increase the MgO solubility and allow for formation of magnesium and phosphate ion pairs. This rapid dissolution of the $Mg(OH)_2$ surface layer is postulated to cause high initial supersaturation in solution, especially near the MgO particle (Stolzenburg, P. et al., 2015).

The saturation index was calculated to determine solution supersaturation using the formula below, defined previously:

$$SI = \log\left(\frac{\gamma_{Mg^{2+}} \cdot \gamma_{NH_4^+} \cdot \gamma_{PO_4^{3-}}}{K_{Struvite}}\right) \quad (16)$$

The saturation index is the log of the SSR equation outlined earlier. Higher saturation index can lead to fast nucleation causing a branched, dendritic structure and smaller particle size of the precipitated struvite. (Stolzenburg, P., et al. 2015). In literature, struvite precipitated utilizing MgO appears more dendritic than the struvite precipitated with $MgCl_2$ at lower Mg:P dosing ratios (<1). When using $MgCl_2$, struvite does not appear dendritic until an Mg:P of 1, which can also be due to the operational pH of 8.2. The dendritic structure of struvite has been

obserbed to be influenced by high degree of supersaturation in solution (Babić – Ivančić, V., et al 2002, Shaddel, S., et al. 2019).

It has also been postulated that the solid MgO particle can provide a Mg^{2+} reserve in the system that can be used until NH_4^+ and PO_4^{3-} ions are consumed and the batch system reaches equilibrium. Due to the additional surface area that MgO provides when precipitating struvite, it is assumed that the particles facilitate heterogeneous nucleation of struvite using the $Mg(OH)_2$ surface layer on the MgO particle (Stolzenburg, P., et al. 2015). Dissolution of the MgO particle can allow for high degrees of supersaturation near the particle. It has been observed that heterogeneous nucleated struvite on MgO particles exhibits the same struvite structure as that of homogeneously nucleated struvite under the same experimental conditions (Kirinovic, E., et al. 2017). Figure 5 exhibits struvite growth (transparent orthorhombic structures) on a MgO particle (yellow and brown irregular structures). Other studies have mentioned the limitation of struvite precipitation when utilizing MgO was not caused by the solubility constraints of MgO but a proposed mechanism of heterogeneous nucleation on MgO particles causing dissolution restrictions and reagent efficiency reduction (Romero-Güiza, M.S., et al. 2015).

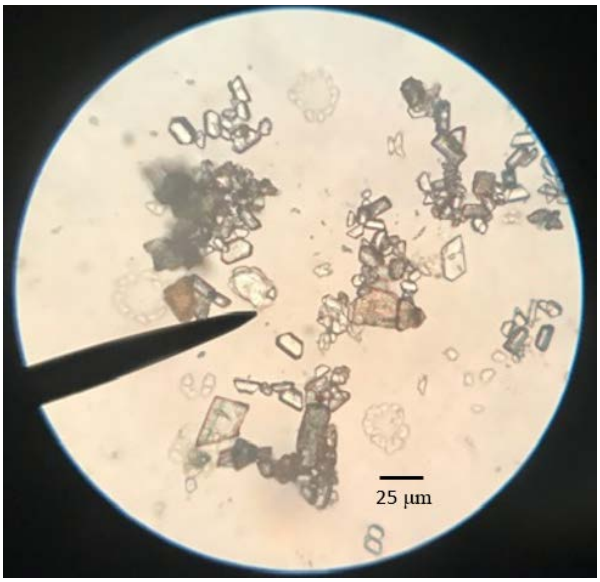

Figure 5:Micrograph of Struvite Formation on MgO Particles

The utilization of MgO to precipitate struvite can provide reactive magnesium hydroxide intermediates that can promote heterogeneous nucleation or homogeneous nucleation (Kirinovic, E., et al., 2017). MgO has been used successfully as an Mg source for struvite precipitation and can promote high supersaturation ratios and rapid precipitation of struvite out of solution. When operating at an Mg:P of 1.56:1 a fast-kinetic regime was observed where 70% of NH_4^+ was removed 5 minutes after MgO addition (Kiani, D., et al. 2018).

Struvite product obtained when utilizing MgO versus MgCl2 was smaller at each Mg:P (0.5, 0.75, and 1) when observing the volume-weighted distributions (Stolezenburg, P. et al., 2015).

Park, N., et al. (2015) observed particle size ranges of 75-150, 150-300, and 300-600 µm. From XRD results, the 75-150 µm particle sizes were consider 100% amorphous structures rather than struvite.

3. Materials and Methodology

3.1. Struvite Recovery Facility

The piloting of MgO product for struvite recovery was performed on a full-scale Ostara Pearl® 500 reactor which is a fluidized bed reactor. HRSD's Nansemond treatment plant anaerobically digests and dewaters waste activated sludge from an EBPR process and the supernatant from dewatering is what supplies the Struvite Recovery Facility (SRF). This nutrient rich influent, labeled centrate, typically has a phosphorus concentration between 200 – 600 mgL^{-1} and a nitrogen ammonia concentration around 430 – 1000 mgL^{-1}. Typically, the influent magnesium concentrations of the centrate do not change immensely throughout time and range from 4 – 29 mgL^{-1}. The centrate pH for the most part is controlled between 6.9 – 6.95 to help limit struvite scale on the feed piping to the SRF. Muriatic acid (HCl) adjustments were manually performed for a large duration of the MgO trial and acid addition eventually became an automated proportional-integrated-derivative (PID) control determined by an online pH probe on the SRF influent. Figure 6 shows the SRF at HRSD Nansemond treatment plant.

Figure 6:HRSD Nansemond Treatment Plant Struvite Recovery Facility (SRF)

HRSD's SRF houses 3 Ostara Pearl 500 reactors and reactor 3 (R3) was designated as the MgO pilot reactor during the MgO trial. Reactor 1 (R1) and reactor 2 (R2) were operated as normal using an $MgCl_2$ and NaOH addition to recover struvite. Included in Figure 6 are the Pearl reactors to the right, and the harvest system to the left, including the dryer and struvite particle silos.

3.2. Magnesium Oxide Pilot Trials

The pilot reactor was operated essentially the same as historically operated, however since MgO provides a source of Mg and alkalinity, NaOH addition was not necessary throughout the trial. The pilot reactor was typically operated under Mg:P molar ratio or pH control, meaning that MgO was dosed as an Mg:P molar ratio or dosed based on effluent pH. Mg:P control utilized the daily reactor loading (kg P/day) as the basis for determining the MgO dosage to the reactor. A Mg:P molar ratio could be targeted and the mass of Mg and MgO required could be solved for by using the stoichiometric conversion between P and Mg and MgO.

$$Mass\ of\ Mg\ (kg\ MgO) = \tag{17}$$
$$P\ Loading\ rate\ \left(\frac{kg\ P}{day}\right)\cdot\left(\frac{kmol\ P}{30.97\ kg}\right)\cdot Mg{:}\,P\ Ratio\ \left(\frac{kmol\ Mg}{kmol\ P}\right)\cdot\left(\frac{24.3\ kg\ Mg}{kmol\ Mg}\right)\cdot\left(\frac{kmol\ Mg}{24.3\ kg}\right)$$
$$\cdot\left(\frac{kmol\ MgO}{kmol\ Mg}\right)\cdot\left(\frac{40.3\ kg}{kmol\ MgO}\right)$$

Effluent pH control was based on conventional Pearl reactor operation and dosed MgO slurry in an Mg:P molar ratio range depending on the deviation of process pH and pH setpoint. MgO was dosed to the reactor as a slurry and the slurry preparation configuration was altered 3 times throughout the trial.

Table 3:MgO Slurry Dosing Configurations

Slurry Configuration	Trial Operation Duration	Description
2018 Trial	June – Nov 2018	Dosed MgO continuously to reactor at a constant Mg:P
2019 Trial	March 2019 – Dec 2019	Dosed MgO intermittently within Mg:P 1:1 – 1.5:1 to maintain pH Setpoint
2020 Trial	April 2020 – Present	Trialed pH control, OP effluent control, and continuous vs. intermittent dosing

The 2.5-year MgO pilot trial contained different MgO slurry dosing configurations, MgO product (Timab M98 and Baymag 30 HP) and control strategies. All trial tests were performed with R3 initially seeded with 90 SGN material, no NaOH addition and a targeted influent centrate pH of 6.9 – 6.95. Table 4 defines each test performed on reactor 3.

Table 4:MgO Pilot Trial Specifications

Test Name, Design Load	**Month; Year**	**MgO**	**Dosing**	**Other Notes**

MgO + Acid, 1X	June 2018	Timab M98	Continuous direct dosing	Mg:P control
MgO, 1X	June–July 2018	Timab M98	Continuous direct dosing	Mg:P control
MgO +Acid, 1X repeat	July–August 2018	Timab M98	Continuous direct dosing	Mg:P control
MgO, 1X repeat	August 2018	Timab M98	Continuous direct dosing	Mg:P control
MgO, 2X	September-October 2018	Timab M98	Continuous direct dosing	Mg:P control
MgO, 3X	October-November 2018	Timab M98	Continuous direct dosing	Mg:P control
$Mg(OH)_2$	December 2018	$Mg(OH)_2$ 60%	Continuous direct dosing	Mg:P control
MgO, 3X	March-April 2019	Baymag 30 HP	Intermittent, recirculation loop	pH Control
MgO, 2X	April-July 2019	Baymag 30 HP	Intermittent, recirculation loop	pH control
MgO, 2X	July-August 2019	Baymag 30 HP and Timab M98	Intermittent, recirculation loop	pH control, Increased Reactor Upflow Velocity
Heated MgO, 2X	September-October 2019	Timab M98	Intermittent, recirculation loop	pH control, MgO heated at 55 °C (131 °F)
Unhydrated MgO, 2X	October 2019	Baymag 30 HP	Intermittent, Eductor	Dosed MgO slurry instantly with an eductor on the recycle line
Heated MgO, 2X Repeat	December 2019	Timab M98	Intermittent, recirculation loop	pH control, MgO heated at 55 °C (131 °F)
Low Hydration MgO, 2X	April-July 2020	Timab M98 and Baymag 30 HP	Intermittent, recirculation loop, batching	Different MgO hydration extents tested
Effluent OP Control, 2X	September 2020	Baymag 30 HP	Intermittent, recirculation loop, batching	30 – 50% hydrated MgO, cascade effluent OP control

3.2.1. 2018 Pilot Trial: Continuous Direct Magnesium Oxide Dosing

The MgO dosing configuration that was used during 2018 MgO trial is depicted attached in Figure 7 and 8. This configuration was referred to as the continuous direct dosing strategy. The 2018 dosing configuration consisted of MgO slurry being dosed continuously

to the reactor from a continuously mixed 330-gallon tank by a peristaltic metering pump. The pilot reactor was operated under Mg:P control during the phase 1 configuration, e.g. a constant MgO addition achieved a specific Mg:P molar dosing ratio in the range of 1.12 – 1.5. Due to the insolubility of MgO, the slurry was assisted from the hose pump to the reactor through the piping with non-potable water (NPW), labeled "carrier water", which is the disinfected treatment plant effluent. The MgO slurry was typically prepared at a 10% m/m in the tote by manually adding MgO bags to NPW. When dosing to the reactor, the slurry was carried by 10 L/min addition of carrier water (NPW) which created a ~1% m/m slurry to be dosed to the reactor continuously. Two 330-gallon tanks were used to alternate slurry feed each day because MgO slurry batches were prepared and mixed continuously 22 – 24 hours in advance. This trial phase was performed with and without sulfuric acid addition to the MgO slurry when the batch was being prepared. Regarding early tests, sulfuric acid (H2SO4) was added to push the hydration reaction by adding hydrogen ions and promoting the dissolution of MgO. Figure 8 exhibits the setup during the 2018 trial testing of MgO for struvite precipitation.

Figure 7:Two 330-gallon Tanks used in the 2018 MgO Pilot Trial

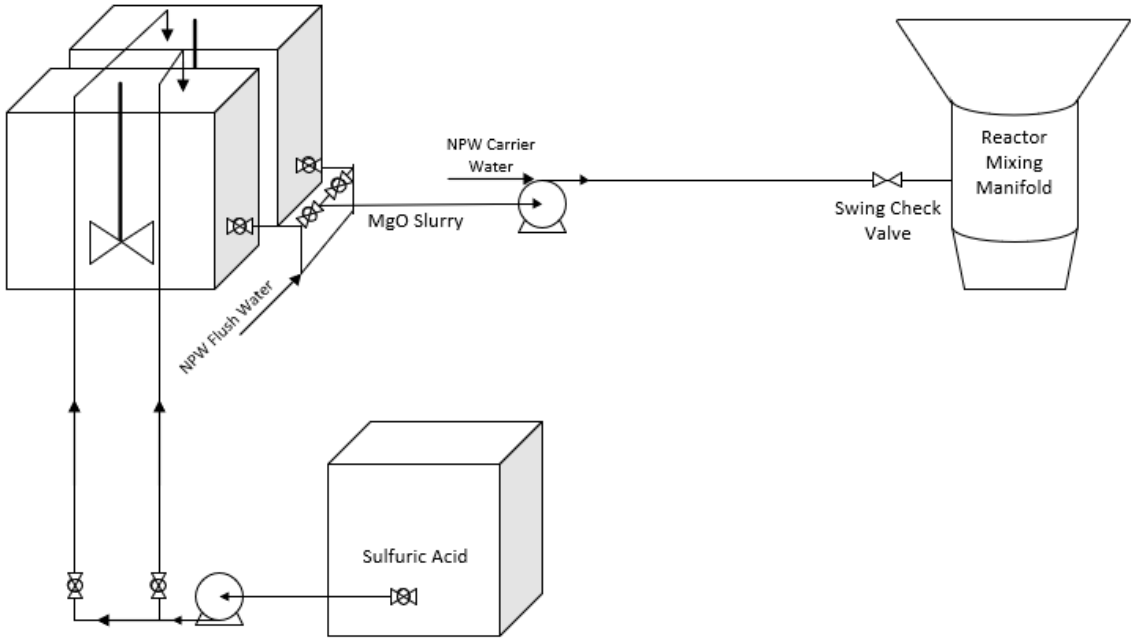

Figure 8:2018 Trial Configuration – Continuous Direct MgO Slurry Dosing Process Flow Diagram (June 2018 – Nov 2018)

This configuration was mainly used when dosing the reactor at its optimal design phosphorus loading rate of 65 kg/day, or 1X loading. 65 kg/day loading rate is the original design capacity of the Pearl® 500 that was previously observed when using $MgCl_2$ to optimally recover struvite, after increasing the loading rate the P removal has the potential to drop below the optimal operation (<70% phosphorus removal). A 1X loading rate can produce 0.5 metric tons (500 kg/day) of struvite each day based on the stoichiometric conversion between phosphorus and struvite.

The design phosphorus loading rate to the reactor was exceeded by 2X (130 kg P/day) and 3X loading (195 kg P/day) for two trial tests using this dosing configuration. Unfortunately, the MgO slurry totes could not hold enough volume to effectively feed previous MgO slurry concentrations to the reactor for 24 hours at 2X loading. The insolubility of MgO and higher slurry concentrations caused many line plugging issues and hose replacements in the hose pump leading to inaccurate Mg:P dosages. Because of these limitations another process flow diagram was proposed by Ostara and installation was completed in March 2019.

3.2.2. 2019 Pilot Trial: Intermittent Magnesium Oxide Dosing

The 2X phosphorus loading rate trials started in March 2019 with a new dosing configuration to determine if MgO addition could effectively yield more fertilizer than MgCl2 addition. Figure 9 depicts the 2019 trial dosing configuration used from March

2019 – January 2020. The idea behind this dosing configuration was to keep MgO suspended and mixing with the use of a centrifugal pump and recirculation loop. This recirculation loop maintained a pressure setpoint with a pressure sensor by manipulating variable-frequency drive (VFD) on the centrifugal pump motor output. An automated pinch valve was incorporated after the recirculation loop in order to dose a specific amount MgO intermittently to the reactor to within 1:1 – 1.5:1 Mg:P based on a PID loop controlled by the effluent pH. As the MgO provided alkalinity addition to the pilot reactor, the MgO has a direct effect on the effluent pH. The automated pinch valve was programmed to normally be closed and open fully for 1 second at an inputted frequency that corresponded with a minimum time necessary for a 1:1 Mg:P and a maximum time necessary for a 1.5:1 Mg:P. After the MgO pinch valve dosed and closed the flushing water valve would open and clean the line of any MgO for an inputted duration of time (seconds). This dosing strategy was referred to as intermittent recirculation loop dosing strategy and represents a typical full-scale system. The larger tank allowed higher loading rates to be tested without running out of MgO slurry and the recirculation loop and centrifugal pump configuration eliminated the consistent line plugging seen in 2018 trial configuration. The recirculation loop easily allowed the slurry to stay suspended even with higher slurry concentration (% MgO m/m). A submersible heater was also flanged into the side of the tote in September 2019 to provide heat to the slurry and promote MgO hydration while mixing. Figure 10 shows the dosing system. A pinch valve where the recirculation loop enters the tote to provide back pressure to the recirculation loop and relieve to the centrifugal pump. This dosing system was successful at preventing line plugging and keeping the MgO in suspension due to the pressure of the recirculation loop and intermittent dosing at higher and more reliable flow rates. However, this configuration did not allow for every test that was later considered in late 2019 and 2020.

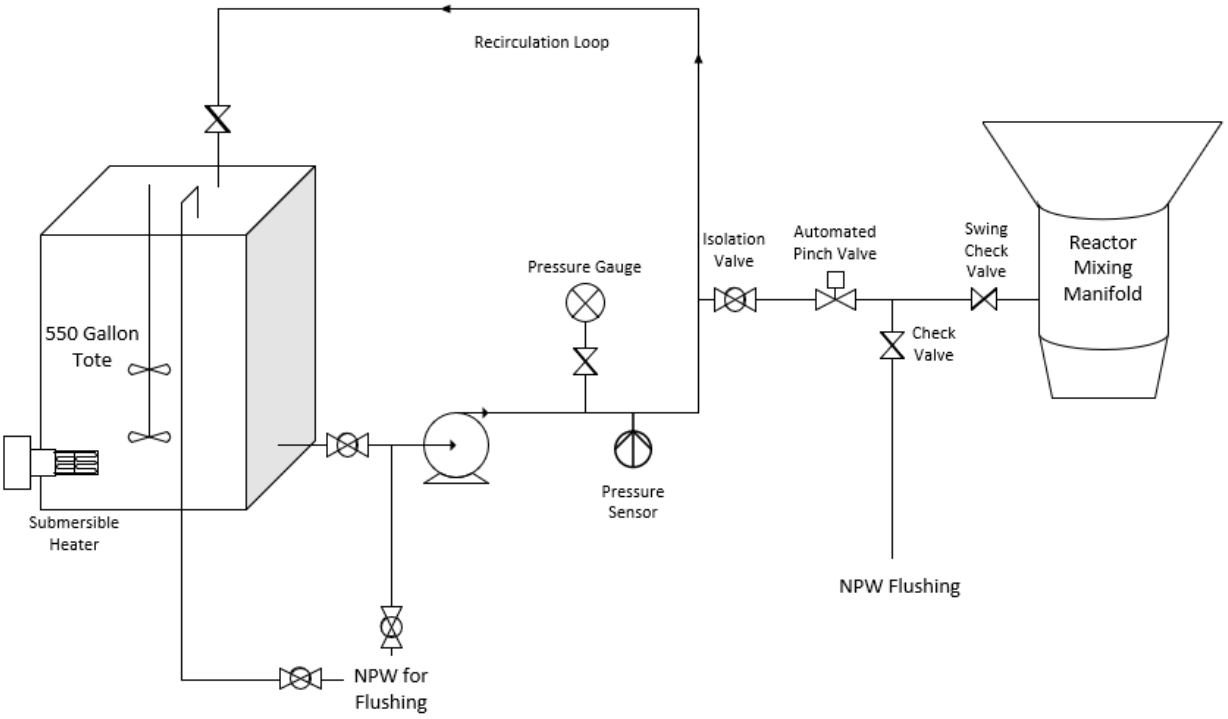

Figure 9:2019 Trial Configuration – Intermittent Recirculation Loop MgO Slurry Dosing Process Flow Diagram (March 2019 – January 2020)

Figure 10:Intermittent Slurry Dosing Configuration

With the hydration of MgO better understood, it became of interest to test the effect of low hydration extent of MgO for struvite precipitation.

3.2.3. 2020 Pilot Trial: Automated Batching Process

It was essential to know if optimal reactor operation could only be achieved when utilizing MgO exceeding a certain hydration extent. Low hydration testing could solidify necessary slurry retention times corresponding to certain hydration extent ranges and determine tank volumes required for full-scale implementation. If substantial hydration was not necessary for optimal operation than the slurry would not need to be retained in a tank for an extended period of time and the tank volume could be smaller. Other modes of control were also of interest, such as effluent ortho-phosphate concentration control and continuous dosing repeated with the improved dosing configuration.

Figure 11 and 12 shows the pipe flow diagram for the phase 3 slurry dosing configuration. Before phase 3 dosing strategy was constructed, an unsuccessful low hydration test took place by piping an eductor (venturi) to the suction side of the recycle pump of reactor 3 and intermittently dosing MgO slurry to the reactor. Due to the MgO being introduced

outside of the injection port, optimal reactor operation was not achieved, and this configuration was discontinued after 4 weeks and consequently phase 3 was implemented.

The 2020 trial dosing configuration included an automated batching process that maintained the slurry volume in the 60-gallon tote between a high level and low level. The batching process was performed using an eductor providing NPW as the driving fluid on the inlet side and MgO from the hopper on the suction side. The desired MgO slurry was premixed using the eductor and dosed to the slurry tote. The control system batched an appropriate volume of NPW and MgO to achieve the inputted MgO m/m slurry each time a low level was measured by the level indicator on the slurry tote. After the slurry was batched to the tote the dosing configuration was setup essentially the same as the previous design with a recirculation loop pressurized to a pressure setpoint by the VFD on the centrifugal pump motor. The automated pinch valve off the recirculation loop was used for intermittent MgO dosing. Intermittent dosing used the valve fully open for 1 second with the opening frequency input manipulated to achieve a 1:1 – 1.5:1 Mg:P dosing range and utilizing PID control based on effluent pH or OP to determine the molar ratio. A "maximum time (seconds) between opening" was inputted to achieve a minimum Mg:P (1:1) dosing and a "minimum time (seconds) between opening" was inputted to achieve a maximum Mg:P (1.5:1) dosing. The 2020 dosing configuration was relatively multifaceted in that it could operate under different control strategies e.g. pH control, OP removal control, Mg:P control, intermittent or continuous dosing. Continuous dosing could be performed by manually setting the automated pinch valve % open position and measuring the tote drawdown over a given time range to ensure dosing was at a flow rate necessary to meet a desired Mg:P dose. Figure 12 exhibits the automated batching configuration that was completed in April 2020.

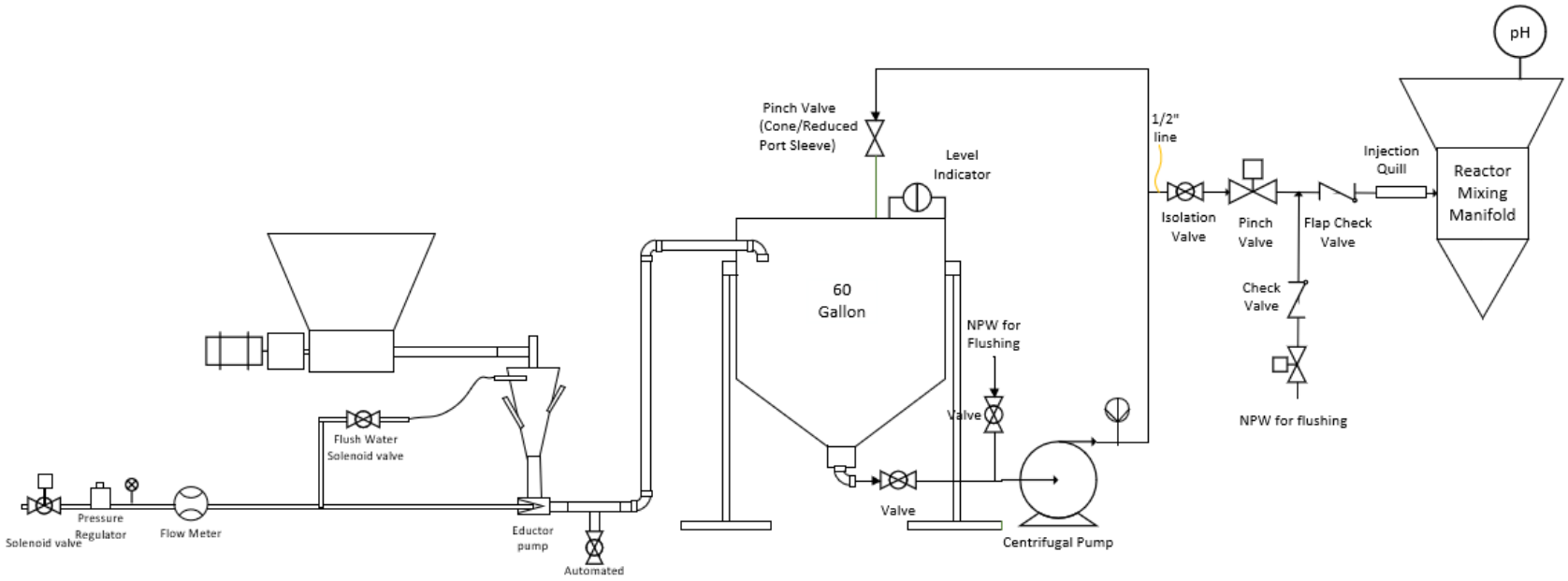

Figure 11:2020 Trial Configuration – Automated Batching Intermittent MgO Slurry Dosing Process Flow Diagram

Figure 12:Automated Batching Configuration containing (from right to left) an MgO dry hopper, eductor cone, and recirculation loop for intermittent MgO slurry dosing

3.3. Reactor Operation

Reactors 1 and 2 were operated as previously described, utilizing $MgCl_2$ and NaOH addition for pH control in the FBR. The pilot was performed on a full-scale Ostara Pearl® 500 reactor. Throughout the trial, reactor 3 (R3) was operated relatively the same as Ostara Pearl reactors are typically operated. The only deviation from typical operation was R3 did not have NaOH added for pH control because MgO provided enough alkalinity for optimal operation and the MgO product required slight pretreatment before being dosed to the reactor. A trial test was defined as a time duration of at least 3 weeks where the reactor operation remains relatively constant in order to understand how given operating parameters affected process efficiency and if MgO caused significant adjustments to daily operation. A test began after initial seeding with existing bagged material, typically 90 SGN, and then began treating influent centrate. Daily samples and analysis were performed on the pilot reactor to monitor performance. Reactor 1 and 2 were also monitored every other day when running continuously. This section discusses methods used for monitoring all reactor operation.

The operation of reactor 3 was typically done to achieve a specific Mg:P. The Mg:P dosing was performed continuously at a constant Mg:P and intermittently within a specified Mg:P range. The amount of MgO dosed to the reactor was determined by the following formula.

$$\boldsymbol{MgO\ Dosage\ Volume}\left(\frac{\boldsymbol{L}}{\boldsymbol{min}}\right) = \tag{18}$$

$$\frac{P\ Loading\ rate\left(\frac{kg}{day}\right)\cdot\left(\frac{day}{1440\ min}\right)\cdot\left(\frac{kmol\ P}{30.97\ kg}\right)\cdot Mg{:}P\ Ratio\left(\frac{kmol\ Mg}{kmol\ P}\right)\cdot\left(\frac{kmol\ Mgo}{kmol\ Mg}\right)\cdot\left(\frac{40.3\ kg}{kmol\ MgO}\right)}{MgO\ slurry\ density\left(\frac{kg}{L}\right)\cdot slurry\ conc.\left(\frac{mass\ MgO}{mass\ slurry}\right)\cdot MgO\ purity\left(\frac{mass\ MgO}{mass\ product}\right)}$$

The MgO slurry density varies depending on slurry concentration (%MgO m/m) used to dose the reactor. The formula used for slurry density determination is below where the density (ρ) of MgO is 3.58 kg/L and the ρ of water is 1 kg/L.

$$\boldsymbol{Slurry\ \rho\left(\frac{kg}{L}\right)} = \left(\frac{MgO\ slurry\ conc\left(\frac{m}{m}\right)}{MgO\ \rho\left(\frac{kg}{L}\right)} + \frac{1-MgO\ slurry\ conc\left(\frac{m}{m}\right)}{Water\ \rho\left(\frac{kg}{L}\right)}\right)^{-1} \quad (19)$$

Slurry concentration calculations and dry feeder motor calibration curves used for slurry batch makeups are further defined in the Appendix (Supplemental Information). Influent and effluent phosphorus concentrations were typically measured each weekday to determine the reactor operation. Influent phosphorus concentration was inputted into the control system to alter the centrate feed flow to the reactor and maintain the specified phosphorus loading rate. Magnesium was also measured each weekday on the influent and the effluent to help monitor the system and verify Mg dosing to the reactor was adequate. Table 5 defines the laboratory methods used to measure constituent ion concentrations and other parameters of interest during operation. Hach dr2800 and dr3900 spectrophotometers were used for Hach tube daily analysis.

Table 5:Daily Reactor Operation Laboratory Analysis

Parameter	**Method**
Ortho Phosphate	Hach TNT 845, Ascorbic Acid
Total Phosphorus	Hach TNT 845, Ascorbic Acid
Magnesium	Hach TNT 849, Metal phthalein
pH	. Orion Star pH Meter

Total phosphorus (TP) concentrations were quantified as PO_4-P present in solution and in solid material after digesting the samples in a Hach digestion block at 100 °C. Magnesium measured using Hach tubes and the spectrophotometer only captured the soluble form. The Central Enviromental Laboratory (CEL) at HRSD also analyzed samples from the SRF influent and effluent on Tuesday, Thursday and Sunday each week. The results from the CEL are inputted into HRSD process operation reports and PARCView PRISM which is a real-time data visualization program used for the SRF. Tests that were performed at the CEL are specified in table 6.

Table 6: HRSD CEL SRF Sample Analysis

Parameter	Method
Total Magnesium	ICP-AES (EPA 200.7 rev 4.4)
Soluble Magnesium	Filtering w/ ICP-AES (EPA 200.7 rev 4.4)
Total Phosphorus	Auto Analyzer Flow Injection Analysis (Lachat 10-115-01-1-E)
Ortho Phosphorus	Flow Injection Analysis
Total Ammonia	Auto Analyzer Flow Injection Analysis (Lachat 10-107-06-1-J)
Total Alkalinity	Auto Analyzer Flow Injection Analysis

Daily influent and reactor effluent analysis performed with Hach tubes were used to monitor the daily efficiency of the pilot process. Struvite precipitation efficiency is determined by how much phosphorus is removed from the system and recovered as struvite. Phosphorus removal is important when monitoring the struvite precipitation real-time as it can infer how well influent centrate is being treated for phosphorus and how much struvite is being produced in the reactor.

$$\boldsymbol{Phosphorus\ Removal}\ (\%) = \left(\frac{Influent\ Phopshorus\left(\frac{mg\ PO4-P}{L}\right) - Effluent\ Phosphorus\ \left(\frac{mg\ PO4-P}{L}\right)}{Initial\ Phosphorus\ \left(\frac{mg\ PO4-P}{L}\right)}\right) \times 100 \quad (20)$$

This equation assumes pure struvite has been precipitated in the system and phosphorus is either recovered as struvite or released from the system as soluble phosphorus or small struvite fines in the effluent. This assumption is reasonable as the pH is not intentionally operated above a pH of 8.2 where other solid P-containing impurities can start precipitating. Phosphorus removal can be calculated for OP or TP removal. OP removal is measured to quantify the soluble phosphorus removed from the centrate and TP removal measured the soluble and particulate phosphorus removed from the centrate. TP removal can quantify how well fines are being contained within the reactor. Whatever is washed out of the reactor as soluble phosphorus or struvite fines will return to the head of the wastewater treatment plant. Struvite precipitation was also monitored by defining a theoretical struvite recovery that could be achieved based on the known amount of phosphorus load into the system throughout time:

$$\boldsymbol{Theoretical\ PO_4 - P\ Recovery\ as\ Struvite}\ (\boldsymbol{g\ PO_4 - P}) = \quad (21)$$

$$PO_4 - P\ Mass\ Load\ (g\ PO_4 - P) \cdot \left(\frac{245.41\ g\ Struvite}{mol\ Struvite}\right)\left(\frac{mol\ Struvite}{mol\ PO_4 - P}\right)\left(\frac{mol\ PO_4 - P}{30.97\ g\ PO_4 - P}\right)$$

$$\boldsymbol{Struvite\ Recovery\ (Yield)}\ (\%) = \frac{Total\ Weight\ of\ Struvite\ Harvested\ (kg)}{Theoretical\ PO_4 - P\ Recovery\ as\ Struvite\ (kg)} \times 100 \quad (22)$$

This mass balance calculation is used to determine the yield, or theoretical struvite production based on total influent phosphorus mass and compare to the amount of struvite that was physically harvested from the system (Adnan, A., et al. II, 2003). Fines wash out during operation can diminish the recovered struvite mass and cause deviation from the theoretical recovery, create an inefficient process and affect downstream infrastructure and plant treatment.

Imhoff cones were taken when reactors were sampled to measure the settled solid volume and quantify the centrate solids in the system and/or fines washout that was occurring. The pilot reactor also has a turbidity meter at the top of the reactor in the clarifier launder to qualitatively monitor performance and compare TP removal to the turbidity measured in real-time.

3.3.1. Reactor Operation: Harvesting

Struvite was initially harvested from the pilot at the beginning of a trial after 3-4 days of efficient operation and as the differential pressure in the reactor (dP) measured around 7.0 kPa. After the initial harvest, 1 ton of struvite was harvested every other day or every day to control the reactor inventory and limit fines accumulating and settling on the side walls of the clarifier, referred to as beaching. The amount of struvite beaching settled in the clarifier was estimated throughout the trials after it was initially noticed above the clarifier surface in December 2018 and became a frequent occurrence in the Summer of 2019. Occasionally, fines were pushed back down into the reactor to fluidize the material.

Struvite was harvested by dewatering the product on a vibrating sieve screen to separate the struvite from the liquid and sending the dewatered product through a hot-air fluidized bed dryer. Once the material was dried it was classified by sieve screens and stored in the respective product size silo. Dried struvite was manually sieved to determine the average size being harvested from the reactor in SGN (Size Guide Number). The dryer was limited on the product size that could effectively be dried and when product was too small it would be manually pulled out of the reactor harvest leg, which is known as wet harvesting. Wet harvest supersacks were dried for at least 2 weeks on plant site before being sent off site for additional refining. Quality control samples were taken of supersack from wet harvest or from the silo bagging system for nutrient analysis to ensure that the bagged struvite had an acceptable purity. XRD analysis was also performed on specified QC samples and grab samples from the pilot during different trials to determine if there were any distinguishable impurities.

Once a pilot test was finished, the reactor was emptied of all leftover material by wet harvesting. Typically, the reactor would need to be cleaned every 3 months or after 3 pilot tests. Cleaning the reactor consisted of capturing the struvite product, draining the remaining liquid, inspecting the upper clarifier and lower injection port area, removing the recycle line below the injection port, removing scale, and then acid washing the reactor once reassembled. Scale build up would occur in the lower reactor early in the trial and

scaling seemed to shift to the upper portion of the reactor in late 2019. Thicker scale would be in the lower portion of the reactor and was better removed by chipping away fragments.

3.4. Magnesium Oxide

Two different MgO products were used throughout the duration of the full-scale pilot test. These MgO products were Timab M98 MgO and Baymag 30 HP (Baymag) MgO. Both MgO products are high purity, reactive caustic MgO. Timab MX95, MX97 and AK98 are three other MgO products that were used during bench-scale jar testing. MgO product purities and specifications are provided in the table below.

Table 7:MgO Product Specifications from Manufacturer

MgO Product	Purity (%)	Size	Reactivity	Specific Surface Area (m^2/g)
Baymag 30 HP	**96.5**	**96% < 75 µm**	**–**	**30**
Timab M98	**97**	**min. 77% < 75 µm**	**–**	**15 – 35**
Timab MX95	**95.6**	**90% < 75 µm**	**30 – 40 seconds in Acetic Acid**	**–**
Timab MX97	**97**	**90% < 75 µm**	**30 – 40 seconds in Acetic Acid**	**–**
Timab AK98	**98**	**98% < 45 µm**	**20 – 30 seconds in Citric Acid**	**50 – 70**

Based on the information provided from manufacturer product specification sheets, it is known that Baymag is a smaller particle with a more constant specific surface area and Timab M98 has greater portion of larger material and a large range of specific surface areas to be expected. The purity of Baymag and Timab M98 are relatively similar and no information was provided by the manufacturer regarding reactivity. As for the other Timab material used in jar tests Timab AK98 (AK98) has the highest reactivity, purity and majority of the material smaller than 45 µm. Timab MX95 and MX97 are similar and only vary in the purity of the product based on available data. Conventionally, MgO activity time is measured when neutralizing acid of 1M concentration, however, the manufacturers did not specifiy the acid concentration.

3.5. Magnesium Oxide Activity

The magnesium oxide activity was determined in this study to understand the reactivity of the products relative to each other. This test was done by neutralizing 1 M acetic acid with 5.0 g of MgO. The 1 M acetic acid was prepared from glacial acetic acid stock solution and deionized water. Typically, 7 drops (350 uL) of phenolphthalein indicator were added to the acetic acid to allow for a visible color change. An Orion Star pH probe was placed into solution to measure the pH throughout the reaction. The reaction was conducted on a stir plate set at 600 rpm to ensure the MgO could properly mix in suspension with the acetic acid. A timer was started as

the MgO sample entered the acid solution and continued until the solution color changed to pink and a pH value around 8.2 was observed. This test was performed for 6 different products of MgO to understand their relative reactivities. The MgO products that were tested are listed in the Table 8 below:

Table 8:MgO Product for Activity Analysis

MgO Products
Baymag-30
Timab M98
Timab MX95
Timab MX97
Timab AK98
Feed Grade Baymag (un-milled)

3.6. Magnesium Oxide Hydration

The quantitative measurement of MgO conversion or MgO hydration extent can be determined as a variation of solid weight (Smithson, G.L. and Bakhshi, N.N. 1969; Birchal, V.S.S., et al. 2000; Tang, X., et al. 2014; Castro, S.R., et al. 2015). The MgO hydration extent represents how much of the initial MgO is converted to $Mg(OH)_2$. The methodology used in this paper was based off literature and MgO manufacturer procedures. A sample is grabbed from a hydrating MgO slurry, which in this work was typically a volume of 20 mL or greater. The sample is then filtered through a glass fiber filter (1.5 µm nominal diameter) using a vacuum pump to remove the water from the sample. The sample is then washed with at least a 10 mL volume of acetone as it remains filtering with the vacuum pump. A tared porcelain crucible is used to dry the solid sample for at least a day in an oven heated to about 105 °C. After drying the sample, it is cooled in a crucible and the dry aliquot mass (m_d) is recorded. The sample is then heated in muffle furnace as 600 °C for 2 hours (Tang, X., et al. 2014). The heated aliquot mass (m_h) can then be recorded. The values for m_d and m_h can be inputted into the following formula to determine hydration extent.

$$Hydration\ Extent\ (\%) = \frac{m_d - m_h}{m_h} \times \frac{M_{MgO}}{M_{H_2O}} \times \frac{100}{purity} \quad (23)$$

The molecular weight of MgO, M_{MgO}, is 40.3 g/mol and the molecular weight of water, M_{H2O}, is 18.1 g/mol. The hydration extent can also be normalized by the purity of the MgO that is being used, which is a fraction of the product that is purely MgO. There are some metal oxide impurities that can remain in the product after calcination and are reported by the manufacturer. Typical MgO purities used in this study have been between 0.95 – 0.98 mass MgO/mass product. Hydration measurements were taken through time of each milled MgO product listed in Table 8 at bench scale. Hydration extents of Timab (M98) and Baymag were also performed in both full-scale MgO dosing systems.

4. Manuscript 1: Effect of Magnesium Oxide Properties on Struvite Precipitation

4.1. Abstract

Magnesium oxide (MgO) can be produced from magnesite calcination ($MgCO_3$). Different calcination conditions can provide MgO product of various quality and characteristics. Hydration of MgO used during full-scale operation was investigated. As it was determined material being dosed to the full-scale Ostara Pearl 500 reactor was predominantly hydrated, converted to magnesium hydroxide ($Mg(OH)_2$), it became of interest to test lower hydration extent ranges effect on struvite precipitation. Through jar testing, the effect of MgO product quality on struvite precipitation was investigated. Various MgO products of different reactivities and hydrations extents were used during jar tests for struvite precipitation from anaerobically digested supernatant (centrate). The MgO product quality effect on solution saturation index and phosphorus (P) removal through time could reason that MgO properties can impact struvite precipitation kinetics and possibly equate jar testing results to the full-scale pilot reactor operation. On-site jar testing analysis showed that the more reactive (lower activity time) products were able to achieve higher OP removal (%) within 45 and 150-minute jar tests. Utilizing the hydrated MgO slurries did show higher OP removal (%) than the unhydrated MgO slurries (mixed for 1-2 minutes) when adding to centrate. Jar testing samples gathered to understand how each MgO product of different reactivities and hydration extents affects saturation index and total P removal (%) of filtered and preserved samples through time. The most reactive MgO showed fast P removal and depletion of the solution saturation index (approaching 0 saturation index where struvite precipitation is not favored). MgO of lower reactivity showed steady P removal and depletion of saturation index. It is hypothesized that behavior of lower reactive MgO may exhibit the ability of MgO to provide a magnesium ion (Mg^{2+}) reserve to the struvite precipitation and infers the same for full-scale operation.

4.2. Introduction and Background

It is hypothesized here that a more accessible and naturally abundant Mg compound can decrease struvite recovery operational costs and create an attractive phosphorus recovery method. MgO is a naturally occurring mineral and can also be created from the calcination of magnesite (Birchal, V.S.S., et al. 2000). Calcination is defined as the thermal treatment of ores causing a release of carbon dioxide. In addition, the treatment can also remove impurities and moisture. Depending on calcination conditions and previous magnesite quality, MgO can vary in particle size, reactivity, and porosity (Birchal, V.S.S., et al. 2000). MgO can undergo a hydration/dissolution (commonly known as slaking) reaction with water to produce magnesium hydroxide ($Mg(OH)_2$) (Kiani, D. et al. 2018). This hydration reaction of MgO to $Mg(OH)_2$ is strongly influenced by the physical properties of MgO which are determined by the calcination conditions of magnesite (Birchal, V.S., et al. 2001). The method of adding MgO into the struvite precipitation process has been shown to affect process operation and

optimization. The solid nature of MgO is hypothesized to provide a Mg2+ reserve attributed to the MgO dissolution during hydration. The variability of MgO product quality and hydration reaction along with the observed successful struvite precipitation and cost effectiveness all represent good reasoning for further investigating MgO.

It has been defined in literature that the limiting step of MgO hydration is the dissolution of MgO into solution (Birchal, V.S.S., et al. 2000; Rocha, S.D.F., et al., 2004; Stolzenburg, P., et al. 2015). It is also thought that the reactivity of the MgO product can infer how the MgO will hydrate when in solution. Typically, the reactivity of MgO product is measured in terms of activity, or the time required to neutralize an acid. The shorter the activity time, the more reactive the MgO product (Birchal, V.S.S., et al. 2000). Relating the MgO reactivity and hydration with struvite precipitation kinetics was also of interest.

Nucleation and crystal growth kinetics of struvite are dependent on the supersaturation of solution. It has been observed that the most basic orthorhombic struvite morphology is present at lower supersaturation conditions. As the supersaturation is increased over the value of 3 by increasing struvite constituent ion concentrations or the pH, the crystal tends to change to a hopper, or butterfly, crystal morphology. Increasing the pH can elongate the crystal and increasing the ammonium concentration can trigger sharp faces on the crystal to form. Dendritic crystals begin to form when supersaturation is increased above a value of 5 and the branching of the crystals amplify as ammonium concentrations are increased (Shaddel, S., et al. 2019).

Results from Stolzenburg, P., et al. (2015) study show that MgO slurry is an effective reagent for precipitating struvite and can achieve better results than that of $MgCl_2$ addition at all corresponding Mg:P dosages tested. MgO addition at an Mg:P of 1 achieved >90% recovery of phosphorus while $MgCl_2$ addition at an Mg:P of 1 achieved around 85% . This study also shows that while MgO addition caused struvite particles to be smaller than $MgCl_2$ addition for struvite precipitation, particles did increase in size as the Mg:P was decreased. The dissolution of the $Mg(OH)_2$ surface layer is encouraged by the solution's initial low pH and high phosphorus concentration that can increase the MgO solubility and allow for formation of magnesium and phosphate ion pairs. This rapid dissolution of the $Mg(OH)_2$ surface layer is postulated to cause high initial supersaturation in solution, especially near the MgO particle (Stolzenburg, P. et al. 2015).

The variability of MgO product quality and MgO reactivity with various product manufacturers was of interest with as the effect that these differences had on struvite precipitation was unidentified. The two products used at full-scale, Timab M98 and Baymag 30 HP, were investigated as well as 3 other Timab products used during bench-scale jar tests, Timab MX95, Timab MX97 and Timab AK98. Testing of these MgO products for struvite precipitation were done with MgO slurry dosed to centrate and monitored for a specific time duration.

In the summer of 2019, it was determined that the MgO being dosed to the reactor was at a high hydration extent for much of the trial. Low hydration was predominantly observed during the initial slurry batch makeup when a test was started. The MgO was able to hydrate to a high extent due to the continuous mixing of the slurry and the size of the slurry tank used to ensure a 24-hour supply. Hypotheses developed around the manipulation of the hydration extent to understand the effect it could have on the subsequent struvite precipitation reaction. The effect on MgO reactivity and hydration extent was tested on the full-scale pilot reactor as well as in jar tests on bench-scale.

At bench-scale, it was thought that dosing MgO of different reactivity and hydration extent to centrate could further optimize the precipitation of struvite when using MgO. Saturation indices were measured to understand how struvite kinetics may be impacted by different MgO products. Saturation index in terms of ion activity product is calculated by:

$$SI = \log_{10}\left(\frac{IAP}{K_{SP}}\right) = \log_{10}\left(\frac{\gamma Mg^{2+}[Mg^{2+}]\cdot\gamma NH_4^{+}[NH_4^{+}]\cdot\gamma PO_4^{3-}[PO_4^{3-}]}{K_{SP}}\right) \quad (24)$$

During the 2020 MgO trial, the updated slurry dosing configuration allowed for testing of variable MgO hydration extents to occur. The two MgO products available for full-scale testing were both used at lower hydration extents to observe any differences in reactor operation and performance caused by different product reactivities and/or hydration extents.

4.3. Materials and Methodology

4.3.1. Magnesium Oxide

Five different MgO products were used during various bench-scale jar tests. These MgO products were Timab M98 MgO and Baymag 30 HP (Baymag) MgO. Both MgO products are high purity, reactive caustic MgO. Timab MX95, MX97 and AK98 are three other MgO products that were used during bench-scale jar testing. MgO product purities and specifications are provided in the Table 9 below.

Table 9: MgO Product Specifications from Manufacturer

MgO Product	Purity (%)	Size	Reactivity	Specific Surface Area (m^2/g)
Baymag 30 HP	**96.5**	**96% < 75 µm**	**–**	**30**
Timab M98	**97**	**min. 77% < 75 µm**	**–**	**15 – 35**
Timab MX95	**95.6**	**90% < 75 µm**	**30 – 40 seconds in Acetic Acid**	**–**
Timab MX97	**97**	**90% < 75 µm**	**30 – 40 seconds in Acetic Acid**	**–**
Timab AK98	**98**	**98% < 45 µm**	**20 – 30 seconds in Citric Acid**	**50 – 70**

Based on the information provided from manufacturer product specification sheets, it is known that Baymag is a smaller particle with a more constant specific surface area and Timab M98 has greater portion of larger material and a large range of specific surface areas to be expected. The purity of Baymag and Timab M98 are relatively similar and no information was provided by the manufacturer regarding reactivity. As for the other Timab material used in jar tests Timab AK98 (AK98) has the highest reactivity, purity and majority of the material smaller than 45 μm. Reactivity is reported in the terms of activity time required to neutralize an acid. Conventionally, these tests are done with acid of 1M concentration, however the manufacturer did not specify acid concentration. Timab MX95 and MX97 are similar and only vary in the purity of the product based on available data.

4.3.2. Magnesium Oxide Activity

The activity of magnesium oxide is determined operationally using time-based measurement that can indicate how reactive an MgO product is relative to other MgO product activity values. An activity test is the time required for MgO to neutralize an acid– acetic acid or citric acid activity tests are common (Birchal, V.S.S, et al. 2000, Tang, X., et al. 2014). Highly reactive/light-burned MgO have activities < 60 seconds, medium reactivity is represented by an activity value between 180 – 300 seconds and low reactivity/hard-burned have activities > 600 seconds (Romero-Güiza, M.S., et al. 2015). The larger the activity, the less reactive an MgO product is (Birchal, V.S.S., et al. 2000). As the calcination temperature decreases the specific surface area increases and activity time decreases which indicates that an MgO product with a larger specific surface area is more reactive (Birchal, V.S.S., et al. 2000). An activity test can provide information about the MgO product production, quality, how it compares to other MgO products and possibly how it hydrates from MgO to $Mg(OH)_2$. In terms of utilizing MgO for struvite precipitation, it is important to understand the reactivity of a slightly soluble Mg product, such as MgO, as it influences the efficiency of phosphorus removal in the system (Salutsky, M.L., et al. 1972).

4.3.3. Magnesium Oxide Slurry Preparation

A specific slurry concentration (MgO % m/m) was prepared by determining the necessary MgO mass to add to a specified volume of NPW. The mass of MgO product was solved for by using the following equations:

$$\boldsymbol{Total\ Slurry\ Mass\ (kg)} = \frac{Volume\ of\ NPW\,(L)\cdot\left(\frac{1000\ kg}{m^3}\right)\cdot\left(\frac{m^3}{1000\ L}\right)}{\left(1-MgO\ Slurry\ Conc\ \left(\frac{m\ MgO}{m\ slurry}\right)\right)} \tag{25}$$

$$\boldsymbol{Mass\ MgO\ (kg)} = Slurry\ Conc\ \left(\frac{m\ MgO}{m\ slurry}\right)\cdot Total\ Slurry\ Mass\ (kg) \tag{26}$$

Once the slurry was made, it was mixed on a stir plate/overhead impeller between 350-500 rpm to keep MgO in suspension. A piece of parafilm was secured on top of the Erlenmeyer flask to prevent evaporation from the exothermic hydration reaction.

4.3.4. Magnesium Oxide Hydration

The quantitative measurement of MgO conversion or MgO hydration extent was determined as a variation of solid weight (Smithson, G.L. and Bakhshi, N.N. 1969; Birchal, V.S.S., et al. 2000; Tang, X., et al. 2014; Castro, S.R., et al. 2015). The methodology used was based off literature and MgO manufacturer procedures. A sample is grabbed from a hydrating MgO slurry, which in this work was typically a volume of 20 mL or greater. The sample is then filtered through a glass fiber filter (1.5 μm nominal diameter) using a vacuum pump to remove the water from the sample. The sample is then washed with at least a 10 mL volume of acetone as it remains filtering with the vacuum pump. A tared porcelain crucible is used to dry the solid sample for at least a day in an oven heated to about 105 °C. After drying the sample, it is cooled in a crucible and the dry aliquot mass (m_d) is recorded. The sample is then heated in muffle furnace as 600 °C for 2 hours (Tang, X., et al. 2014). The heated aliquot mass (m_h) can then be recorded. The values for md and m_h can be inputted into the following formula to determine hydration extent.

$$Hydration\ Extent\ (\%) = \frac{m_d - m_h}{m_h} \times \frac{M_{MgO}}{M_{H_2O}} \times \frac{100}{purity} \quad (27)$$

The molecular weight of MgO, M_{MgO}, is 40.3 g/mol and the molecular weight of water, M_{H2O}, is 18.1 g/mol. The hydration extent can also be normalized by the purity of the MgO that is being used, which is a fraction of the product that is purely MgO. There are some metal oxide impurities that can remain in the product after calcination and are reported by the manufacturer. Typical MgO purities used in this study have been between 0.95 – 0.98 mass MgO/mass product.

4.3.5. Magnesium Oxide Slurry Analysis

The slurry temperature, viscosity, and specific gravity were measured at times to understand how hydration extent effected affected these other slurry qualities. The slurry temperature was measured with a Digi-Sense resistance temperature detector (RTD). The probe was submersed in the slurry and the temperature was recorded once the reading was stable. Slurry viscosity was determined by using an Elcometer Zahn 1 cup. A stopwatch was started once the slurry sample was collected in the Zahn cup and the orifice on the bottom of the cup was removed from the slurry. The stopwatch was stopped once a continuous stream of slurry from the small orifice stopped and the slurry began to drip from the orifice. Specific gravity was measured by using a hydrometer. Prior to taking the specific gravity and viscosity measurements it was ensured that the slurry was well mixed, especially when adding to a graduated cylinder to use the hydrometer. These measurements were done throughout time as hydration extent samples were taken.

4.3.6. MgO Slurry Dosing for Jar Testing

Struvite precipitation jar tests were performed under specific Mg:P. To achieve a desired Mg:P it was necessary to measure the centrate OP concentration and dose MgO slurry appropriately. The equations below define the necessary steps to dose a targeted Mg:P. The MgO mass and slurry volume was calculated once the mass of phosphorus was solved for. Equations

$$\boldsymbol{Mass\ of\ P\ (g\ P)} = \tag{28}$$

$$Measured\ P\ Conc\left(\frac{mg\ PO4-P}{L}\right)\cdot Volume\ of\ Jar\cdot\left(\frac{g}{1000\ mg}\right)$$

$$\boldsymbol{Mass\ of\ MgO\ (g\ MgO)} = \tag{29}$$

$$Mass\ of\ P\ (g\ P)\cdot\left(\frac{1\ mol\ P}{30.97\ g}\right)\cdot Mg{:}P\ ratio\left(\frac{mol\ Mg}{mol\ P}\right)\cdot\left(\frac{mol\ MgO}{mol\ Mg}\right)\cdot\left(\frac{40.3\ g\ MgO}{mol\ MgO}\right)$$

$$\boldsymbol{MgO\ Slurry\ Volume\ (mL)} = \frac{Mass\ of\ MgO\ (g\ MgO)}{slurry\ \rho\left(\frac{kg}{L}\right)\cdot slurry\ conc\left(\frac{m}{m}\right)\cdot MgO\ Purity\left(\frac{m}{m}\right)} \tag{30}$$

The slurry volume varied based on slurry concentration (MgO % m/m) and can be calculated using the following equation where ρ is density:

$$\boldsymbol{Slurry\ \rho\left(\frac{kg}{L}\right)} = \left(\frac{MgO\ slurry\ conc\left(\frac{m}{m}\right)}{MgO\ \rho\left(\frac{kg}{L}\right)} + \frac{1-MgO\ slurry\ conc\left(\frac{m}{m}\right)}{Water\ \rho\left(\frac{kg}{L}\right)}\right)^{-1} \tag{31}$$

4.3.7. Struvite Precipitation Jar Testing and On-site Analysis

Struvite precipitation jar tests were performed with a Phipps & Bird 6-paddle jar tester. Jars were used as stirred tank reactors to observe struvite precipitation when dosing MgO slurry to centrate. MgO slurry was hydrated to various extents. Jars were initially filled with 2 liters of centrate, mixed at 100 rpm, and dosed with the appropriate volume of MgO slurry to achieve a desired Mg:P (typically 1:1).

Table 10: Centrate Analysis Performed for Jar Testing

Analysis	Method
Initial pH	Orion Star pH meter, Portable Milwaukee pH meter
Ortho-phosphorus (mg PO_4-P/L)	Hach TNT 845, Ascorbic Acid Method
Soluble Magnesium (mg/L)	Hach TNT 849, Metal phthalein Method
Ammonia (mg/L)	TNT 832, Salicylate Method
Alkalinity (mg/L $CaCO_3$)	TNT 870

The alkalinity was measured when pH was to be adjusted with muriatic acid prior to beginning a jar test. Acid volume necessary for specific pH adjustments was determined using the method outlined in Supplemental Information. MgO of different hydration

extents and different activities were dosed to the centrate and struvite would begin to precipitate. The duration of the jar test was typically 45 minutes to analyze the initial supersaturation and phosphorus removal experienced in the jars. MgO of different activity at different hydration extents were used to understand if the activity and hydration extent had a significant effect on struvite precipitation.

If analysis was to be performed on site after struvite precipitation jar tests than the soluble struvite constituent concentrations were measured with Hach tubes and the spectrophotometer. All tubes that were used for centrate analysis listed in the table below were used for analysis of the final jar struvite constituent concentrations. Since there was potential for struvite to still be actively precipitating after the jar test had stopped, Hach TNT 846 reactive phosphorus tubes (vanadate method) were used as these tube instructions were less intensive than the TNT 845 tubes.

Samples for analysis were taken from the jars with a pipette or syringe at a specific time (45 or 150 minutes), instantly filtered with a vacuum pump and analyzed on-site. Analysis performed during jar testing is listed in Table 12. Analysis allowed for phosphorus removal to be determined for each test.

Table 11: On-Site Jar Test Analysis

On-site Analysis
pH
Ortho Phosphorus Concentration (mg PO_4-P/L)
Soluble Magnesium (mg/L)

4.3.8. Struvite Precipitation Jar Testing and CEL Analysis

Jar tests for CEL analysis were prepared in a 6-blade paddle mixer as previously described with centrate and MgO slurry of various hydration extents. MgO slurries utilized for jar testing were filtered with a vacuum pump and the filtrate was sent to the CEL for total Mg analysis (EPA 200.7, Rev. 4.4) to quantify how much soluble Mg was present in solution when dosing slurry to centrate. The filter residue collected on the glass fiber paper was then used to quantify the hydration extent of the MgO slurry dosed to the jars. Hydratoin extent is determined by following the previously defined method.

An initial centrate sample was grabbed for analysis and once the MgO slurry was dosed to the jars, 5 samples were grabbed at times 0, 5, 15, 30, and 45 minutes. On-site pH and electrical conductivity measurements were also performed for each sample. Samples were taken with a 100 mL syringe and immediately filtered through glass fiber paper using a vacuum pump. Jar testing analysis performed by the CEL allowed for the phosphorus removal and saturation index to be quantified through time 0-45 minutes.

Table 12: CEL Analysis Performed for Struvite Precipitation Jar Test at Times 0, 5, 15, 30, and 45 Minutes

Sample Type	On-Site Analysis	CEL Analysis of Filtered Samples
MgO Slurry Hydration	**MgO Slurry Hydration Extent (%)**	**Total Mg of MgO Slurry Sample (mg/L) – EPA 200.7, Rev 4.4**
Struvite Precipitation Samples @ 0, 5, 15, 30, and 45 minutes	**pH**	**Total Mg (mg/L) – EPA 200.7, Rev. 4.4**
	Electrical Conductivity (mS/cm) – Hach	**Total Phosphorus – Lachat 10-115-01-1-E**
		Total Ammonia-N – Lachat 10-107-06-1-J

Once data from the CEL was received the OP removal was determined and the saturation index was calculated by Visual MINTEQ 3.1 for each sample time.

4.3.9. Struvite Precipitation Equilibrium Modeling

Visual MINTEQ was run for each sample time with the given pH and ionic strength measured at that time. Ionic strength, I, was approximated from the electrical conductivity (EC) at 25 °C measurement using an empirical formula commonly used when assuming a linear relationship, where electrical conductivity at 25 °C (EC_{25}) is in µS/cm:

$$I = 1.6 \times 10^{-5} EC_{25} \tag{32}$$

The electrical conductivity was measured with a portable Hach high-range conductivity meter and the pH was measured with a portable Milwaukee pH meter. Due to the relatively constant temperature of centrate experienced in the jar tests, noticed between 23 – 26 °C the complex temperature correction was not used.

The activity coefficients for each struvite constituent were solved for by inputting the ionic strength into Visual MINTEQ which uses the Davies activity coefficient equation to determine the saturation index. Visual MINTEQ solves for the SI utilizing the IAP:

$$SI = \log_{10}\left(\frac{IAP}{K_{SP}}\right) \tag{33}$$

4.4. Results and Discussion

4.4.1. Magnesium Oxide Activity Determination

An activity test was performed on the MgO products used in full-scale operation and jar tests to understand how reactive the products were. The magnesium oxide products used

in full-scale operation and jar testing are listed below with their corresponding activity, or time taken to neutralize 1M acetic acid.

Table 13: MgO Product Activity Analysis

MgO Products	Activity/Time to Neutralize Acid
Baymag-30	23 seconds
Timab M98	46 seconds
Timab MX95	36 seconds
Timab MX97	28 seconds
Timab AK98	13 seconds
Feed Grade Baymag (un-milled)	• minutes 52 seconds

The activity tests revealed how reactive each MgO product was relative to the others. A lower activity time, or time taken to neutralize 1M acetic acid, represents a more reactive MgO product and a higher activity time represent a less reactive MgO product. The most reactive MgO was AK98 while the least reactive milled product was Timab M98. Feed Grade Baymag was larger un-milled MgO product that was the least reactive, neutralizing acetic acid after almost 16 minutes. The effect of the milled MgO product activity on struvite precipitation was tested on bench-scale in a series of jar tests.

4.4.2. Magnesium Oxide Hydration Extent Determination – MgO Pilot 2019

MgO hydration extent was first investigated in June 2019 when using Baymag MgO product and it was discovered that Baymag hydrates relatively fast and is ~70% hydrated after only 4.75 hours of mixing the slurry. After 20 hours of mixing right before the next slurry batch was made the Baymag MgO had been hydrated 97.8%. This considered the maximum achievable hydration extent when considering the average purity of Baymag product is 96.5% MgO. The slurry hydration was not monitored throughout the night, so it is not well known how quick the slurry hydration plateaus. The high hydration extent was assumed to be typical for the MgO trial up to this point in time as the larger tote and recirculation loop was installed in November 2018 and the previous dosing configuration with 2 small totes pre-hydrated the slurry for 22-24 hours prior to dosing. With the undetermined effect of MgO slurry hydration extent on struvite precipitation, it was of interest to test a hybrid design where MgO hydration could be maintained in specific ranges and investigated on the pilot reactor. Performance struvite precipitation– e.g. product size, P removal, and yield– with lower hydration extent MgO could solidify full-scale MgO slurry slaking system design specifications.

Figure 38 shows the hydration and viscosity of the 20% m/m Baymag MgO slurry through time. It is noticed that the increase of slurry viscosity, in centipoise reflects the increase in MgO hydration to $Mg(OH)_2$ through time. This correlation is due to the density of the solid changing as the denser $Mg(OH)_2$ precipitates and the MgO dissolves to reach equilibrium with the solution and solid phases.

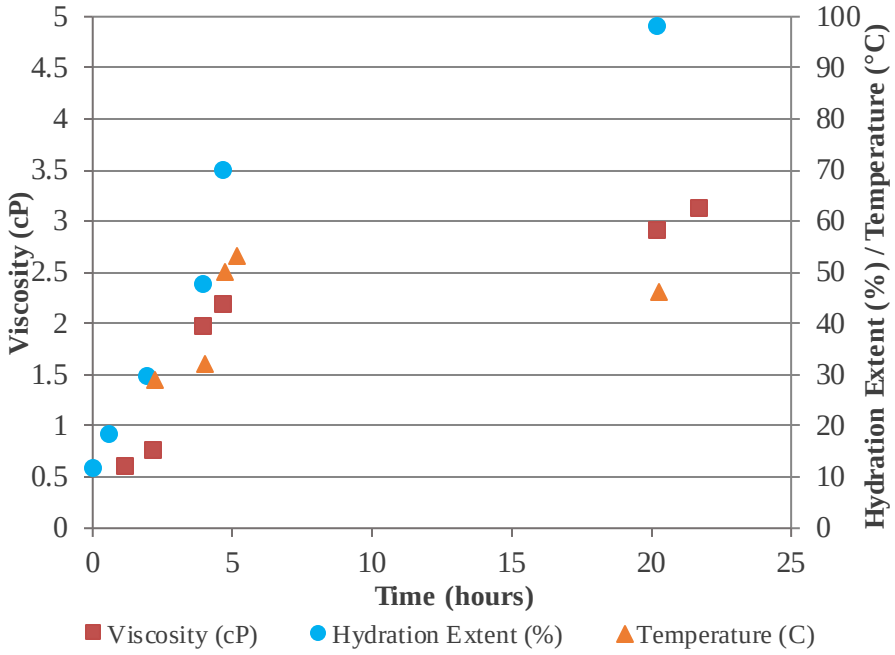

Figure 13: 20% m/m Baymag 30 HP MgO Slurry Hydration Extent and Viscosity Through Time (June 2019)

Figure 13 exhibits the fast hydration rate of Baymag during the first 5 hours of slurry mixing. There was a noticeable color change of MgO as it became predominantly hydrated, it shifted from a white-colored slurry to a muted green-colored slurry. Temperature can also be observed to increase at a fast rate during the first 5 hours as Baymag MgO hydrates from 11% to 70%. The increase in temperature is explained by the exothermic hydration reaction occurring and the mixing of slurry under pressure. The temperature leveled off after 20 hours to 46 °C compared to 53 °C observed at 4.75 hours. The developing interest in the hydration extent of MgO material prompted analysis on Timab (M98) MgO when used again in August 2019. Figure 14 represents the hydration of Timab through time. It is observed that Timab does not initially hydrate at the rapid rate observed with Baymag.

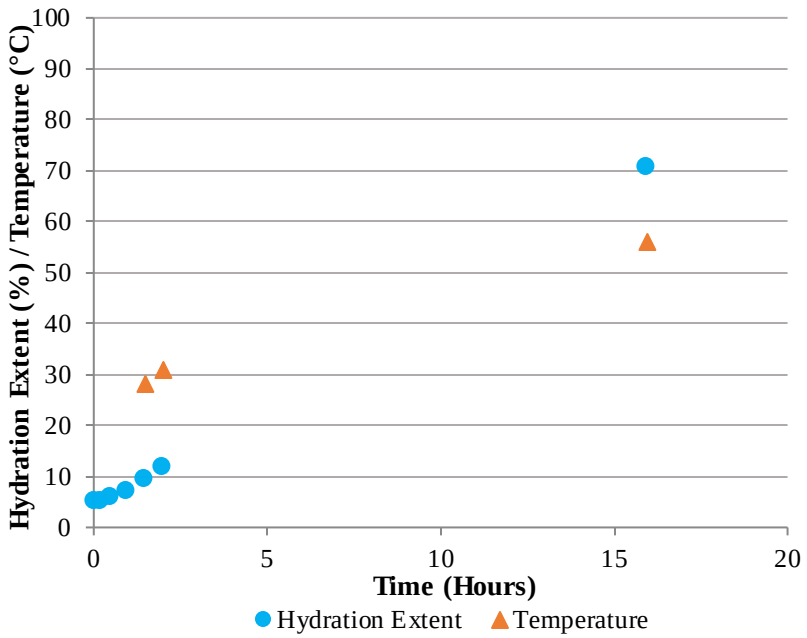

Figure 14: 20% m/m Timab M98 MgO Slurry Hydration

Timab hydrated to almost 71% after 16 hours of mixing in the tote. Temperature also increased when hydrating Timab, reaching an observed high of 56 °C after 16 hours prior to re-batching the slurry. The achieved hydration extent and activity of the MgO product used, Baymag and Timab, seem to have an indirect relationship. This has also been shown in literature as the lowest activity (highest reactivity) MgO products corresponding to the highest level of hydration extent within a 300-minute timeframe. This indirect relationship is hypothesized to be attributed to the calcination temperature used for MgO production and its effect on surface area and thus MgO product reactivity (Birchal, V.S.S., et al., 2000).

A submersible heater and thermocouple were implemented into the tote and pilot test was started using heated Timab MgO slurry. The heated slurry was made by initially heating the 3/4-full tote of NPW to 55 °C, then adding bags to prepare desired 20% m MgO/m slurry and topping off the tote with NPW to fill the total volume. The heated slurry was initially around the 55 °C target temperature and increased due to the exothermic hydration reaction. Figure 15 exhibits the hydration extent and temperature throughout 21 hours for the heated Timab hydration. The morning prior to remaking the tote batch it was observed that the temperature had since returned toward the temperature setpoint and the slurry was not supplementing measurable heat.

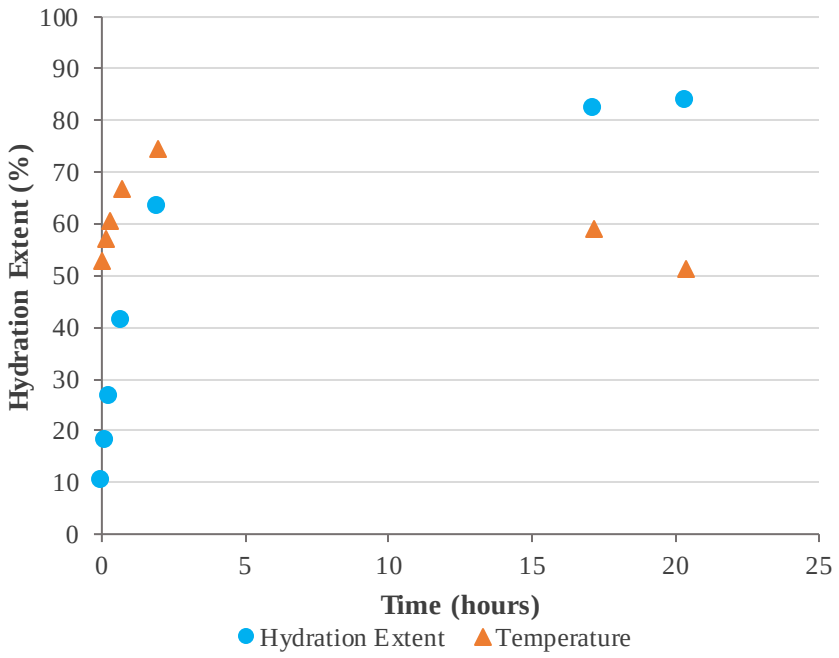

Figure 15: Heated 20% m/m Timab M98 MgO Slurry Hydration

When heating a 20% m/m Timab MgO slurry continuously the hydration extent reached prior to re-batching the slurry was 84%. This is greater than the hydration extent reached with Timab when not heated and the hydration conversion through time is sharper for the heated Timab. Figure 16 show this hydration of heated Timab monitored for the first 3 days of operation to observe the effect of re-batching slurry to the remaining hydrated slurry in the tote. Figure 16 contains the data used in Figure 15 in conjunction with data collected after that timeframe. As mentioned previously, the slurry was continuously heated at 55 °C using a submersible heater and thermocouple.

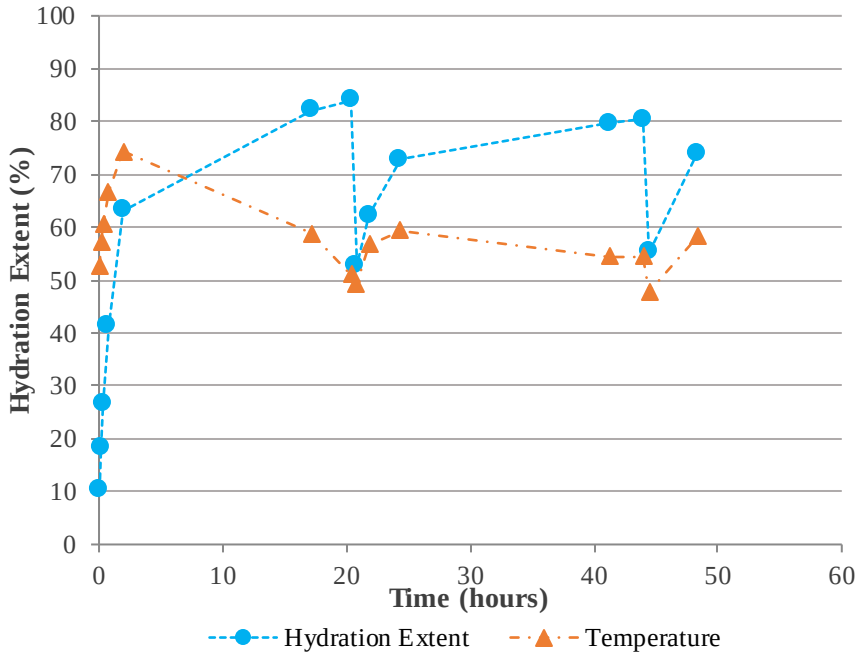

Figure 16: Heated 20% m/m Timab M98 Slurry Hydration Throughout Two Slurry Re-batches (September 9-11, 2019)

Re-batching of MgO slurry preceded the samples taken at hour 21 and hour 44. It is observed that the re-batching does lower the hydration of the overall slurry as some MgO particles are almost fully hydrated and some have just been added to water to begin hydrating. After the slurry batch done before hour 21 it seemed that the slurry hydration extent started to plateau just above 80% as it had done previously before re-batching. Temperature is once again noticed to trend with the hydration extent initially but as the hydration extent rate plateaus the temperature returns near the temperature setpoint of 55 °C. The faster hydration rate produces additional heat and when the hydration rate lessens this is observed as a temperature drop. Slurry temperature was seen to go below 55 °C when the batch was being made each day due to NPW being added, which is typically between 15 – 29 °C.

4.4.3. Magnesium Oxide Hydration Extent Determination – MgO Pilot 2020

When the MgO slurry configuration was updated in 2020 to an automated batching system with a smaller MgO slurry tank it was anticipated that different slurry concentrations would produce different hydration extent ranges dosed to the reactor. This was expected due to different slurry concentrations achieving different retention times based on reactor dosing of MgO satisfying an Mg:P of 1:1 – 1.5:1. The higher the slurry concentration (% MgO m/m), the less MgO slurry needed to be dosed to the reactor and thus the higher the hydration extent achieved during the longer retention time of the slurry. A lower slurry concentration (% MgO m/m) meant slurry needed to be dosed more frequently to the reactor to achieve the necessary Mg:P. This relationship between slurry concentration and hydration extent was observed when testing various slurry concentrations (% MgO m/m)

and grabbing samples for hydration extent determination. Hydration Extent ranges were higher for the first few days of slurry batching as the reaction was occurring at a faster pace, the hydration extent leveled off after the initial few days and hydration extents ranges in Table 15 were measured.

Table 14: Hydration Extent Range Measured for Various MgO Products and Slurry Concentrations used During Full-Scale Operation

MgO Product, Slurry Concentration (% MgO m/m)	Hydration Extent Range (%)
Baymag, 5%	10-17%
Baymag, 8%	25-55%
Timab, 6.5%	15-25%
Timab, 12%	12-65%, leveled off between 30-50%

4.4.4. Magnesium Oxide Activity and Hydration Extent Effect on Struvite Precipitation – On-site Analysis

Magnesium oxide activity effect was observed in jar tests with the use of various MgO products. These products of differing reactivities were tested with respect to different Mg:P dosing ratios and different hydration extents. Each Mg:P ratio of 0.85:1, 1:1 and 1.25:1 was performed with an MgO product, both hydrated and unhydrated. Hydrated samples were hydrated for 22 -24 hours prior to dosing to centrate while the unhydrated samples were mixed for 1 minute and then instantly dosed. Not all tests were performed at the same time due to paddle mixer availability, however each Mg:P ratio of each MgO product was performed on the same day. Each test was performed at a mixing speed of 70 rpm for 45 minutes. Below in Figure 17 is a diagram of how each jar test was performed with the different MgO products.

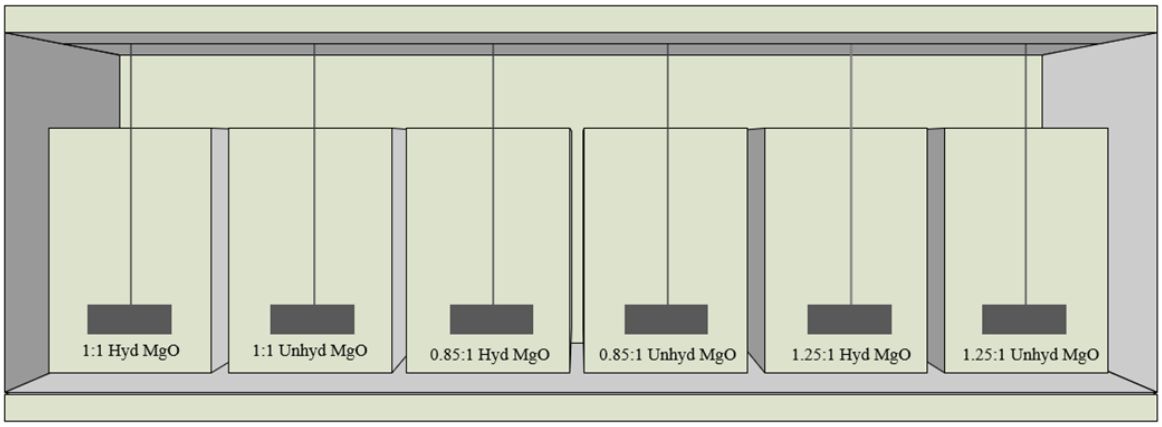

Figure 17: Struvite Precipitation Jar Test Setup with Various Mg:P Dosing Ratios Using MgO

The initial pH was between 6.85 – 7.04 prior to dosing the MgO slurry. After 45 minutes of allowing the slurry and centrate to react and precipitate struvite. Samples were grabbed and immediately analyzed using the Hach tubes and spectrophotometer on-site. The phosphorus removal given of each MgO product either 22-24 hours hydrated as a 15% m MgO/m slurry or unhydrated (mixed for 1 minute as a 15% m MgO/m slurry prior to dosing) can be seen in Figure 18 with respect to each product's activity. Figure 18 shows how material of low activity, and thus more reactivity, were able to remove more phosphorus than the MgO products of higher activity values in the allotted 45-minute jar test.

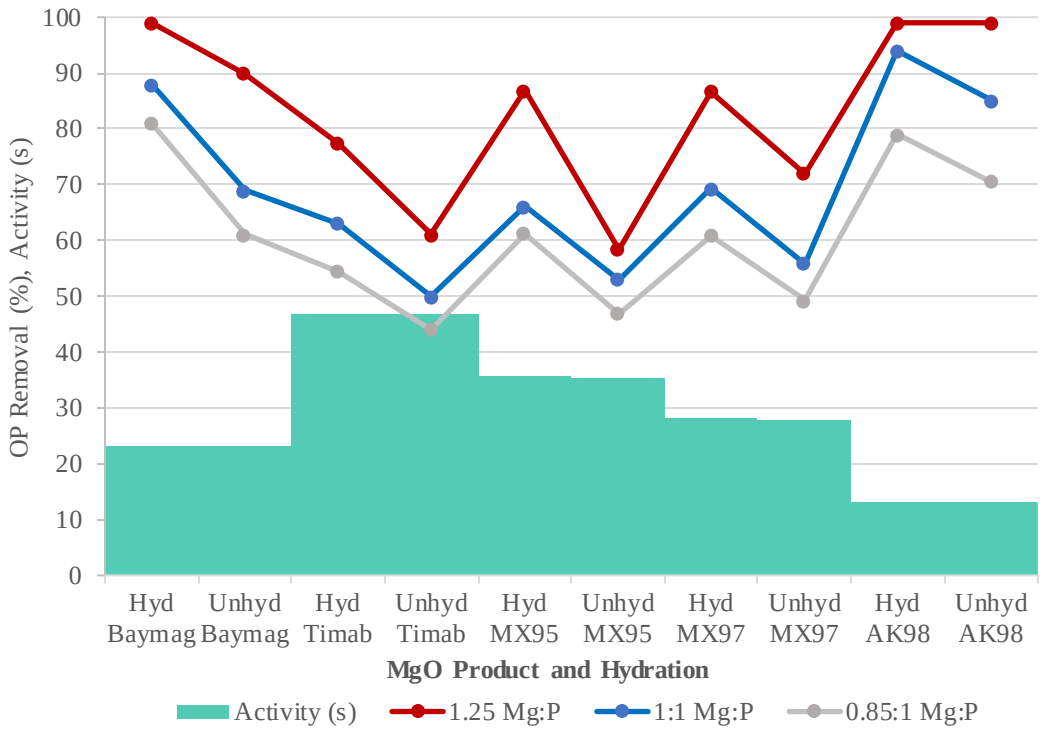

Figure 18:Mg:P and MgO Activity Effect on Orthophosphate Removal during Struvite Precipitation Jar Testing

The increase of Mg:P dosing from 0.85:1 to 1:1 also showed improvement in the phosphorus removal achieved. It is important to note that hydrated reactive material, i.e. Baymag and AK98, dosed at an Mg:P of 0.85:1 achieved a phosphorus removal that would be considered optimal under full-scale operation (>70%). Interestingly, unhydrated AK98 also shows decent performance under the 0.85:1 Mg:P dosing jar test. The moderately reactive material, with respect to the given MgO products, MX95 and MX97, did not achieve optimal operation under 0.85:1 or 1:1 Mg:P with hydrated or unhydrated MgO. Timab (M98) performed poorly, hydrated and unhydrated, in all dosing scenarios minus the 1.25: Mg:P dosage when using hydrated Timab. Table 32 in Supplemental Information defines the phosphorus removals achieved during these jar tests can be seen in tabular form.

The hydration extents of the various MgO products were quantified during this jar testing and the hydration extents can be seen in Figure 19 along with the phosphorus removals.

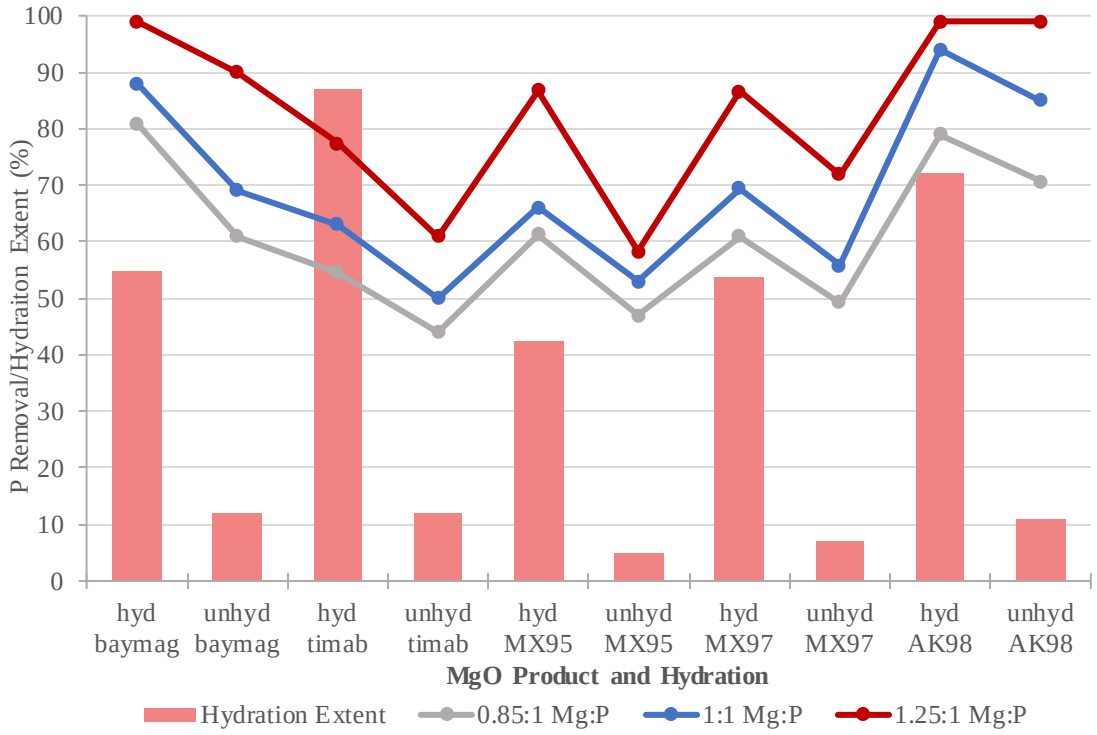

Figure 19: Mg:P and MgO Hydration Extent Effect on Phosphorus Removal During Struvite Precipitation Jar Testing

When looking at MgO products individually, Figure 19 shows that MgO of a higher hydration removed more phosphorus than its unhydrated form when dosed as a slurry to the centrate. An important thing to note is the ability of MgO product to optimally remove phosphorus even when not fully hydrated with respect to its purity. Baymag MgO hydrated to 55% was able to perform optimally under each Mg:P test. This same performance is also seen with 72% hydrated AK98. Unfortunately, the less reactive Timab (M98) was not able to obtain optimal P removal when dosed at 0.85:1 or 1:1 even though it was 87% hydrated. It is hypothesized that less reactive material may require more reaction time during the jar

tests to achieve optimal operation, rather than higher hydration. Optimal operation may be affected by the initial conditions and final pH achieved in the jar test duration. Figure 52 in Supplemental Information defines the initial and final pH of the jars for 1:1 Mg:P 45-minute tests. Several jar tests were performed at 0.85, 1:1, and 1.25: Mg:P without MgO hydration extent determination for each test performed– the average OP removal and pH observed for all jar tests can be seen in Figure 54 of Supplemental Information. The average OP removal trends with the MgO product and hydration extent as observed in Figure 18 and Figure 19. The reactivity of the product shows a direct relationship with the OP removal achieved within 45-minute jar tests.

To observe the effect of a longer mixing time on struvite precipitation and P removal, on-site jar testing was performed for hydrated and unhydrated MgO products at 1:1 Mg:P. Mixing speed was 70 rpm while the mixing time was extended to 150 minutes. All hydrated samples were hydrated as a 15% m MgO/m slurry for 22 hours prior to dosing. The hydration extent of the MgO products used are listed in Table 16 below.

Table 15: Hydration Extents of MgO Products Used for 150 Minute Struvite Precipitation Jar Test

MgO Products	Hydration Extents (%)
Baymag	68.5
Timab	47.2
MX95	37.7
MX97	47.5
AK98	78.7

Phosphorus removals achieved when adding hydrated 15% m MgO/m slurry to centrate during a 150-minute duration jar test were compared to previously outlined jar testing data collected for 45-minutes. Figure 20 depicts the phosphorus removal achieved by dosing 22 hour hydrated MgO product to centrate and mixing for different durations. Figure 20 shows that the longer jar testing time positively impacts the phosphorus removal observed in the jar test, especially when utilizing less reactive MgO products. It is hypothesized that faster MgO dissolution occurs with more reactive MgO and ultimately achieves a higher OP removal and equilibrium between the solution and struvite solid within a short period of time. AK98 MgO product showed similar OP removal at 45-minute and 150-minute jar test durations. Timab, MX95, and MX97 showed an improved OP removal when increasing the jar test from 45 minutes to 150 minutes. When precipitating struvite utilizing Baymag, it is observed that unhydrated Baymag showed improved OP removal when extending the jar test time.

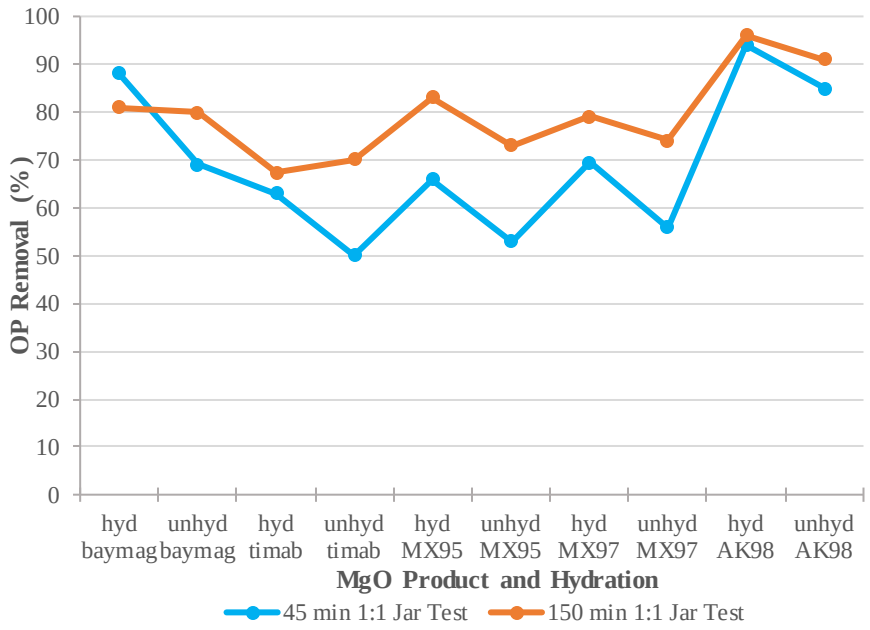

Figure 20: Struvite Precipitation Jar Test Duration Effect on Phosphorus Removal

The majority of jar tests showed improvement except the hydrated Baymag jar test. It is unclear what caused this conflicting result but it is hypothesized based of the final pH obtained during this test that there was not a proper dosage of MgO slurry to the jar test or the slurry was not mixed well enough prior to pipetting the slurry to the centrate. The unhydrated Baymag for the 150-minute struvite precipitation jar test achieved a higher final effluent pH than the hydrated Baymag which is not the typical observation. It is evident, based on Figure 21 that the phosphorus removal is correlated with the final pH achieved.

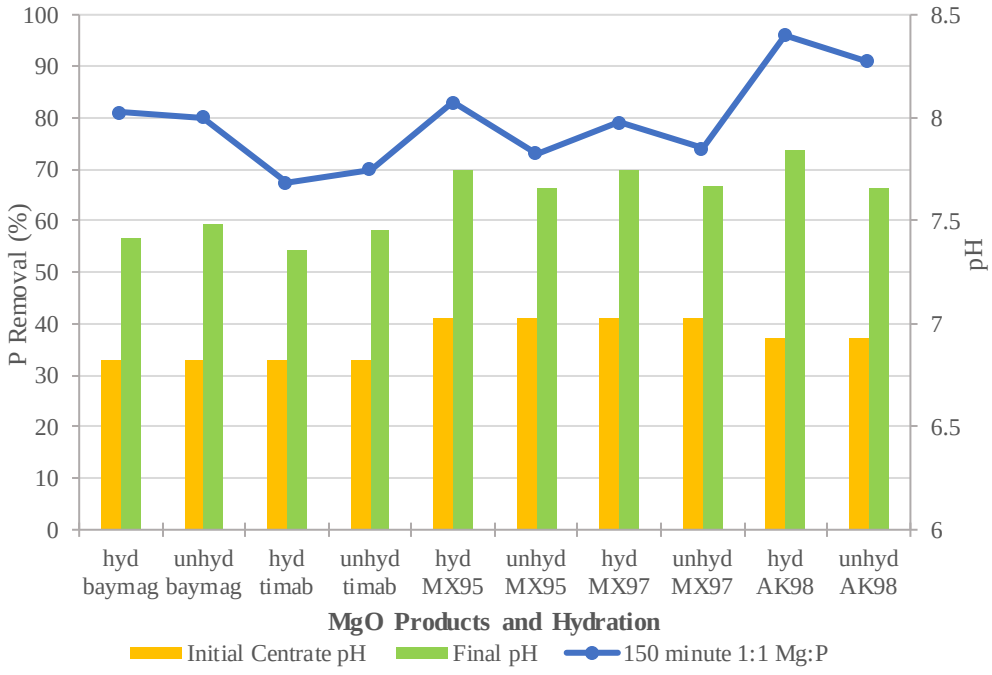

Figure 21: Initial and Final pH during 45-minute Jar Tests Determining the Effect of Various MgO Products and Mg:P on Phosphorus Removal

The final pH seems to be higher for the more reactive material as it is thought the initial low pH and high phosphorus concentration encourage MgO solubility and $Mg(OH)_2$ surface layer dissolution as previously hypothesized by Stolzenburg, P., et al. More investigation of the jar testing was necessary to understand struvite precipitation through time and if reactivity and hydration extent of MgO products influenced the rate and duration of the precipitation reaction. Further testing was performed with the help of the HRSD CEL and are discussed in the next section.

4.4.5. Magnesium Oxide Activity and Hydration Extent Effect on Struvite Precipitation – CEL Analysis

Analysis performed in this section followed a similar procedure to that performed by Stolzenburg, P., et al. (2015). However, the focus of this analysis was to understand the supersaturation and struvite constituent concentrations through time when utilizing different MgO products at an Mg:P of 1:1. Struvite jar tests performed at the SRF for CEL analysis were done with MgO products Baymag, Timab M98, and AK98. Samples were grabbed throughout the allotted 45-minute jar test reaction time while being mixed at 100 rpm then preserved in acid and refrigerated. Total magnesium, phosphate as phosphorus and ammonia as nitrogen were measured by the CEL while pH and electrical conductivity were measured on-site. Conductivity measurements were used to estimate an ionic strength of solution to determine the saturation index of the solution through time with the use of EPA's Visual MINTEQ 3.1 chemical equilibrium model. The first round of jar testing entailed moderately hydrating the MgO products for a certain amount of time before dosing to the centrate for struvite precipitation. The hydration extent with the corresponding total Mg concentrations (mg/L) measured from filtered MgO slurry samples can be observed in Table 17. It can be observed that Baymag and Timab M98 start with high Mg concentrations in solution, which are presumed to be soluble Mg^{2+} concentrations as filtering and sample preservation occurred prior to analysis. As the hydration reaction continued, Mg concentrations decreased, when observing hydrations >23 hours. It is thought that the Mg concentration decreases as equilibrium between MgO and $Mg(OH)_2$ is reached. The Mg^{2+} concentration observed during AK98 MgO hydration is low, not observed to exceed 15 mg/L.

Table 16: MgO Product Hydration Extent for Jar Testing

MgO Product	Date	Hydration Time (hrs)	Hydration Extent (%)	Mg Concentration after Filtering MgO Slurry (mg/L)
	9/24/2020	3	19	236

Timab M98	9/24/2020	7	24	226
	10/14/2020	8	60	228
	10/28/2020	26	64	3.62
Baymag	6/26/2020	0	12	203
	10/13/2020	2	60	223
	9/23/2020	4	64	190
	9/23/2020	7	65	51.9
	10/27/2020	24.5	70	4.04
AK98	6/24/2020	0	11	11.5
	10/12/2020	1	63	0.320
	9/25/2020	5	75	14.8
	10/27/2020	23	>79	1.28

It is noticed that with the more reactive MgO products hydrate to a further extent within certain hydration times. Throughout the 45-minute jar tests samples were taken at time 0, 5, 15, 30, and 45 minutes to monitor the struvite constituent concentrations through time. Figure 22 demonstrates the P removal through time of each hydrated MgO product.

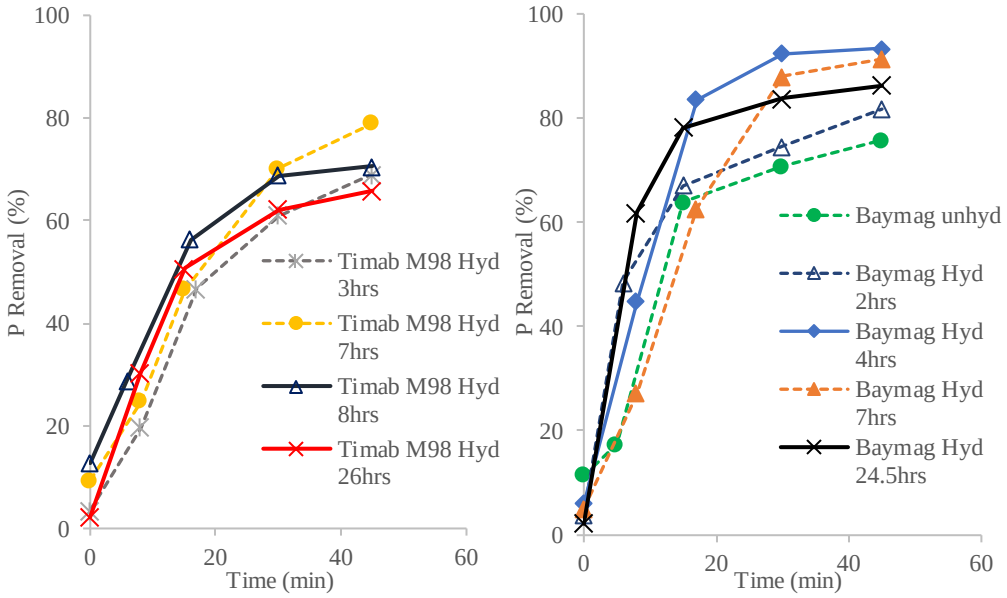

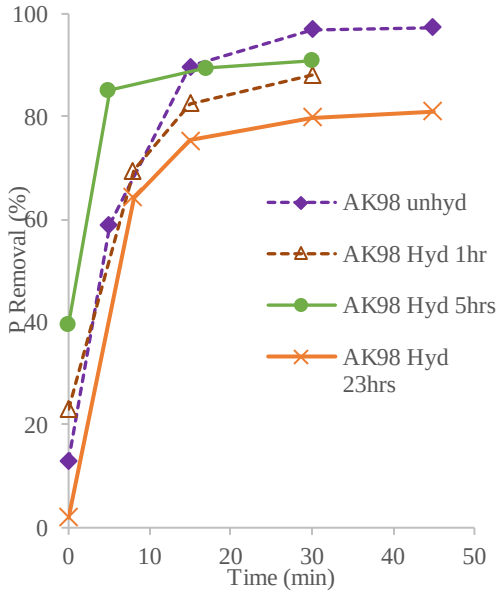

Figure 22: Phosphorus Removal Throughout the 45-minute Struvite Precipitation Jar Test with MgO Products of Various Hydration Extents

With respect to the hydrated MgO jar tests, the most reactive MgO, AK98, at a 5-hour hydration showed the most rapid P removal, removing 40% immediately and 85% after 8 minutes of mixing. All hydrations of AK98 removed >88% of phosphorus after 30 minutes. The trend of P removal utilizing AK98 is similar to $MgCl_2$ addition for struvite precipitation. Baymag of different hydration times show rapid phosphorus removal. 4-hour hydrated Baymag removed 83.5% phosphorus after 17 minutes while the 7-hour hydrated Baymag required 30 minutes to achieve an 89% P removal. Timab, the least reactive MgO used needed a longer time period to approach the optimal phosphorus removal (>70%) for both hydrations used.

The unhydrated AK98 MgO jar test acted similarly to the hydrated tests, while unhydrated Baymag required 30 minutes to achieve optimal phosphorus removal. AK98 unhydrated 1:1 test removed 97.3% phosphorus after 45 minutes and may have been influenced by the initial centrate pH of 7.07 during this test. The pH trends of jar tests can be observed in Figure 53 in Supplemental Information. Given the removals, the saturation index through time after MgO dosing was of interest to understand the kinetics of the precipitation through time. The saturation index was determined by EPA Visual MINTEQ 3.1 model by inputting pH, ionic strength and struvite constituent concentrations of individual sample times. Figure 23 illustrates the saturation index through time.

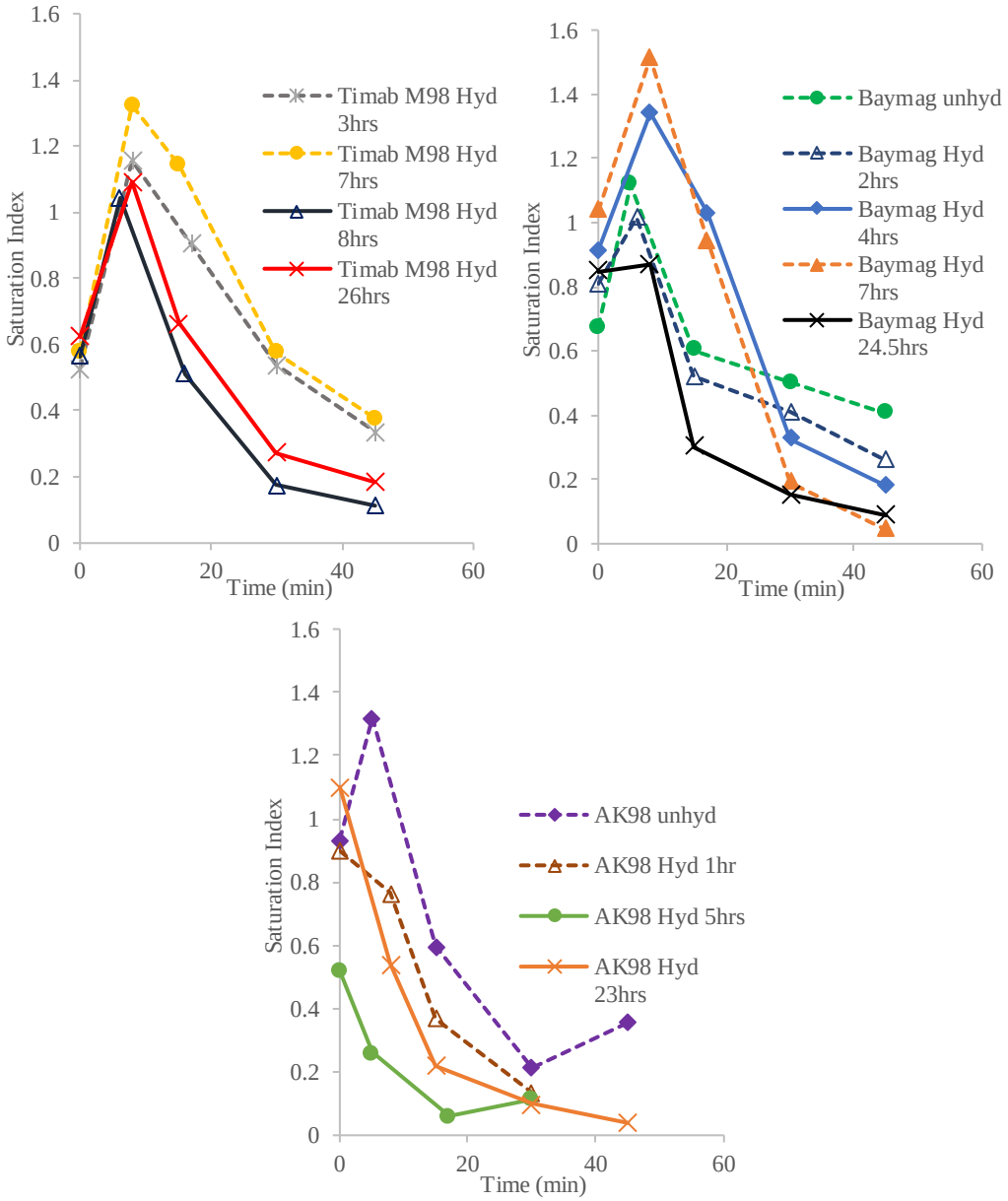

Figure 23: Saturation Index (SI) throughout the 45-minute Struvite Precipitation Jar Test with MgO Products of Various Hydration Extents

The degree of saturation can control struvite precipitation kinetics, determining whether struvite nucleation or crystal growth is favored. A high SI can indicate nucleation is the dominant form of precipitation while a moderate SI, closer to 0, can infer crystal growth would more likely be favored. Understanding SI through time and equating to MgO slurry travel through the full-scale reactor may give insight on the kinetics of precipitation and struvite product size during full-scale operation. It can be observed that a rapid decrease in SI and increase in P removal through time occurs when dosing AK98 MgO slurry. It is hypothesized that the reactivity of AK98 caused instant dissolution of MgO as Mg^{2+} that allows for the reaction to occur at a fast rate. After 30 minutes, P removal approaches 90%

and SI decreases close to 0. It is hypothesized that similarities between AK98 MgO and $MgCl_2$ when precipitating struvite may indicate that AK98 cannot provide a Mg^{2+} reserve but can provide adequate conditions for struvite crystal growth. Contrastingly, Timab M98 did not remove phosphorus rapidly and was able to maintain an SI around 0.4 after 45 minutes showing that conditions are favorable for further precipitation as Timab M98 potentially acts as a Mg^{2+} reserve. Baymag shows different SI trends depending on hydration. Longer Baymag hydration shows rapid P removal and SI depletion when dosed to centrate, while low hydration or unhydrated Baymag shows slightly slower removal and SI depletion. Magnesium concentrations seen during jar testing from MgO dissolution can be observed in Figure 24. Magnesium concentrations are initially observed to be high (100-120 mg/L) for more reactive hydrated MgO products. It is occasionally observed that a peak of Mg^{2+} is not observed and is hypothesized to have already been consumed by the struvite precipitation reaction and dissolution of MgO occurred rapidly. Comparing Mg concentration to P removal at each sample time can shed light on how fast the Mg^{2+} from MgO dissolution is being utilized for struvite precipitation. Mg concentration peaks at time 0 minutes for the most reactive AK98. Baymag, which is the second most reactive MgO, observed high Mg concentrations at time 5 and 10 minutes when using moderately hydrated product (4 or 7-hour hydration). The least reactive MgO product, Timab M98, did not see extreme peaks of Mg concentration in filtered samples from the different time intervals, never exceeding 83.5 mg/L. It is hypothesized that the dissolution of Timab M98 is slower when initially dosed to centrate. This can infer a potential for "slowly available" Mg^{2+} reserve to be in the reactor as MgO, where further dissolution can be promoted by low pH and high phosphate concentration in the centrate.

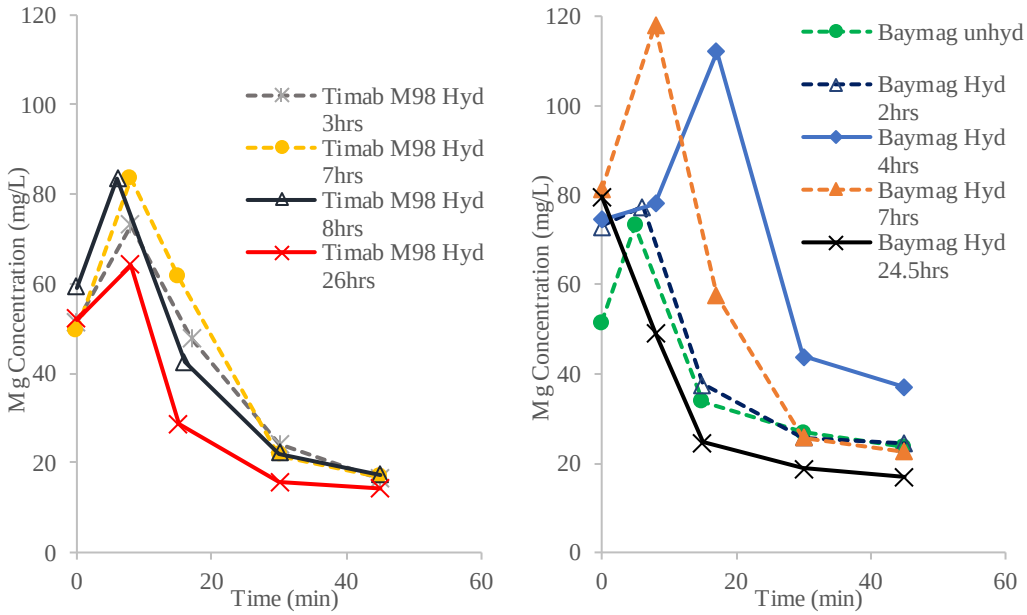

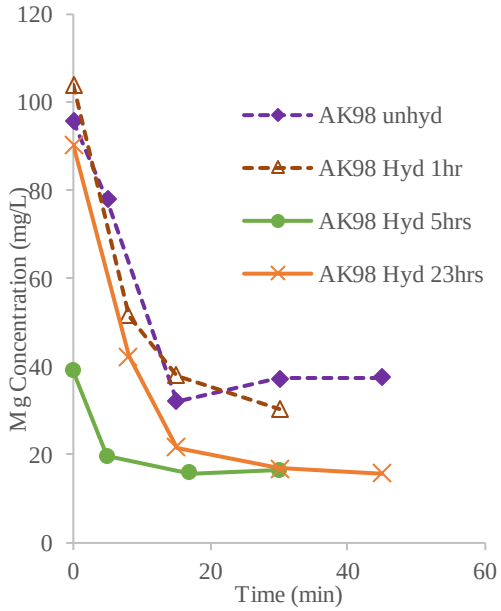

Figure 24: Magnesium Concentrations Throughout the 45-minute Struvite Precipitation Jar Test with MgO Products of Various Hydration Extents

Micrographs can be observed in Figure 25 of the struvite product observed from the jar tests utilizing MgO products of various hydration extent and reactivities. It can be observed that the AK98 MgO, even at lower hydration extents, used for struvite typically forms orthorhombic crystal structures, possibly from total dissolution of MgO when dosed to centrate. When less hydrated, AK98 forms more dendritic struvite morphology, possibly from local higher saturation index from MgO/$Mg(OH)_2$ dissolution. Higher hydration of across all MgO products showed more orthorhombic struvite structures. The higher conversion of MgO to $Mg(OH)_2$ may result in more rapid saturation of solution due to faster dissolution of $Mg(OH)_2$. MgO particles of yellow/brown color can be observed in all struvite micrographs from jar tests utilizing Timab M98, the least reactive MgO products used. The observation of MgO in micrographs can show the "slowly available" Mg^{2+} produced during struvite precipitation when using MgO.

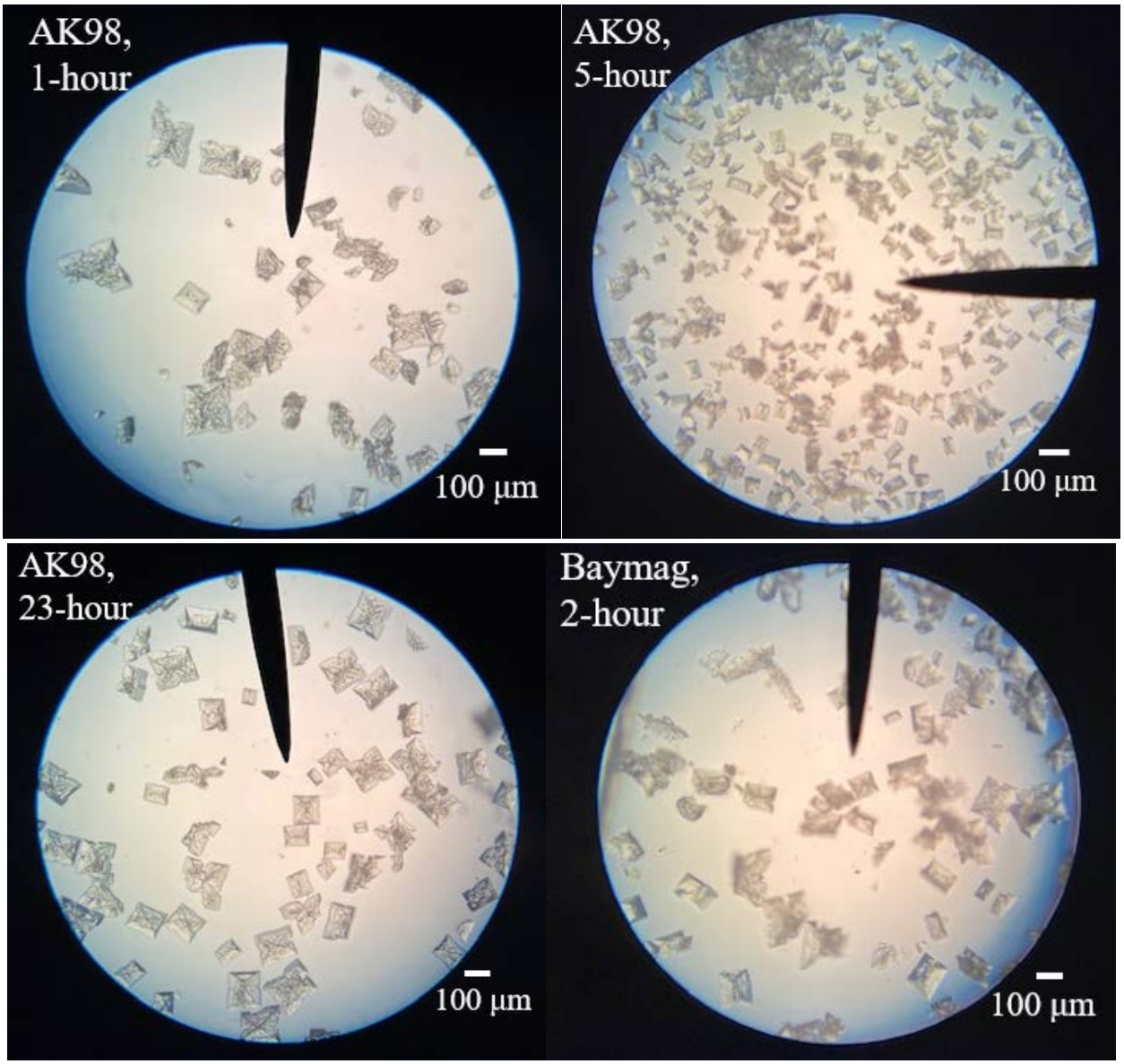
AK98,
1-hour
100 µm
AK98,
5-hour
100 µm
AK98,
23-hour
100 µm
Baymag,
2-hour
100 µm

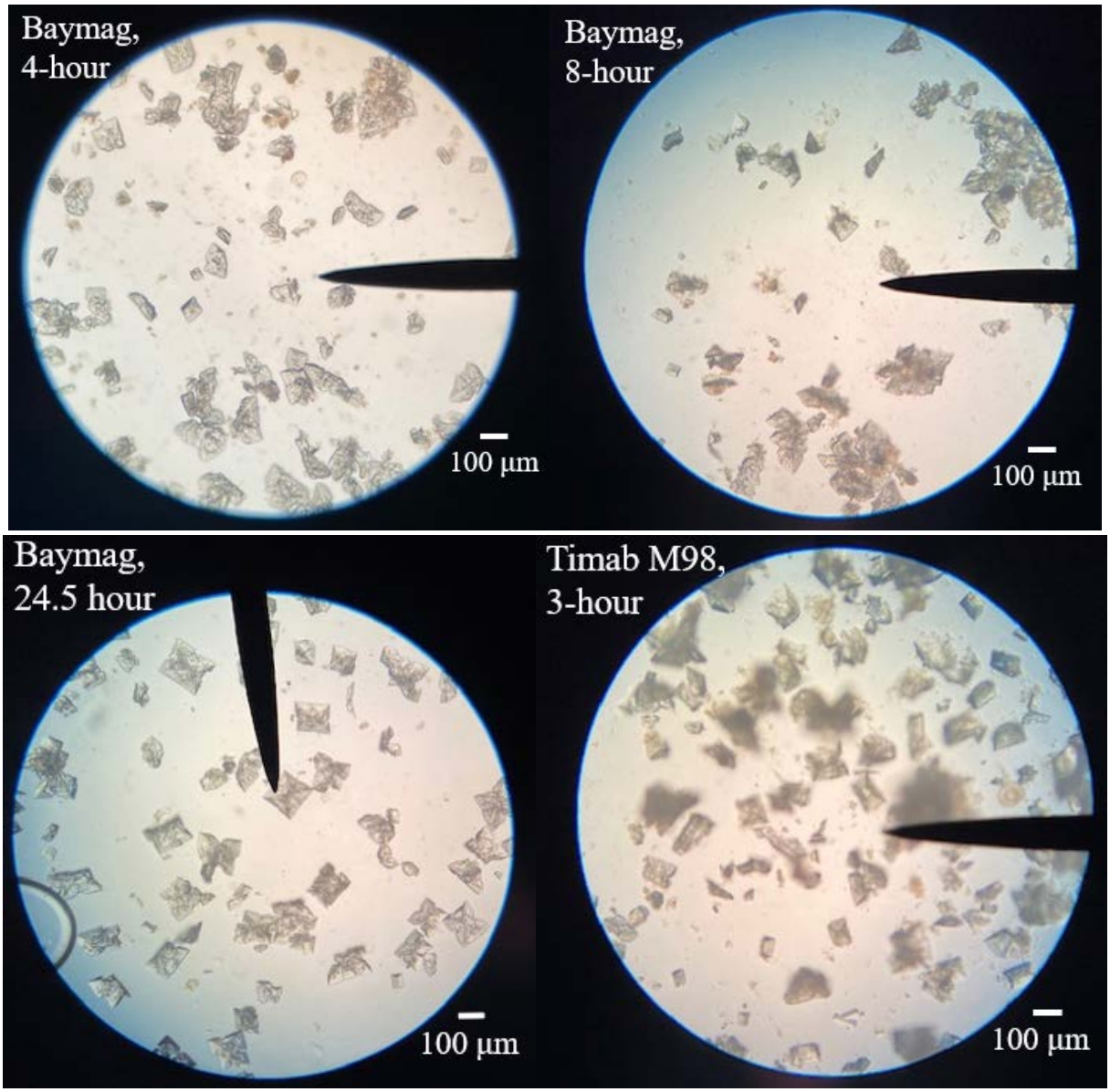
Baymag,
4-hour
100 µm
Baymag,
8-hour
100 µm
Baymag,
24.5 hour
100 µm
Timab M98,
3-hour
100 µm

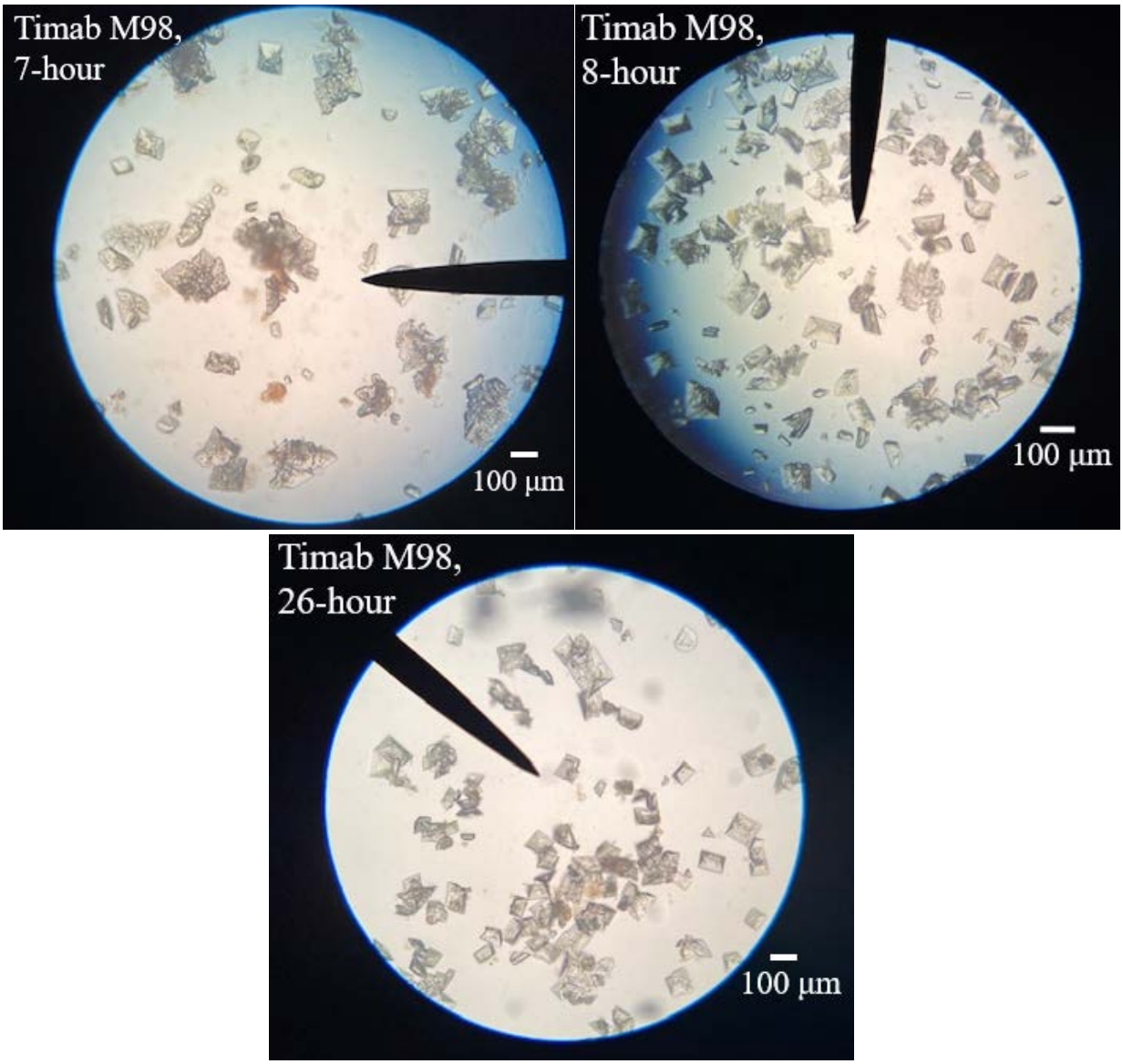

Figure 25:Micograph at 100X of Struvite Jar Test Product with MgO Product

4.5.Conclusions

Through jar testing, MgO hydration and reactivity and Mg:P dosing ratios have been shown to affect struvite precipitation in terms of OP removal and saturation index. Jar testing results demonstrated:

- Higher Mg:P molar ratios of 1.25:1 improved OP removal during 45-minute jar tests for all MgO products
- Low 0.85:1 Mg:P molar ratios only showed close to 80% OP removal for the most reactive MgO products, Baymag and AK98, when hydrated
- At 0.85:1 Mg:P, hydrated less reactive MgO products (Timab M98, MX95, and MX97) and all unhydrated products did not perform well with an Mg:P under 1
- pH can impact the overall performance of an MgO product on struvite precipitation
- Extending the jar test from 45 minutes to 150 minutes was observed to especially benefit the MgO product of lower reactivity (Timab M98, MX95, and MX97).

When further investigating the saturation index and OP removal through time it was observed that:

- More reactive MgO products were observed to achieve rapid OP removal and depletion of saturation index through time
- Low reactive MgO show a more stable, linear OP removal through time and the same goes for the depletion of saturation index observed
- Saturation indices close to zero, observed with AK98, do not seem adequate at providing the struvite precipitation reaction with an "slowly available" Mg^{2+} reserve through the 45-minute jar test
- Struvite precipitation utilizing AK98 MgO resembles the conventional $MgCl_2$ reaction, rapid OP removal within the first few minutes of reaction. However, Timab M98 may possess more potential to provide a "slowly available" Mg^{2+} reserve throughout the 45-minute jar test

As mentioned, less reactive MgO product benefitted more from a longer jar test duration of 150 minutes. More reactive MgO product that had been hydrated showed little benefit in a longer jar testing duration and it can be concluded that a major portion of the MgO had been utilized during the initial reaction, which is supported with data collected throughout time and micrographs of final struvite product (absent of visible MgO product). This understanding could infer that MgO products of certain reactivity and hydration extent can prove the hypothesis that MgO and $Mg(OH)_2$ can provide a Mg^{2+} reserve. Micrographs of the final struvite obtained when utilizing MgO products of various reactivity and hydration further define the Mg reserve that can be present. Further MgO and $Mg(OH)_2$ dissolution can be influenced by the initial low pH and high OP concentration of centrate during continuous operation and provide the "slowly available" Mg^{2+} reserve. When equating the results from jar testing to a full-scale struvite recovery process, such as the Pearl® process, fur-ther research may be necessary to understand the fluidization and travel of a solid "slowly available" Mg^{2+} reserve and if it hinders or benefits full-scale operation.

5. Manuscript 2: Optimization of Struvite Recovery Utilizing Different Modes of Control and Magnesium Oxide Feed Strategies

5.1. Abstract

The conventional Pearl® process for struvite recovery utilizes magnesium chloride ($MgCl_2$) and sodium hydroxide (NaOH) which are responsible for the high operational costs associated with the process. 75% of operational costs can be attributed to $MgCl_2$ addition necessary for struvite precipitation. Utilizing magnesium oxide, a cost effective and environmentally sustainable mineral, can eliminate costs associated with not naturally occurring $MgCl_2$. MgO can also provide the necessary alkalinity for struvite precipitation and eliminate NaOH costs entirely. MgO utilized for full-scale Pearl reactor operation was trialed to understand if optimal operation could be obtained, which is considered baseline performance historically achieved during conventional $MgCl_2$ reactor operation. Due to the solid nature of MgO, it was also of interest to operate the pilot reactor beyond design reactor loading (65 kg P/day) and test the hypothesis that MgO can provide a Mg^{2+} reserve in the reactor. Two high-grade (caustic) MgO products formed from magnesite ($MgCO_3$) calcination were used for pilot testing at 1X reactor design loading (65 kg P/day), 2X loading (130 kg P/day) and 3X loading (195 kg P/day). Struvite recovered (yield), OP removal and TP removal, struvite product size and necessary Mg:P molar ratio dosing were monitored and compared to conventional $MgCl_2$ reactor operation throughout the trial. The MgO pilot trials showed comparable results to baseline $MgCl_2$ Pearl® reactor operation. At times during 2018 and 2019 the MgO pilot reactor achieved baseline struvite yield (P recovered/Theoretical P recovery) (≥50%) and TP removal (≥70%) at reactor design loading (65 kg P/day). The pilot reactor performance at 2X reactor loading (130 kg P/day) surpassed baseline reactor performance (yield and TP removal) observed at 1.3X reactor loading (85 kg P/day). Historically, a P mass imbalance existed within SRF operation– all P entering the system could not be allocated as struvite product, effluent soluble P or effluent fines. In late 2019, baseline performance improved to ≥70% yield and TP removal for 1X and 1.5X reactor loading. The MgO pilot surpassed baseline operation for reactor loading beyond design load (1X), at times obtaining 80% yield and TP removal. Improved reactor operation corresponded with closing of the P mass balance at the SRF observed in later 2019.

5.2. Introduction and Background

Sidestream struvite precipitation from aerobically digested supernatant (centrate) can be performed utilizing various technologies. All technologies require a Mg source and alkalinity to precipitate struvite. Alternative Mg sources were investigated for full-scale Pearl® process operation at Hampton Roads Sanitation District (HRSD). The Struvite Recovery Facility (SRF) at HRSD Nanesmond Treatment Plant (NTP) houses 3 Pearl® 500 reactors that use $MgCl_2$ and NaOH. This conventional Pearl process has high associated chemical costs. $MgCl_2$ can cost $350-700/ton while NaOH can cost between $500-600/ton. Utilizing MgO instead of $MgCl_2$

can save over 60% of costs associated with Mg addition (Verigin, M., et al., WEFTEC 2020). Additionally, MgO production which includes milling and calcining the product has a carbon footprint of 3 tons of carbon dioxide (CO_2)/ ton Mg produced. Meanwhile, $MgCl_2$ production has a carbon footprint of 12.9 tons of CO_2/ ton Mg produced (Kiani, D., et al. 2018).

MgO is produced from the calcination of magnesite ($MgCO_3$) and calcination conditions can alter MgO product characteristics. Caustic magnesia (light-burned MgO) or dead-burned magnesia (hard-burned MgO) are possible products of the calcination that can each be beneficial for different industrial applications. Caustic MgO is obtained from calcination at lower temperatures (<900 °C) which cause the material to be more porous and thus more reactive. Caustic MgO can be used in agriculture, cattle feed, environmental control, and the manufacturing of special cements. Dead-burned MgO is produced at high calcination temperatures (>1200 °C) which result in a low porosity and low reactivity/unreactive product that is beneficial to the refractory industry (Birchal, V.S.S., et al., 2000; Birchal, V.S., et al. 2001). MgO has a density of 3.58 g/cm^3 and is slightly soluble in water. Magnesium oxide can undergo a hydration/slaking reaction with water to create magnesium hydroxide ($Mg(OH)_2$), and the mechanisms of this hydration reaction have been studied since the 1960s (Smithson, G.L., et al., 1969).

It has been observed that dosing a concentrated MgO slurry is more advantageous than dosing bulk MgO powder material due to better dispersion and initial reaction of slurry (Stolzenburg, P., et al. 2015, Capdevielle, A., et al. 2013). Utilization of an MgO byproduct in suspension showed to decrease reaction time and increase quantity and quality of product when precipitating struvite in comparison to bulk MgO dosing (Quintana, M., et al. 2007). Compared to soluble Mg salt, MgO use for struvite precipitation possesses a few obstacles such as the preceding complex hydration reaction that occurs during slurry preparation and its low solubility in aqueous solutions (Stolzenburg, P., et al. 2015).

It has also been postulated that the solid MgO particle can provide a magnesium ion (Mg^{2+}) reserve in the system that can be used until ammonia (NH_4^+) and phosphate (PO_4^{3-}) ions are consumed and the batch system reaches equilibrium. Additionally, due to the additional surface area that MgO provides when precipitating struvite, it is assumed that the particles facilitate heterogeneous nucleation of struvite using the $Mg(OH)_2$ surface layer on the MgO particle (Stolzenburg, P., et al. 2015). Dissolution of the MgO particle can allow for high degrees of supersaturation near the particle (Kirinovic, E., et al. 2017). Results from Stolzenburg, P., et al. (2015) study show that MgO slurry is an effective reagent for precipitating struvite and can achieve better results than that of $MgCl_2$ addition at all corresponding Mg:P dosages tested. MgO addition at an Mg:P of 1 achieved >90% recovery of phosphorus while $MgCl_2$ addition at an Mg:P of 1 achieved around 85% . This study also shows that while MgO addition caused struvite particles to be smaller than $MgCl_2$ addition for struvite precipitation, particles did increase in size as the Mg:P was decreased.

The potential of MgO to provide a Mg^{2+} reserve was of interest for full-scale Pearl® 500 reactor operation at NTP as decommissioning of a neighboring treatment plant would increase phosphorus loading at the SRF in the future. Consideration of WASSTRIP® implementation at NTP would also increase phosphorus loading at the SRF. An MgO pilot was started on a full-scale Pearl® reactor with the intention of operating the reactor beyond design reactor loading (65 kg P/day) to test the hypothesis of MgO providing a Mg^{2+} reserve. The characteristics of MgO were also investigated during full-scale operation to determine if MgO slurry hydration was necessary for optimal struvite precipitation.

5.3. Materials and Methods

5.3.1. Magnesium Oxide

Two different MgO products were used throughout the duration of the full-scale pilot test. These MgO products were Timab M98 MgO and Baymag 30 HP (Baymag) MgO. Both MgO products are high purity, reactive caustic MgO calcined from magnesite ($MgCO_3$).

Table 17:MgO Product Specifications from Manufacturer

MgO Product	Purity (%)	Size	Reactivity	Specific Surface Area (m^2/g)
Baymag 30 HP	**96.5**	**96% < 75 µm**	–	**30**
Timab M98	**97**	**min. 77% < 75 µm**	–	**15 – 35**

Based on the information provided from manufacturer product specification sheets listed in Table 18, it is known that Baymag is a smaller particle with a more constant specific surface area and Timab M98 has greater portion of larger material and a large range of specific surface areas to be expected. The purity of Baymag and Timab M98 are relatively similar and no information was provided by the manufacturer regarding reactivity.

5.3.2. Magnesium Oxide Hydration

The methodology used in this paper was based off literature and MgO manufacturer procedures. A sample is grabbed from a hydrating MgO slurry, which in this work was typically a volume of 20 mL or greater. The sample is then filtered through a glass fiber filter (1.5 µm nominal diameter) using a vacuum pump to remove the water from the sample. The sample is then washed with at least a 10 mL volume of acetone as it remains filtering with the vacuum pump. A tared porcelain crucible is used to dry the solid sample for at least a day in an oven heated to about 105 °C. After drying the sample, it is cooled in a crucible and the dry aliquot mass (m_d) is recorded. The sample is then heated in muffle furnace as 600 °C for 2 hours (Tang, X., et al. 2014). The heated aliquot mass (m_h) can then be recorded. The values for m_d and m_h can be inputted into the following formula to determine hydration extent.

$$Hydration\ Extent\ (\%) = \frac{m_d - m_h}{m_h} \times \frac{M_{MgO}}{M_{H_2O}} \times \frac{100}{purity} \quad (34)$$

The molecular weight of MgO, M_{MgO}, is 40.3 g/mol and the molecular weight of water, M_{H2O}, is 18.1 g/mol. The hydration extent can also be normalized by the purity of the MgO that is being used, which is a fraction of the product that is purely MgO. There are some metal oxide impurities that can remain in the product after calcination and are reported by the manufacturer. Typical MgO purities used in this study have been between 0.95 – 0.98 mass MgO/mass product.

5.3.3. Magnesium Oxide Pilot Trials

The pilot reactor was operated essentially the same as historically operated, however since MgO provides a source of Mg and alkalinity, NaOH addition was not necessary throughout the trial. The pilot reactor was typically operated under Mg:P molar ratio or pH control, meaning that MgO was dosed as a constant Mg:P molar ratio or dosed based on effluent pH. Mg:P control utilized the daily reactor loading (kg P/day) as the basis for determining the required MgO dosage to the reactor. A Mg:P molar ratio could be targeted and the mass of Mg and MgO required could be solved for by using the stoichiometric conversion between P, Mg and MgO.

$$Mass\ of\ MgO\ (kg\ MgO) = \quad (35)$$
$$P\ Loading\ rate\ \left(\frac{kg\ P}{day}\right) \cdot \left(\frac{kmol\ P}{30.97\ kg}\right) \cdot Mg{:}P\ Ratio\ \left(\frac{kmol\ Mg}{kmol\ P}\right) \cdot \left(\frac{24.3\ kg\ Mg}{kmol\ Mg}\right) \cdot \left(\frac{kmol\ Mg}{24.3\ kg}\right) \cdot \left(\frac{kmol\ MgO}{kmol\ Mg}\right) \cdot \left(\frac{40.3\ kg}{kmol\ MgO}\right)$$

Effluent pH control was based on conventional Pearl reactor control, except for utilizing NaOH, and dosed MgO slurry in an Mg:P molar ratio range depending on the deviation of process pH from pH setpoint. MgO was dosed to the reactor as a slurry and the slurry dosing configuration was altered 3 times throughout the trial as defined in Table 19.

Table 18:MgO Slurry Dosing Configurations

Slurry Configuration	Trial Operation Duration	Description
2018 Trial	June – Nov 2018	Dosed MgO continuously to reactor at a constant Mg:P
2019 Trial	March 2019 – Dec 2019	Dosed MgO intermittently within Mg:P 1:1 – 1.5:1 to maintain pH Setpoint
2020 Trial	April 2020 – Present	Trialed pH control, OP effluent control, and continuous vs. intermittent dosing

The 2.5-year MgO pilot trial contained different MgO slurry dosing configurations, MgO product (Timab M98 and Baymag 30 HP) and control strategies. All trial tests were performed with R3 initially seeded with 90 SGN material, no NaOH addition and a targeted influent centrate pH of 6.9 – 6.95. Table 20 defines each test performed on reactor 3.

Table 19:MgO Pilot Trial Specifications

Test Name, Design Load	Month; Year	MgO	Dosing	Other Notes
MgO + Acid, 1X	June 2018	Timab M98	Continuous direct dosing	Mg:P control
MgO, 1X	June–July 2018	Timab M98	Continuous direct dosing	Mg:P control
MgO +Acid, 1X repeat	July–August 2018	Timab M98	Continuous direct dosing	Mg:P control
MgO, 1X repeat	August 2018	Timab M98	Continuous direct dosing	Mg:P control
MgO, 2X	September-October 2018	Timab M98	Continuous direct dosing	Mg:P control
MgO, 3X	October-November 2018	Timab M98	Continuous direct dosing	Mg:P control
Mg(OH)2	December 2018	$Mg(OH)_2$ 60%	Continuous direct dosing	Mg:P control
MgO, 3X	March-April 2019	Baymag 30 HP	Intermittent, recirculation loop	pH Control
MgO, 2X	April-July 2019	Baymag 30 HP	Intermittent, recirculation loop	pH control
MgO, 2X	July-August 2019	Baymag 30 HP and Timab M98	Intermittent, recirculation loop	pH control, Increased Reactor Upflow Velocity
Heated MgO, 2X	September-October 2019	Timab M98	Intermittent, recirculation loop	pH control, MgO heated at 55 °C (131 °F)
Unhydrated MgO, 2X	October 2019	Baymag 30 HP	Intermittent, Eductor	Dosed MgO slurry instantly with an eductor on the recycle line
Heated MgO, 2X Repeat	December 2019	Timab M98	Intermittent, recirculation loop	pH control, MgO heated at 55 °C (131 °F)
Low Hydration MgO, 2X	April-July 2020	Timab M98 and Baymag 30 HP	Intermittent, recirculation loop, batching	Different MgO hydration extents tested

Effluent OP Control, 2X	September 2020	Baymag 30 HP	Intermittent, recirculation loop, batching	30 – 50% hydrated MgO, cascade effluent OP control

5.3.3.1. 2018 Pilot Trial: Continuous Direct MgO Dosing

The 2018 MgO pilot trial was referred to as the continuous direct dosing strategy consisting of MgO slurry being dosed continuously to the reactor from a continuously mixed 330-gallon tank by a peristaltic metering pump. The pilot reactor was operated under Mg:P control during the phase 1 configuration, e.g. a constant MgO addition achieved a specific Mg:P dosing ratio, typically specified an Mg:P within the range 1.12 – 1.5. Due to the insolubility of MgO, the slurry was assisted from the peristaltic metering pump to the reactor through the piping with non-potable water (NPW), labeled "carrier water", which is the disinfected treatment plant effluent. The MgO slurry concentration was typically prepared at a 10% m/m in the tote by manually adding MgO bags to NPW. When dosing to the reactor the slurry was carried by 10 L/min carrier water (NPW) which created a ~1% m/m slurry dosed to the reactor continuously. Two 330-gallon tanks were used to alternate slurry feed each day because MgO slurry batches were prepared and mixed continuously in advance for an average of 22 – 24 hours. This trial phase was performed with and without sulfuric acid (H_2SO_4) addition to the MgO slurry during batch preparation. Regarding early tests, H_2SO_4 was added to push the hydration reaction by adding hydrogen ions and promoting the dissolution of MgO. Figure 26 exhibits slurry configuration utilized during the 2018 trial testing of MgO for struvite precipitation.

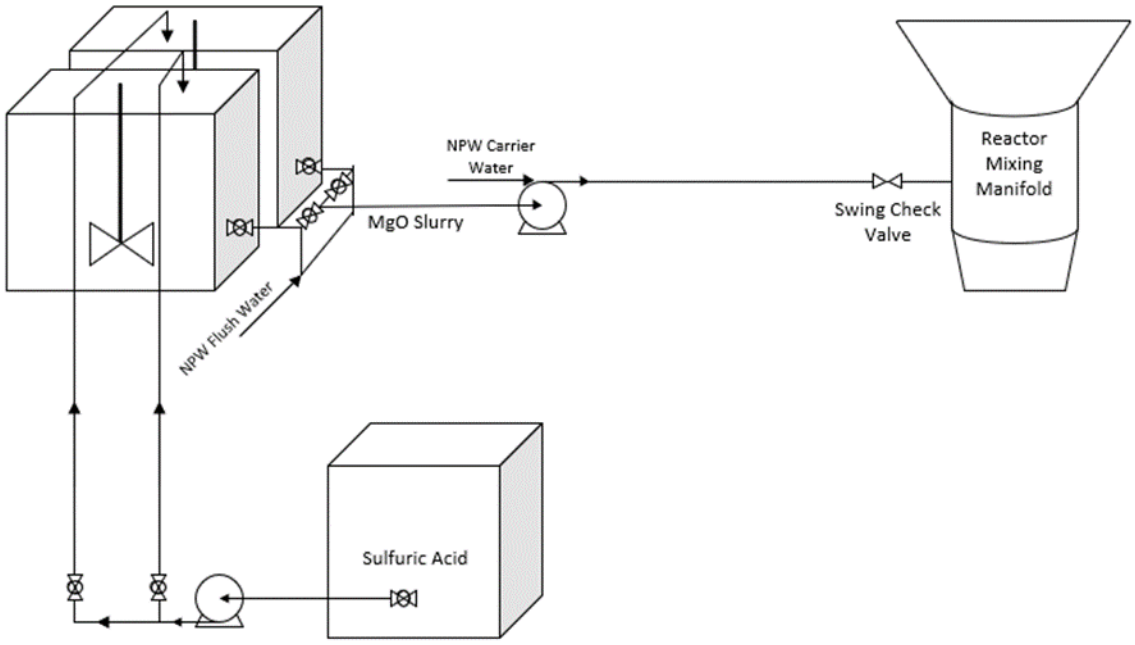

Figure 26:2020 Trial Configuration – Automated Batching Intermittent MgO Slurry Dosing Process Flow Diagram

This 2018 configuration was mainly used when dosing the reactor at its optimal design phosphorus loading rate of 65 kg/day, or 1X loading. 65 kg/day loading rate is the original design capacity of the Pearl 500 that was previously observed when using $MgCl_2$ to optimally recover struvite, after increasing the loading rate the P removal has the potential to drop below the optimal operation (<70% TP removal). A 1X loading rate can produce 0.5 metric tons (500 kg/day)of struvite each day based on the stoichiometric conversion between phosphorus and struvite.

The design phosphorus loading rate to the reactor was exceeded by 2X (1000 kg struvite/day) and 3X loading (1500 kg struvite/day) for two trial tests using this dosing configuration. Unfortunately, the MgO slurry totes could not hold enough volume to effectively feed previous MgO slurry concentrations to the reactor for 24 hours at 2X loading. The insolubility of MgO and higher slurry concentrations for higher loading caused many line plugging issues and hose replacements in the hose pump leading to inaccurate Mg:P dosages. Because of these limitations another process flow diagram was designed by Ostara and HRSD with installation completed in March 2019.

5.3.3.2. 2019 Pilot Trial: Intermittent MgO Dosing

The 2X phosphorus loading rate trials started in March 2019 with a new dosing configuration to determine if MgO addition could effectively yield more fertilizer than MgCl2 addition. Figure 27 depicts the 2019 trial dosing configuration used from March 2019 – January 2020. The idea behind this dosing configuration was to keep MgO

suspended and mixing with the use of a centrifugal pump and recirculation loop. This recirculation loop maintained a pressure setpoint with a pressure sensor by manipulating a variable-frequency drive (VFD) on the centrifugal pump motor output. An automated pinch valve was incorporated after the recirculation loop in order to dose a specific amount MgO intermittently to the reactor to within 1:1 – 1.5:1 Mg:P based on a PID controlled by the effluent pH deviation from setpoint. As the MgO acted as alkalinity addition to the pilot reactor, the MgO has a direct effect on the effluent pH. The automated pinch valve was programmed to normally be closed and open fully for 1 second at an inputted frequency that corresponded with a minimum time necessary for a 1:1 Mg:P and a maximum time necessary for a 1.5:1 Mg:P. After the MgO pinch valve dosed and closed a flushing water valve would open and clean the line of any MgO for an inputted duration of time (seconds). This dosing strategy was referred to as intermittent recirculation loop dosing strategy and represents a typical slaking system.

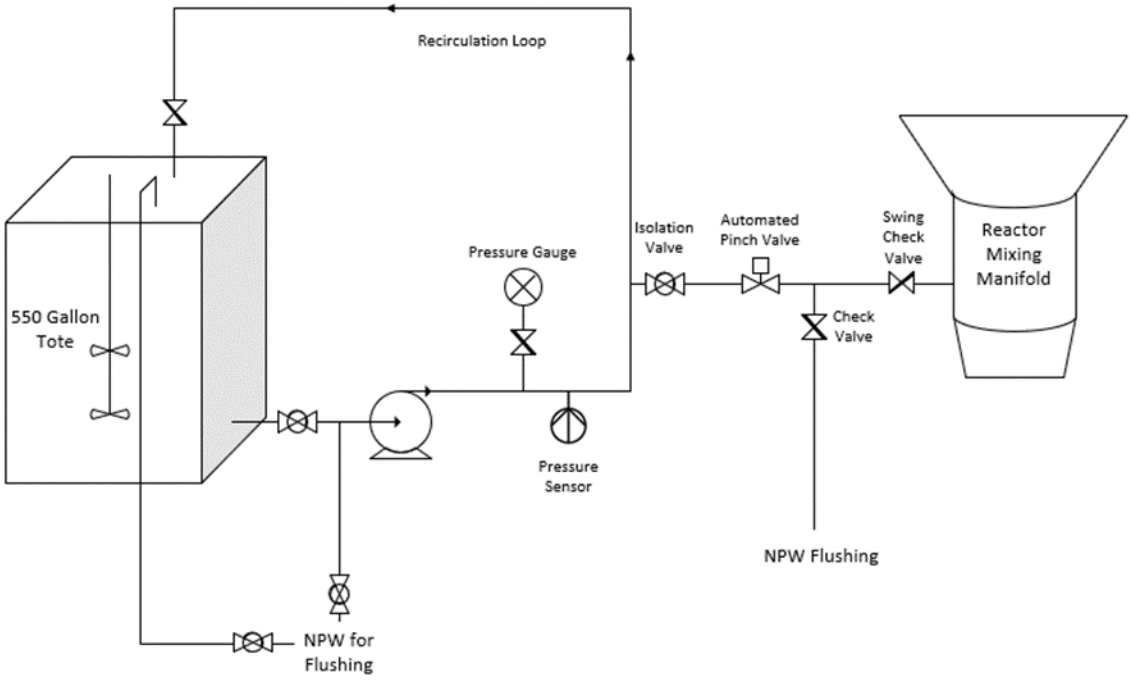

Figure 27:2019 Trial Configuration – Intermittent Recirculation Loop MgO Slurry Dosing Process Flow Diagram (March 2019 – January 2020)

Tank volume was increased to test higher reactor loading rates and incorporating a recirculation loop and centrifugal pump allowed higher slurry concentrations (% m/m) to be tested without line-plugging. A submersible heater was also flanged the side of the tote in September 2019 to provide heat to the slurry and promote MgO hydration while mixing. A pinch valve on the recirculation loop discharge provided back pressure to the recirculation loop and relieve to the centrifugal pump.

This dosing system was successful at preventing line plugging and keeping the MgO in suspension due to the pressure of the recirculation loop and intermittent dosing at higher and more reliable flow rates. However, this configuration did not allow for every test that was later considered in late 2019 and 2020.

5.3.3.3. 2020 Pilot Trial: Automated Batching Process

With the hydration of MgO in 2019 trials better understood it became of interest to test low hydration extent MgO for struvite precipitation. If substantial hydration was not necessary for optimal operation than the slurry would not need to be retained in a tank for an extended period and the tank volume could be smaller.

Before phase 3 dosing strategy was constructed, an unsuccessful low hydration test took place by piping an eductor jet pump to the suction side of the recycle pump of reactor 3 and intermittently dosing MgO slurry to the reactor. Due to the MgO being introduced outside of the injection port, optimal reactor operation was not achieved, and this configuration was discontinued after 4 weeks and consequently phase 3 was implemented in 2020.

The 2020 trial dosing configuration included an automated batching process that maintained the slurry volume in the 60-gallon tote between a high level and low level. The batching process was performed using an eductor (venturi jet pump) providing NPW as the driving fluid on the inlet side and MgO from the hopper on the suction side. The desired MgO slurry was premixed in the eductor and dosed to the slurry tote. The program batched an appropriate volume of NPW and mass of MgO to achieve the inputted slurry concentration (% MgO m/m) each time a low level was measured by the level indicator on the slurry tote. After the slurry was batched to the tote the dosing configuration was set up essentially the same as the previous design with a recirculation loop pressurized to a pressure setpoint by the VFD on the centrifugal pump motor. The automated pinch valve off the recirculation loop was used for intermittent MgO dosing. Intermittent dosing used the valve fully open for 1 second with the opening frequency input manipulated to achieve a 1:1 – 1.5:1 Mg:P dosing range utilizing PID control. A "maximum time (seconds) between opening" was inputted to achieve a minimum Mg:P (1:1) dosing and a "minimum time (seconds) between opening" was inputted to achieve a maximum Mg:P (1.5:1) dosing. The 2020 dosing configuration was multifaceted in that it could operate under different control strategies e.g. pH control, OP removal control, cascade OP removal control, Mg:P control, intermittent or continuous dosing. Continuous dosing could be performed by manually setting the automated pinch valve % open position and measuring the tote drawdown over a given time range to ensure dosing was at a flow rate necessary to meet a desired Mg:P dose. Figure 28 shows the pipe flow diagram for the phase 3 slurry dosing configuration.

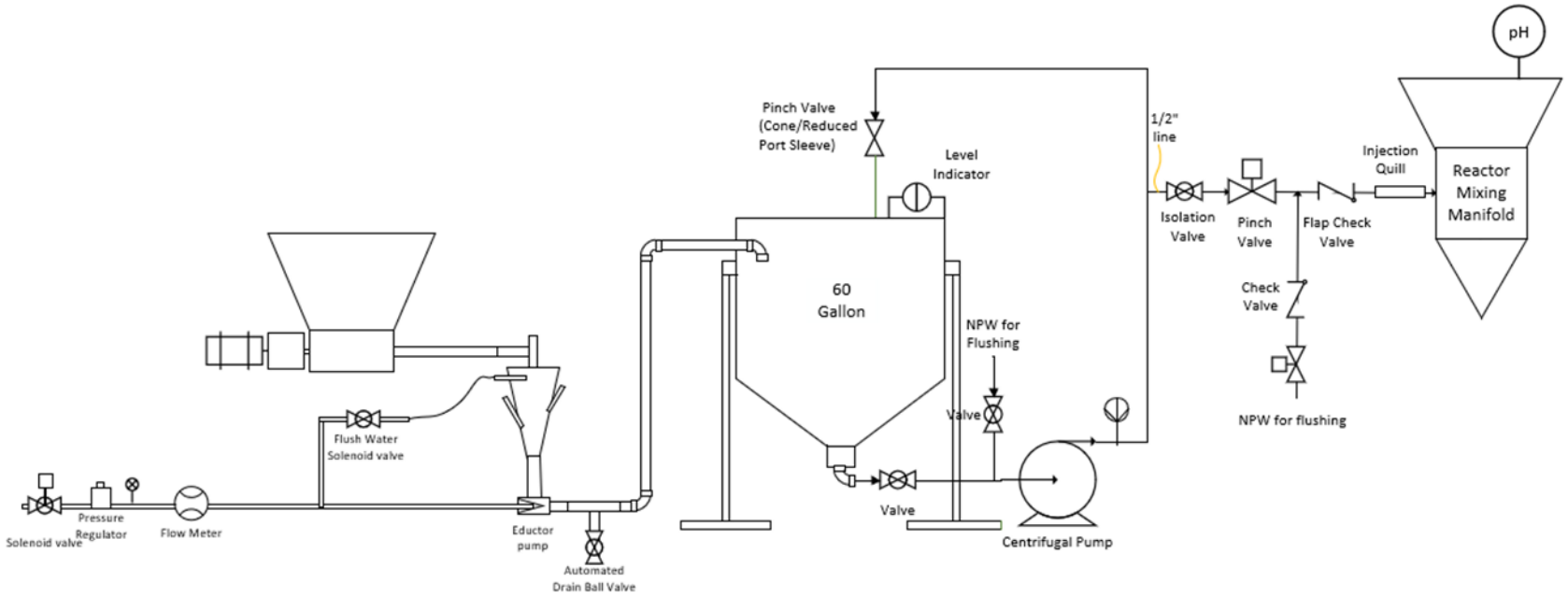

Figure 28: 2020 Trial Configuration – Automated Batching Intermittent MgO Slurry Dosing Process Flow Diagram

Other modes of control were also of interest, such as OP removal (%) control, cascade OP removal (%) control and continuous dosing repeated with the improved dosing configuration. Cascade control, flow diagram in Figure 29, utilized a cascade PID with the primary controller obtaining an OP removal (%) setpoint by manipulating the pH setpoint. The pH setpoint outputted from the primary controller was then used as the process variable for the secondary controller that was responsible for manipulating the MgO dosing valve frequency (seconds).

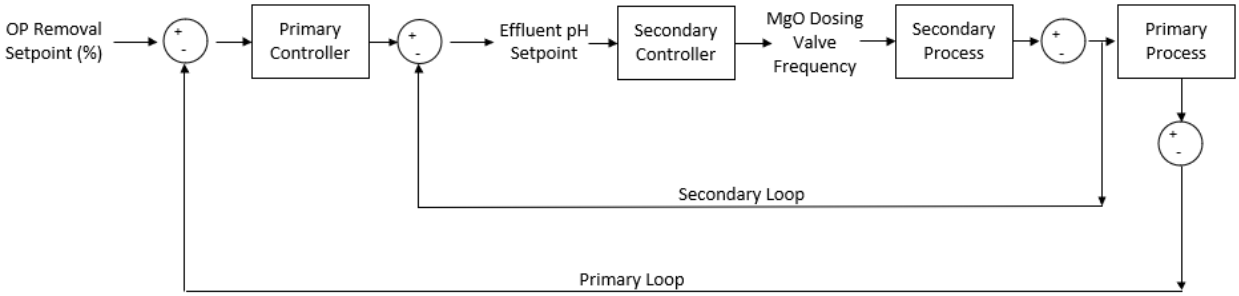

Figure 29:OP Removal Cascade Controller Flow Diagram

The controller was tuned utilizing the root mean square error (RSME) method which used the following equation for a certain number of observations throughout a defined time duration:

$$RMSE = \sqrt{\frac{\sum_{i=1}^{N}(observed_i - setpoint_i)^2}{N}} \quad (36)$$

Firstly, iterations were done for the secondary loop under typical pH control with different P&I parameters to evaluate which P&I was best when using the RMSE method. After the secondary loop was tuned, the RMSE method was performed on the primary controller under cascade control to determine the primary P&I parameters that worked best.

5.3.4. Pilot Reactor Operation

The piloting of MgO for struvite precipitation was performed utilizing a Pearl 500 reactor. Operation was typical to conventional MgCl2 reactor operation with the exception of $MgCl_2$ and NaOH addition. The conventional Pearl process can be seen in Figure 30.

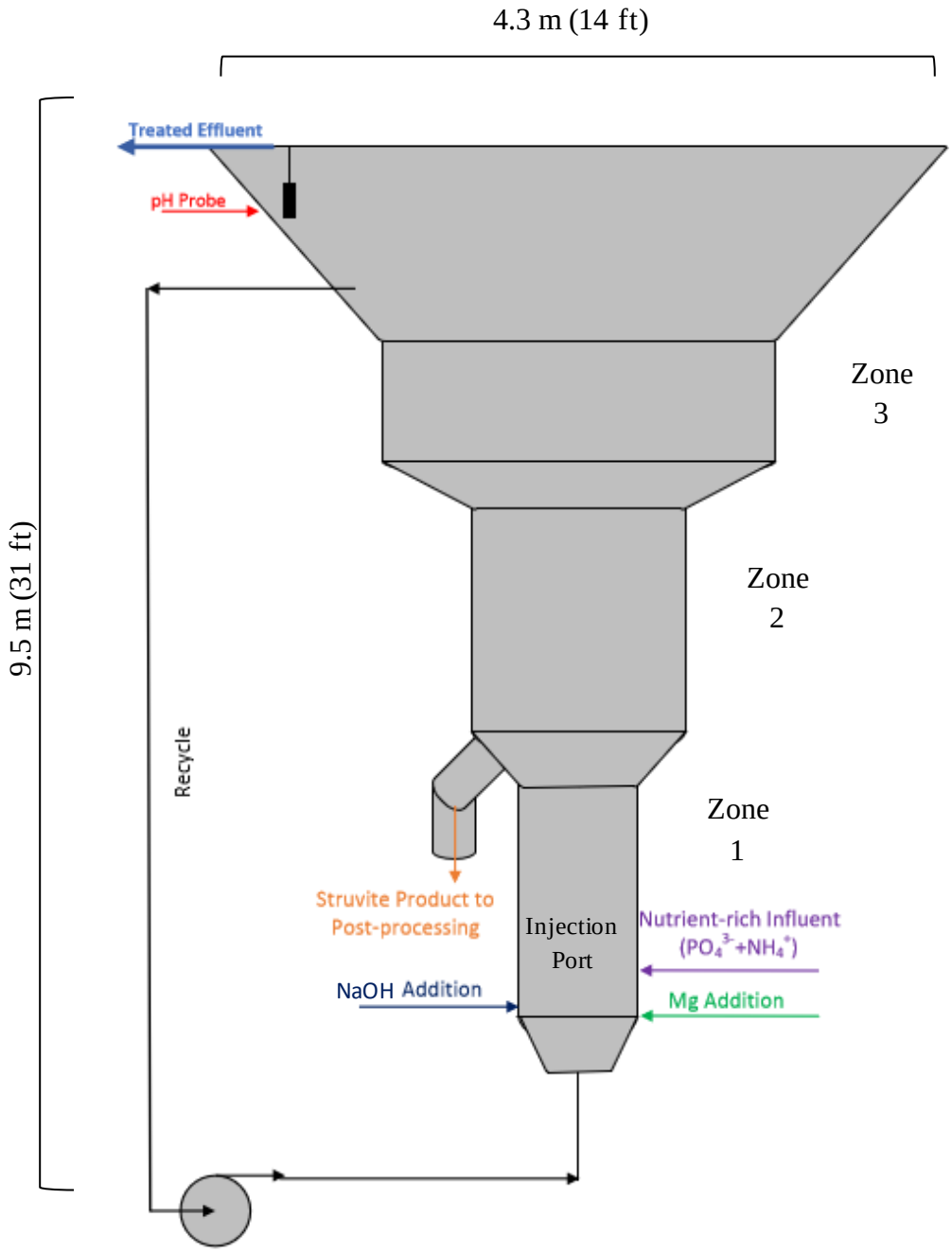

Figure 30: Conventional Pearl Reactor Schematic

The operation of reactor 3 was typically done to achieve a constant Mg:P or an Mg:P molar ratio range to achieve an effluent pH setpoint. The Mg:P dosing was performed continuously at a constant Mg:P and intermittently within a specified Mg:P range. The amount of MgO dosed to the reactor with respect to time was determined by the following formula.

$$\boldsymbol{MgO\ Dosage\ Volume}\left(\frac{\boldsymbol{L}}{\boldsymbol{min}}\right) = \quad (37)$$

$$\frac{P\ Loading\ rate\ \left(\frac{kg}{day}\right)\cdot\left(\frac{day}{1440\ min}\right)\cdot\left(\frac{kmol\ P}{30.97\ kg}\right)\cdot Mg{:}P\ Ratio\left(\frac{kmol\ Mg}{kmol\ P}\right)\cdot\left(\frac{kmol\ Mgo}{kmol\ Mg}\right)\cdot\left(\frac{40.3\ kg}{kmol\ MgO}\right)}{MgO\ slurry\ density\ \left(\frac{kg}{L}\right)\cdot slurry\ conc.\left(\frac{mass\ MgO}{mass\ slurry}\right)\cdot MgO\ purity\ \left(\frac{mass\ MgO}{mass\ product}\right)}$$

The MgO slurry density varies depending on slurry concentration (%MgO m/m) used to dose the reactor. The formula used for slurry density determination is below where the density (ρ) of MgO is 3.58 kg/L and the ρ of water is 1 kg/L.

$$\boldsymbol{Slurry\ \rho\left(\frac{kg}{L}\right)} = \left(\frac{MgO\ slurry\ conc\left(\frac{m}{m}\right)}{MgO\ \rho\left(\frac{kg}{L}\right)} + \frac{1-MgO\ slurry\ conc\left(\frac{m}{m}\right)}{Water\ \rho\left(\frac{kg}{L}\right)}\right)^{-1} \quad (38)$$

Slurry concentration calculations and dry feeder motor calibration curves used for slurry batch makeups are further defined in the Appendix (Supplemental Information).

Influent and effluent phosphorus concentrations were typically measured each weekday to determine the pilot reactor operation. Influent phosphorus concentration was inputted into the control system to alter the centrate feed flow to the reactor and maintain the specified phosphorus loading rate (kg P/day). Magnesium was also measured each weekday on the influent and the effluent to help monitor the system and verify Mg dosing to the reactor was adequate. Table 21 defines the laboratory methods used to measure constituent ion concentrations and other parameters of interest during operation. Hach dr2800 and dr3900 spectrophotometers were used for Hach tube daily analysis.

Table 20: Daily Reactor Operation Laboratory Analysis

Parameter	**Method**
Ortho Phosphate	Hach TNT 845, Ascorbic Acid
Total Phosphorus	Hach TNT 845, Ascorbic Acid
Magnesium	Hach TNT 849, Metal phthalein
pH	Orion Star pH Meter

Total phosphorus (TP) concentrations were quantified as PO_4-P present in solution and in solid material after digesting the samples in a Hach digestion block at 100 °C. Magnesium measured using Hach tubes and the spectrophotometer only captured the soluble form. The Central Enviromental Laboratory (CEL) at HRSD also analyzed samples from the SRF influent and effluent on Tuesday, Thursday and Sunday each week. The results from the CEL are inputted into HRSD process operation reports and PARCView PRISM which is a real-time data visualization program used for the SRF. Tests that were performed at the CEL are specified in Table 22.

Table 21:HRSD CEL SRF Sample Analysis

Parameter	Method
Total Magnesium	ICP-AES (EPA 200.7 rev 4.4)
Soluble Magnesium	Filtering w/ ICP-AES (EPA 200.7 rev 4.4)
Total Phosphorus	Auto Analyzer Flow Injection Analysis (Lachat 10-115-01-1-E)
Ortho Phosphorus	Flow Injection Analysis
Total Ammonia	Auto Analyzer Flow Injection Analysis (Lachat 10-107-06-1-J)

Parameters in Table 22 were monitored and recorded to further compare pilot reactor operation to conventional $MgCl_2$ operation. Reactor operation and performance included OP removal, TP removal, struvite yield, average particle size and Mg:P dosing. These parameters listed in Table 23 created a systematic way of comparing the pilot reactor utilizing MgO with the conventional reactors utilizing $MgCl_2$.

Table 22:Pilot Reactor Monitored Parameters

Parameter	Unit
OP Removal	%
TP Removal	%
Reactor Loading Rate	kg P/day
Mg:P Dosage	Mol Mg/Mol P
Effluent Turbidity	NTU
Reactor Differential Pressure	kPa
Harvested Product Size	SGN (Size Guide Number) = mm × 100
Total Harvested Product	kg or US tons
Struvite Yield	% Harvested Struvite from Theoretical Production

Effluent concentrations and pH values were utilized to ensure the Mg:P and pH leaving the reactor were optimal for struvite precipitation. Reactor differential pressure was measured to estimate of reactor inventory and trigger the harvest system by a pressure setpoint. The parameters in Table 23 were used to show overall performance of each pilot test and baseline $MgCl_2$ operating durations to determine if MgO usage was successful and comparable to typical reactor operation.

Daily influent and reactor effluent analysis performed with Hach tubes were used to monitor the daily efficiency of the pilot process. Struvite precipitation efficiency is determined by how much phosphorus is removed from the system and recovered as struvite. Phosphorus removal is important when monitoring the struvite precipitation real-time as it can infer how well influent centrate is being treated for phosphorus and how much struvite is being produced in the reactor.

$$\boldsymbol{Phosphorus\ Removal}\ (\%) = \left(\frac{Influent\ Phopshorus\left(\frac{mg\ PO4-P}{L}\right) - Effluent\ Phosphorus\ \left(\frac{mg\ PO4-P}{L}\right)}{Initial\ Phosphorus\ \left(\frac{mg\ PO4-P}{L}\right)}\right) \times 100 \quad (39)$$

This equation assumes pure struvite has been precipitated in the system and phosphorus is either recovered as struvite or released from the system as soluble phosphorus or small struvite fines in the effluent. This assumption is reasonable as the pH is not intentionally operated above a pH of 8.2 where other solid P-containing impurities can start precipitating. Phosphorus removal can be calculated for OP or TP removal. OP removal is measured to quantify the soluble phosphorus removed from the centrate and TP removal measured the soluble and particulate phosphorus removed from the centrate. TP removal can quantify how well fines are being contained within the reactor. Whatever is washed out of the reactor as soluble phosphorus or struvite fines will return to the head of the wastewater treatment plant. Struvite precipitation was also monitored by defining a theoretical struvite recovery that could be achieved based on the known amount of phosphorus load into the system throughout time:

$$\boldsymbol{Theoretical\ PO_4 - P\ Recovery\ as\ Struvite}\ (\boldsymbol{g\ PO_4 - P}) = PO_4 - P\ Mass\ Load\ (g\ PO_4 - P) \cdot \left(\frac{245.41\ g\ Struvite}{mol\ Struvite}\right)\left(\frac{mol\ Struvite}{mol\ PO_4 - P}\right)\left(\frac{mol\ PO_4 - P}{30.97\ g\ PO_4 - P}\right) \quad (40)$$

$$\boldsymbol{Struvite\ Recovery}\ (\boldsymbol{Yield})(\%) = \frac{Total\ Weight\ of\ Struvite\ Harvested\ (kg)}{Theoretical\ PO_4 - P\ Recovery\ as\ Struvite\ (kg)} \times 100 \quad (41)$$

This mass balance calculation is used to determine the yield, or theoretical struvite production based on total influent phosphorus mass and compare to the amount of struvite that was physically harvested from the system (Adnan, A., et al. II, 2003). Fines wash out during operation can diminish the recovered struvite mass and cause deviation from the theoretical recovery. Imhoff cones were taken when reactors were sampled to measure the settled solid volume and quantify the centrate solids in the system and/or fines washout that was occurring. The pilot reactor also had a turbidity meter at the top of the reactor in the clarifier launder to qualitatively monitor performance and compare TP removal to the turbidity measured in real-time.

5.3.4.1. Pilot Reactor Operation: Harvesting

Struvite was initially harvested from the pilot at the beginning of a trial after 3-4 days of efficient operation and as the differential pressure in the reactor (dP) measured around 7.0 kPa. After the initial harvest, 1 ton of struvite was harvested every other day or every day to control the reactor inventory and limit fines accumulating and settling on the side walls of the clarifier, referred to as beaching. The amount of struvite beaching settled in the clarifier was estimated throughout the trials after it was initially

noticed above the clarifier surface in December 2018 and became a frequent occurrence in the Summer of 2019. Occasionally, fines were pushed back down into the reactor to fluidize the material.

Struvite was harvested by dewatering the product on a vibrating sieve screen to separate the struvite from the liquid and sending the dewatered product through a hot-air fluidized bed dryer. Once the material was dried it was classified by sieve screens and stored in the respective product size silo. Dried struvite was manually sieved to determine the average size being harvested from the reactor in SGN (Size Guide Number). The dryer was limited on the product size that is could effectively be dried and when product was too small it would be manually pulled out of the reactor harvest leg, which is known as wet harvesting. Wet harvest supersacks were dried for at least 2 weeks on plant site before being sent off site for additional refining. Wet harvesting was performed on the main harvest leg of the reactor as well as a retrofitted upper harvesting leg. Quality control samples were taken of supersack from wet harvest or from the silo bagging system for nutrient analysis to ensure that the bagged struvite had an acceptable purity. XRD analysis was also performed on specified QC samples and grab samples from the pilot during different trials to determine if there were any distinguishable impurities.

Once a pilot test was finished, the reactor was emptied of all leftover material by wet harvesting. Typically, the reactor would need to be cleaned every 3 months or after 3 pilot tests. Cleaning the reactor consisted of capturing the struvite product, draining the remaining liquid, inspecting the upper clarifier and lower injection port area, removing the recycle line below the injection port, removing scale, and then acid washing the reactor once reassembled. Scale build up would occur in the lower reactor early in the trial and scaling seemed to shift to the upper portion of the reactor in late 2019.

5.3.5. Continuously Monitoring Ortho-Phosphorus Analyzer

An analyzer was placed on the reactor clarifier launder to measure the effluent ortho-phosphorus concentration continuously. The continuously monitoring analyzer consists of a two-stage filtration system with the first filter in the reactor effluent and the second filter used for analyzer protection. The analyzer measures phosphorus on a scale from 2-50 mg/L PO4-P and is capable of diluting samples by 2X, 5X or 10X as necessary. Sample dilution and flushing of analyzer and filtration system is done with DI water. Pressure readings of the filter on the reactor effluent can prompt a cleaning cycle to remove any fines or small particulates on the effluent filter. The analyzer measures phosphorus utilizing the molybdovanadophosphoric acid method. The phosphorus concentrations were sent to the distributed control system (DCS) from the PLC in the analyzer and visible on the computer.

5.4. Results and Discussion

5.4.1. Baseline Reactor Operation: $MgCl_2$ with pH Control

Prior to 2018 all Pearl reactors were run with $MgCl_2$ and NaOH and typically operated between design load (1X) and 1.5X design load to process centrate accordingly. Typical reactor operation is a pH-controlled process using the pH probe on the reactor effluent. Data used in this section are from reactor grab samples and CEL analysis performed on Tuesday, Thursday, and Sunday. Struvite product size from the reactors is typically between 90 – 350 SGN (average diameter of 0.9 – 3.5 mm). The phosphorus removal and struvite yield of the SRF prior to the pilot startup was considered the baseline operation for the MgO pilot to be compared to. Data from 2017-2019 were utilized to develop this baseline performance which can be seen in Figure 31. Data were analyzed for an individual reactor, a composite of 2 reactors or the whole SRF depending on the centrate inventory and reactor demand during that time. Durations were chosen based on consistency of reactor(s) operation to avoid long periods of time where the reactors were idled or off.

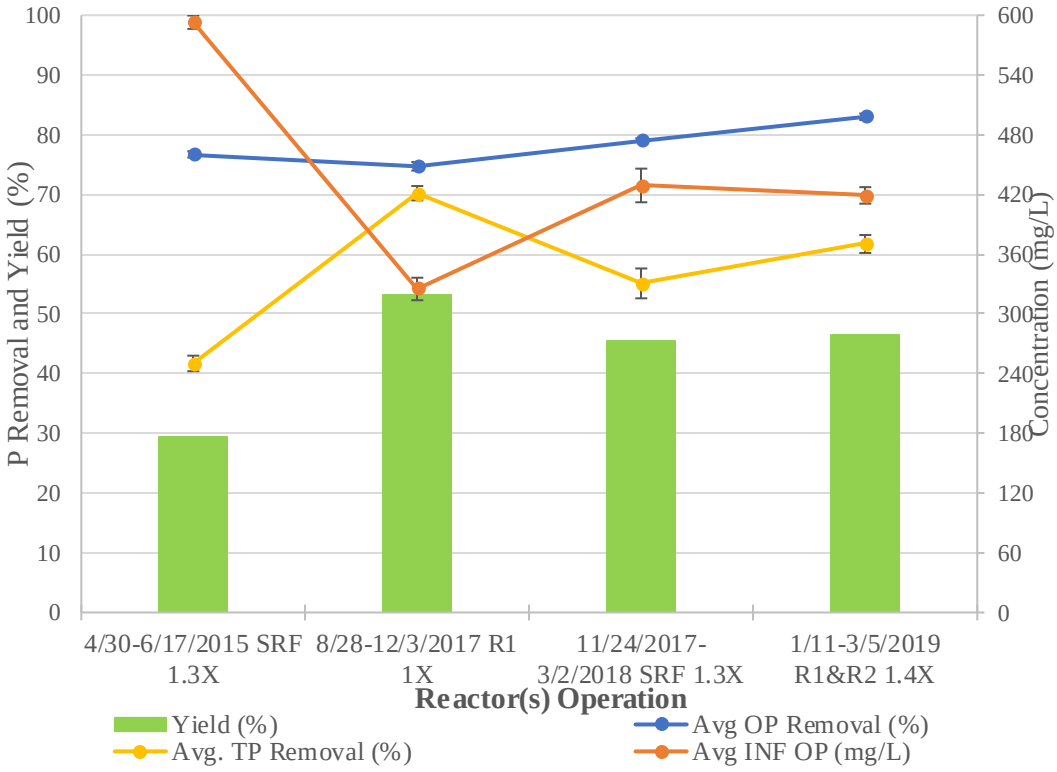

Figure 31:Reactor Baseline Performance Prior to MgO Pilot

Based on these operation durations in Figure 31, it is observed that the baseline performance historically operated between 74-84% OP removal while the TP removal was between 62-72%. It seems that during these reactor operations the influent phosphorus concentrations inversely correlated with the baseline performance yield of the reactors. For these operations, the yield of the reactors/SRF seemed to be lower as the influent

phosphorus concentrations were greater. Traditionally, the OP and TP removal never aligned with the yield when trending performance throughout multiple test durations. Theoretically the TP removed from the system should account for all the struvite recovered; however, this is not observed. Figure 31 shows lower yields than theoretically achieved based on removals, with struvite yield typically 50% or less of the influent phosphorus loading. Based on grab samples, the SRF removed 10% or more TP than was recovered as struvite depending on reactor operation. This historical gap (poor closure of mass balance) between removal and yield has been researched and analyzed on numerous occasions to no avail. An error at times as large as 30% of theoretical struvite product formation seems unthinkable when considering tons of material lost after months of operation. Figure 32 shows the mass imbalance between influent phosphorus loading and effluent phosphorus forms. There is a loss of phosphorus mass that cannot be accounted for as soluble or particulate phosphorus leaving in the reactor effluent or struvite recovered through harvesting the reactor, this is defined as absent phosphorus (absent P).

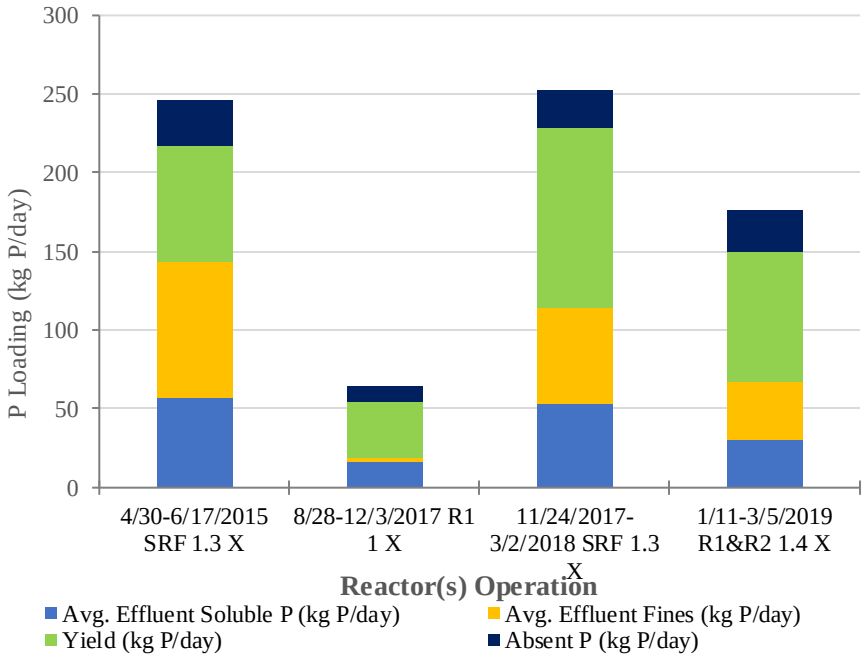

Figure 32:Phosphorus Mass Allocation at the SRF During Baseline Operation

The data in Figures 31 and 32 generated curiosity about what could be causing the low yield and the phosphorus mass imbalance at the SRF. Theories for the inconsistency between removal and yield were:

- durations the reactor had been in service without being cleaned
- influent supersaturation
- reactor loading rates
- inaccuracy of effluent pH probes and reactor control
- the time that the reactor had spent idled

- loss through the dewatering screen
- degradation of struvite in dryer
- inaccurate reactor effluent sampling

Reactor effluent sampling by operators for CEL analysis was a concern until June 2018 when sampling procedures were clarified. Correct reactor effluent samples were taken from the reactor weirs. Reactor effluent samples were occasionally grabbed where the effluent was introduced to the SRF drain, which at the time was supplied with NPW dilution. Invalid effluent samples could not be identified from data prior to June 2018. NPW dilution to the SRF drain was eliminated in June 2018. This theory was debunked later in 2019 as operator samples were consistently grabbed from the reactor weirs and a mass imbalance was still observed. Other theories for the mass imbalance were also invalidated by:

- Measuring OP and TP samples off dewatering screen effluent during harvest
- Analyzing historical trends of mass imbalance with influent P concentrations and reactor loading
- Nutrient and XRD analysis of dried struvite product

It was noticed in late 2019 that the baseline operation performance gap between removal and struvite recovery of the pilot reactor and the $MgCl_2$ reactors had dissipated. A theory for the sudden convergence of phosphorus removal and yield is the baffle removal from the reactors which happened in late 2019. Vertical sections of the reactors were baffled into quadrants to promote turbulence and mixing; which could have also promoted disturbance, struvite scaling, or fines washout (not well capture in effluent sampling) due to irregular flow patterns through the length of the reactor. The P mass balance convergence correlates with baffle removal and the previously observed mass imbalance was not justified by other theories. R1 and R2 had all three baffles while R3 had only the lower baffle in 2019. The two upper baffles of R3 were removed prior to 2014 due to the excessive scale build up that halted reactor operation and could not be removed effectively with acid washing. The last remaining baffle from R3 was removed in July 2019. All baffles from R1 and R2 were removed in July 2019 and October 2019, respectively, along with the scale that had accumulated on the baffles. A picture of a baffled reactor, viewed from the top clarifier portion of the reactor, can be seen below in Figure 33.

Figure 33:Reactor Baffle

Substantial scaling was noticed in the lower portion of the reactor where scale cavities were present from recycle flow patterns. Scaling that occurred in the lower region of the reactors can potentially alter the area that flow passes through, thus influencing upflow velocity experienced in different sections of the reactor. Differences in upflow velocity throughout the cross-sectional area could be the cause of the observed billowing of fines in the clarifier by irregular flow rates and flow patterns. Figure 34a shows the scaling that occurred after 3 months of reactor operation prior to being acid washed. When looking into a sight glass of the reactor in June 2019 it was noticed that scale present above the injection port in the reactor shown in Figure 34a could not allow for the injection port area of the reactor to be inspected when viewing from above. Where the reactor meets the injection port portion of the recycle line was covered with scale and the lower baffle, which is the vertical structure seen in Figure 34a, had 2-3" of scale in areas. It can be seen how the scale can potentially obstruct flow by decreasing the cross-sectional area in the lower portion of the reactor. It is hypothesized that the presence of the lower baffle and high influent phosphorus concentration, and thus solution supersaturation, could have promoted the excessive scaling and inverse relationship between influent phosphorus concentration and yield when considering baseline $MgCl_2$ reactor operation. Figure 34b represents the lower portion of the reactor after 9 months of reactor operation prior to acid washing.

Figure 34:a. Scaling of Lower Portion of Reactor 1 after 3 Months of Operation (July 2019); b. Scaling of Lower Portion of Reactor 1 after 9 Months of Operation (September 2020)

Both Figure 34a and 34b were taken from the same location of reactor 1 at similar angles, the only physical difference between these pictures is the existence of the lower baffle. The difference in scale observed during these reactor inspections is noteworthy and the presence of the lower baffle observed in Figure 34 may have aided to the development of the scale in the bottom of reactor 1 in June 2019, making the lower portion of the reactor indistinguishable. Reactor performance after baffle removal from the $MgCl_2$ reactors between 2015 – 2020 can be observed in Figure 35 (data in Supplemental Information) and the results for phosphorus removal and yield show more consistency. The yield values seem to represent the average removal experienced throughout the duration of reactor operation with less error. When analyzing operation after baffle removal, it does not seem the yield is inversely correlated to the influent OP concentrations as it had once appeared to when the baffles were in place.

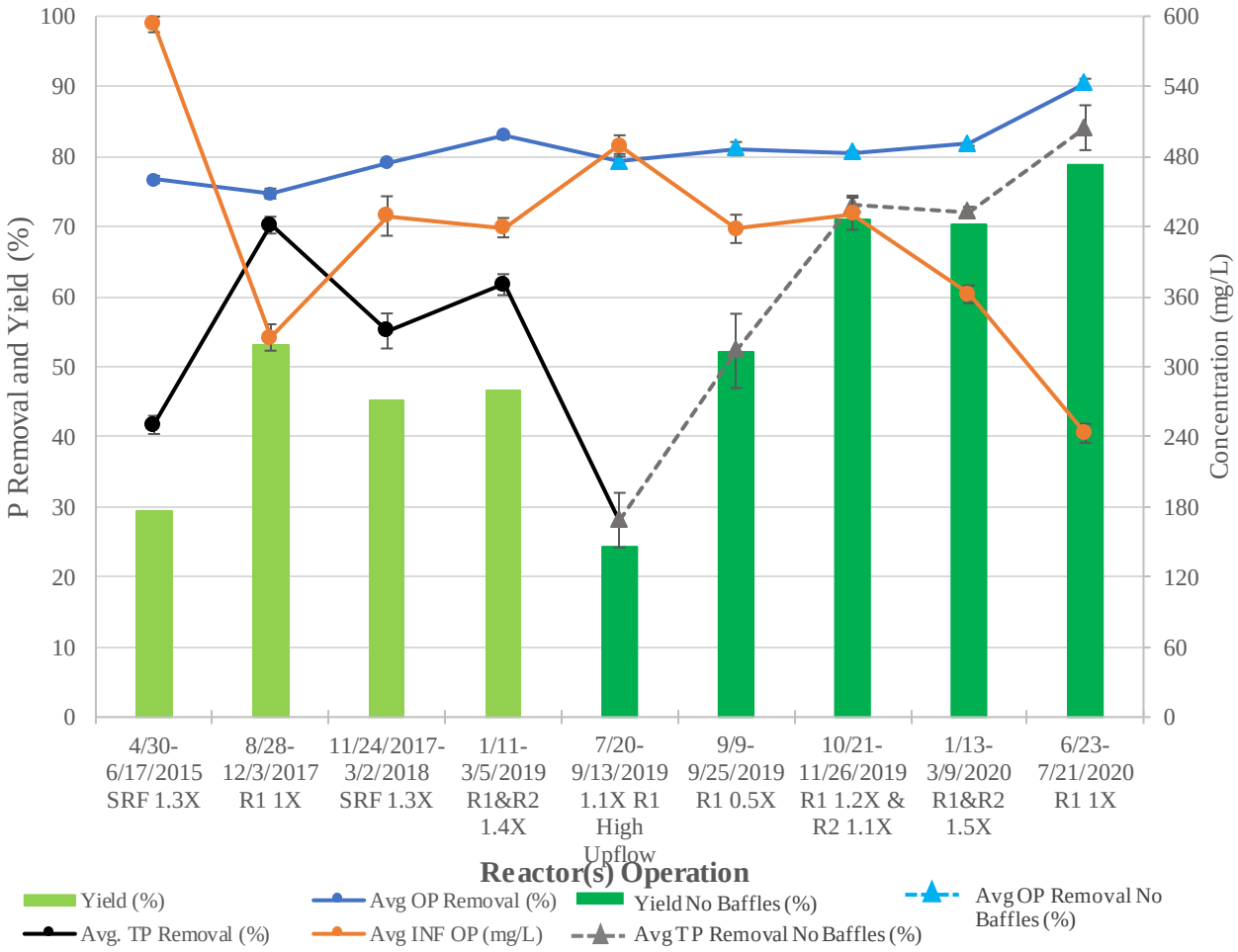

Figure 35:Average Reactor Baseline Performance with and without Baffles

The removal of the baffles eliminated mass balance problem under normal reactor operation as current loss of yield could be better explained by average TP removal. It can also be observed that the OP and TP removals improved even with reactor loading greater than design capacity after the baffles were removed. Previously, reactor loading greater than 1X resulted in TP removal around 60%; however, in January 2020 R1 and R2 operating at 1.5X design load were able to remove 72% TP.

With the closing of the phosphorus gap noticed in 2019, it was desirable to classify all phosphorus loading to the SRF or reactor as a form of effluent phosphorus. Ideally, phosphorus can leave the reactor as soluble P, fines, or harvested struvite. Based on the influent P loading, it was possible to allocate all P to an effluent type and determine if there was a significant fraction still missing after baffle removal. Figure 36 displays the absent P observed during baseline reactor operation and how convergence of phosphorus removal and yield occurs after the baffle removal of reactor 1 during July of 2019.

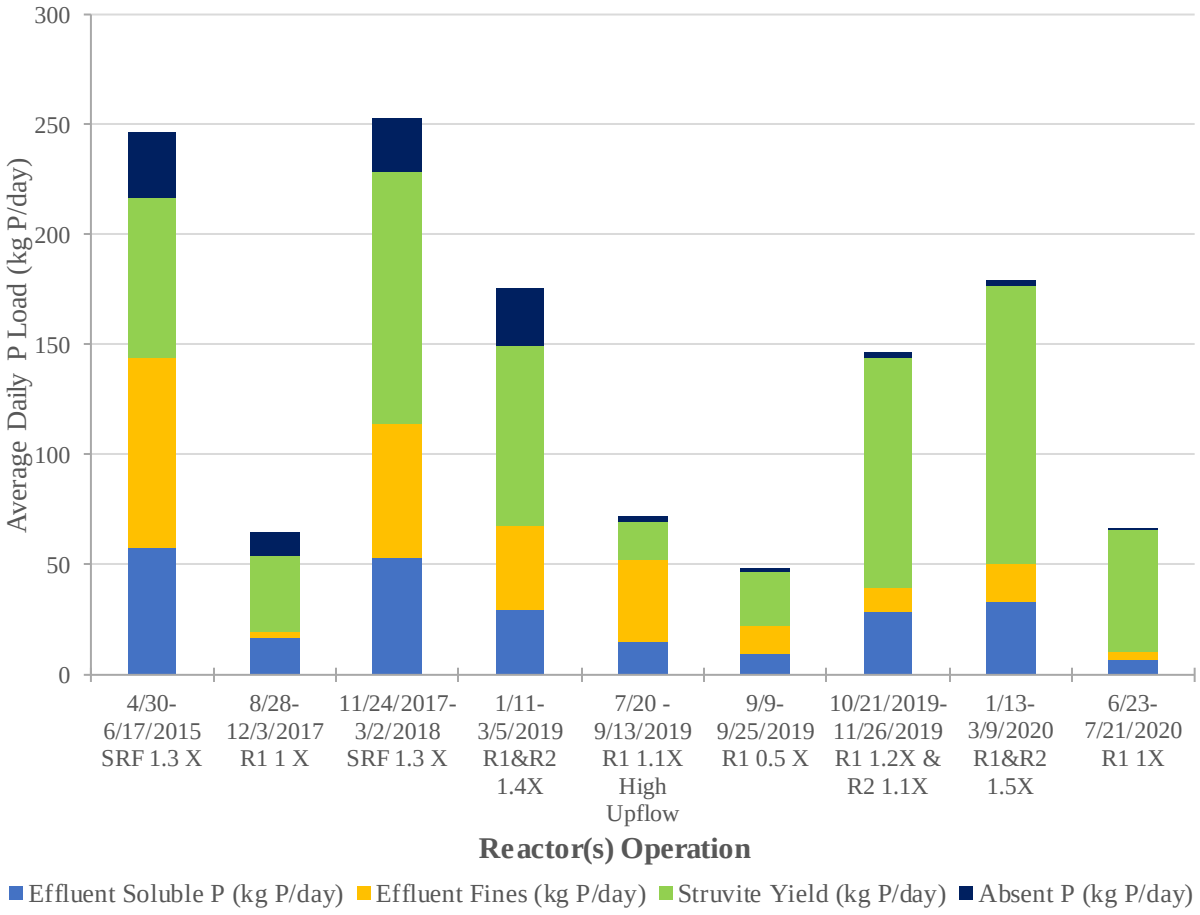

Figure 36:Phosphorus Allocation of the SRF Reactor(s)

It was observed during the high upflow reactor operation in July 2019 that a larger portion of phosphorus was allocated as effluent fines due to the fines washout that occurred. The most current phosphorus allocation of the MgCl2 occurred in July 2020, a year after baffle removal, and almost all phosphorus entering the SRF can be allocated to a form of effluent phosphorus. To further investigate the effects of the baffles, data were analyzed from November 2017 – April 2018 and March – April 2019 when both reactor 1 and 2 had all baffles, while reactor 3 only had the lower baffle present. Prior to 2015 the upper two baffles of reactor 3 were removed because the scale that had accumulated on the baffles was extremely problematic and resistant to the reactor acid washes. Figure 37 shows the allocation of phosphorus of the SRF from each reactor during the specified operation times and Figure 38 shows each reactor yield during this time. These durations were analyzed as there was historical data available for the harvesting system that allowed struvite product to be allocated to the individual reactors as all were being operated.

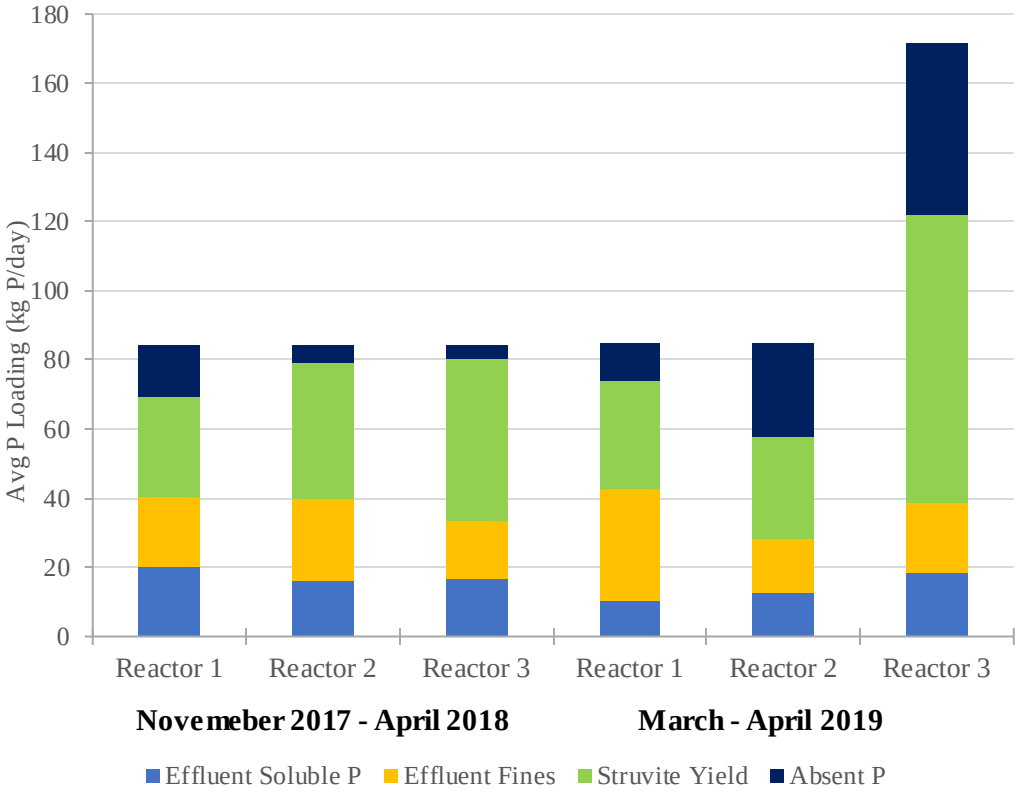

Figure 37: Phosphorus Allocation for each SRF Reactor for Specific Durations

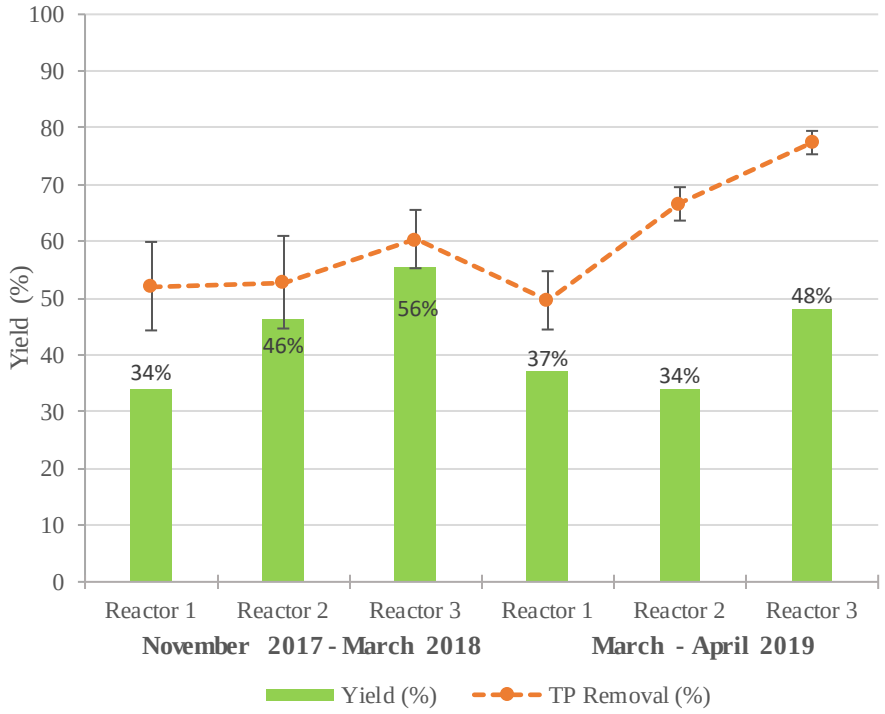

Figure 38: Struvite Yield and TP Removal of each SRF Reactor for Specific Durations

Figure 37 defines the total mass of the influent reactor loading as either struvite harvested, soluble phosphorus in the effluent, or solid struvite in the effluent. It can be observed in Figure 38 that reactor 3 yielded more struvite than reactor 1 or 2 during these durations, while sometimes obtaining higher phosphorus removal. Reactor 3 still shows a considerable amount of phosphorus that cannot be accounted for as effluent fines or soluble phosphorus, especially with a higher P loading rate in March – April 2019. During March – April 2019, an autosampler was placed on the SRF effluent to try and close the gap between P removal and struvite yield. The missing phosphorus from the SRF was not accounted for when compositing each hour of SRF operation during the day and this may have been due to the randomness of struvite fines billowing in the reactor clarifiers or the sampling method from the SRF drain line. A billow of fines from reactor 1 can be observed in Figure 39 below.

Figure 39: Billow of Struvite Fines in Reactor 1 Clarifier (July 2019)

The yield of R3 seemed to slightly outperform R1 and R2, based on the data for these specific durations, and it was thought that the prior removal of the upper 2 baffles helped reactor performance. Even with two baffles removed from reactor 3, billowing of fines was still possible to observe in the reactor clarifier, with increasing opportunity after 2 – 3 months of operation most likely due to scale buildup in the lower reactor. The slight outperformance of R3 was the original factor that prompted R3 to be used for the MgO pilot to determine if MgO addition could be as effective as $MgCl_2$ for struvite precipitation and exceed baseline performance.

5.4.2. MgO Pilot Operation: Mg:P Control

The first trials performed on the full-scale pilot reactor were in June 2018 and included Timab M98 MgO slurry dosing at a constant Mg:P to the reactor utilizing the previously described phase 1 slurry dosing configuration (June 2018 – Nov 2018). Due to MgO being a new chemical utilized in a Pearl reactor for struvite precipitation it was not known if it would behave the same as $MgCl_2$ and require pH control or another mode of control. Once starting the trial, it was noticed that MgO could supply enough alkalinity to not require any NaOH addition. Slurry was pumped from the tank to the reactor to reach an Mg:P of at

least 1:1 for optimal struvite precipitation. MgO slurry feed was rotated between 2 tanks as slurry preparation was done a day in advance prior to dosing the reactor. This phase was performed with and without H_2SO_4 addition to the MgO slurry batch preparation to act as a hydrating agent by promoting the dissolution of MgO and accelerating the hydration of MgO to $Mg(OH)_2$. The first trials were operated at 1X loading to process 65 kg of P/day while initially targeting an Mg:P of 1.125:1 and later in the trial adjusting the Mg:P between 1.125:1 – 1.5:1 to understand the effluent pH effect on reactor performance. Table 24 and Figure 40 show the average performance and daily performance of R3, respectively, in terms of effluent pH, influent OP, and OP and TP removal during the initial tests with and without acid addition to the MgO slurry.

Table 23: MgO Pilot Trial 2018 – Average Operation of Reactor 3

Test Name	Duration	Effluent pH	Avg OP Removal (%)	Avg TP Removal (%)	Avg CEL OP Removal (%)	Avg CEL TP Removal (%)	Avg Influent OP (mg/L)
1X w/ Acid	6/12-7/10/2018	7.29	69	62	86	73	313
1X w/o Acid	7/10-7/25/2018	7.52	82	69	92	72	341
1X w/ Acid Repeat	7/30-8/7/2018	7.53	82	69	83	72	390
1X w/o Acid Repeat	8/9-8/23/2018	7.76	76	74	82	73	392

Based on the results in Figure 40 it is observed that pretreatment of MgO slurry with acid did not indicate better results than no acid pretreatment of the slurry. Acid was not used for slurry pretreatment after August 2018 due to its invariable effect on struvite precipitation.

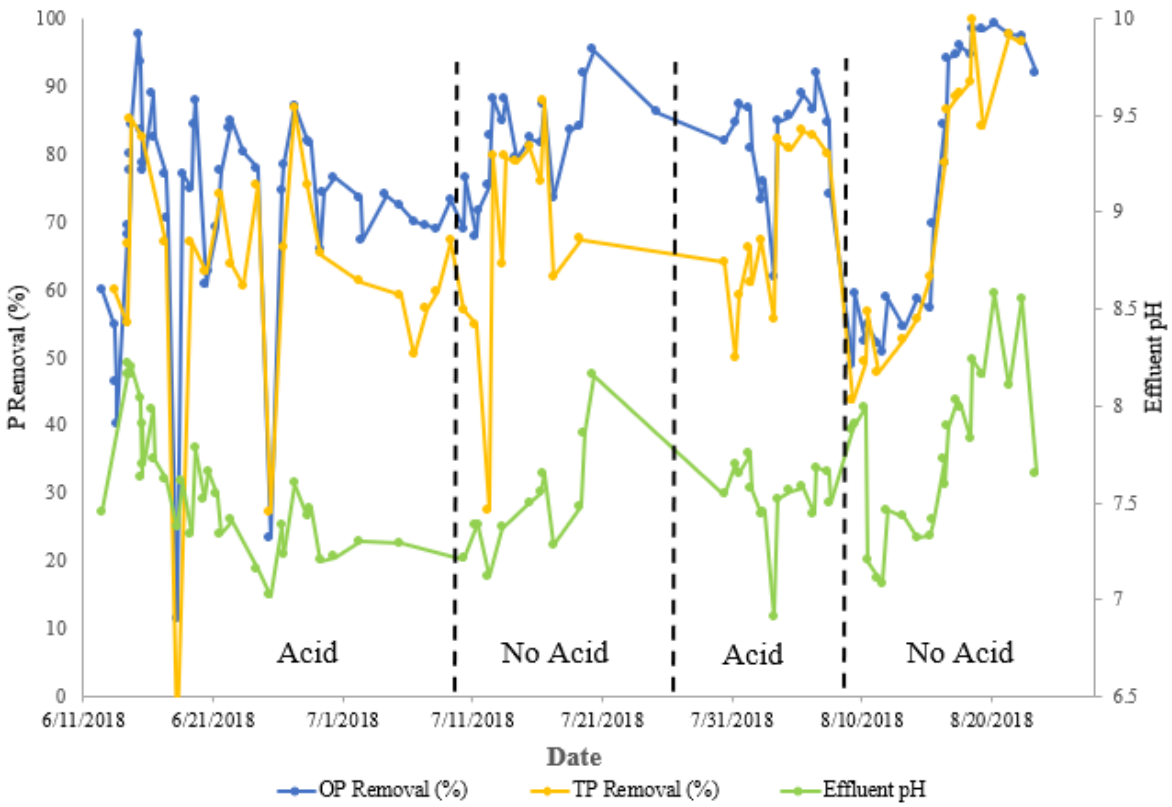

Figure 40: MgO Pilot Trial – 1X Design Load Utilizing Continuous Timab M98 MgO Pretreated with and without H2SO4

Phosphorus removals achieved throughout tests indicated that MgO can achieve adequate phosphorus removal at 1X loading. Effluent samples analyzed around a pH of 7 were noticed to have lower removal in the reactor and typically indicated a plug in the MgO slurry line to the reactor. Operation near an 8 pH, observed in the No Acid Repeat test, achieved almost 100% OP removal and correlated with an Mg:P of 1.5:1. Ultimately, a constant Mg:P of 1.5:1 was considered excessive as a high pH has previously correlated with substantial fines washout. Due to the success of the MgO addition at 1X design load, it was of interest to understand if surpassing the design load was possible and more effective than $MgCl_2$. In previous operation of reactors with $MgCl_2$, the TP removal in the reactor was not consistently optimal (<70%) once the design loading rate for the reactor was exceeded. For example, prior to pilot startup, reactor 1 and 2 were operated at an average of 1.3X load in November 2017 to March 2018 with $MgCl_2$ and achieved an average OP removal of 79% and this removal decreases as loading rate increases. Higher loadings are sometimes necessary depending on the volume of digested solids that needs to be dewatered and how much centrate needs to be processed. This lower removal at higher loading rates is not considered optimal when run for long durations as less struvite is recovered from the reactor and more phosphorus is recycled to the head of the wastewater treatment plant. Average test results when operating under 2X design loading with

continuous MgO dosing to the reactor starting in October 2019 can be seen in Table 25 below.

Table 24: Timab M98 MgO Pilot Trial Test Performance when Exceeding Design Load

Test Name	Trial Duration	Avg Effluent pH	Average OP Removal (%)	Average TP Removal (%)	Avg CEL OP Removal (%)	Avg CEL TP Removal (%)	Avg INF OP Concentration (mg/L)
Timab 2X	9/4-10/3/2018	7.8	84	79	82	64	442
Timab 3X	10/26-11/18/2018	8.06	79	67	83	72	538

Overall, the initial pilot tests achieved adequate P removal at 2X and 3X design load. Based on TP removal, fines were not an immense issue and it was decided to continue testing high loading rates utilizing MgO. Figure 41 shows the 2018 trial test summary including average OP removals and yields compared to the baseline $MgCl_2$ performance outlined in the previous section. When using MgO, the yield is not correlated with the influent phosphorus concentration (Avg INF OP) and does not meet the baseline performance specification for each trial. The phosphorus gap between removal and yield was still present and at this point in the trial the lower baffle of R3 was still present.

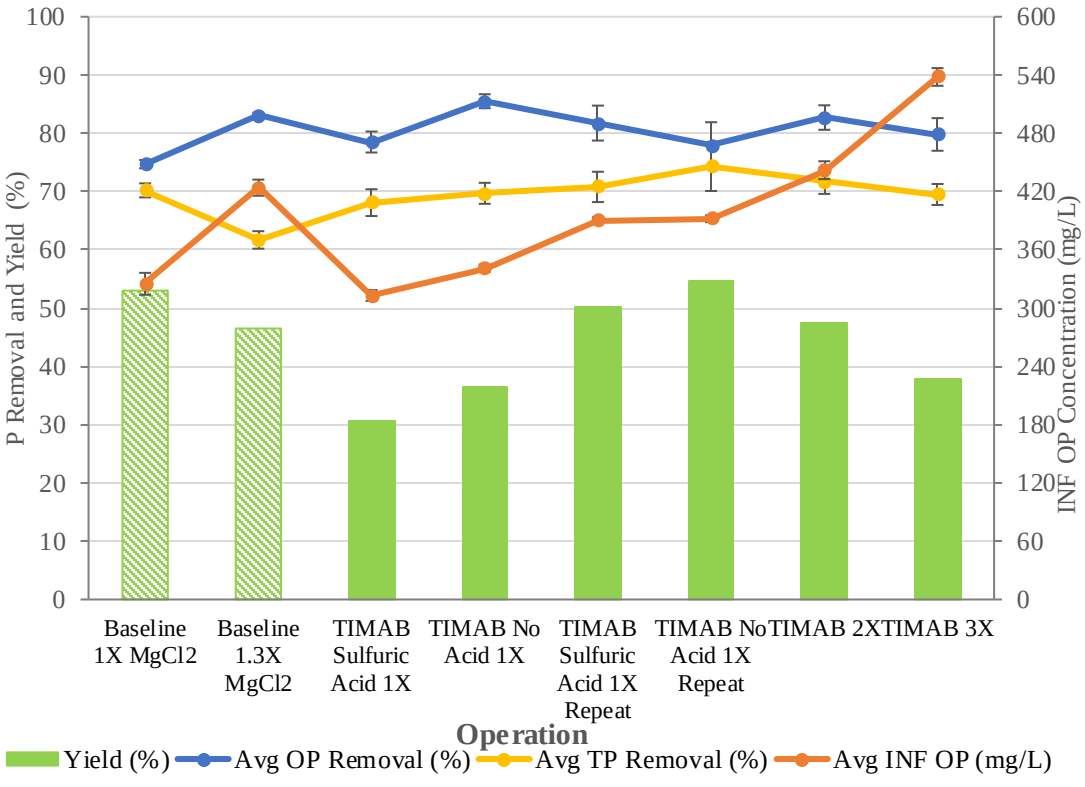

Figure 41: MgO Pilot Trial 2018 Summary

Operation at 2X and 3X design load tests utilizing MgO were able to achieve performance comparable to that of design load, but there were occasional low removals throughout each pilot test. As reactor performance data were being taken, struvite particle size distributions were also being measured when harvesting from the pilot reactor. The average particle size for each test in 2018 are in Table 26 below.

Table 25:MgO Pilot Trial 2018 Struvite Particle Size

Test Name	Average Particle Size Harvested (SGN)
1X w/ Acid	92
1X w/o Acid	83
1X w/ Acid Repeat	94
1X w/o Acid Repeat	90
Timab 2X	131
Timab 3X	108

An average particle size of 131 SGN from the Timab 2X test did not necessarily align with average particle sizes observed in future high loading tests. It is hypothesized that the documented average particle size during the Timab 2X test was insufficient due to 80% of shaker box samples being taken from the harvest system during the first 2.5 weeks of reactor operation which lasted 4 weeks total. When allocating the average daily phosphorus load to the 2018 pilot trial tests it is observed that there is a portion of phosphorus that cannot be accounted for by reactor effluent or struvite yield. Phosphorus allocation during the 2018 MgO pilot tests can be seen in Figure 42.

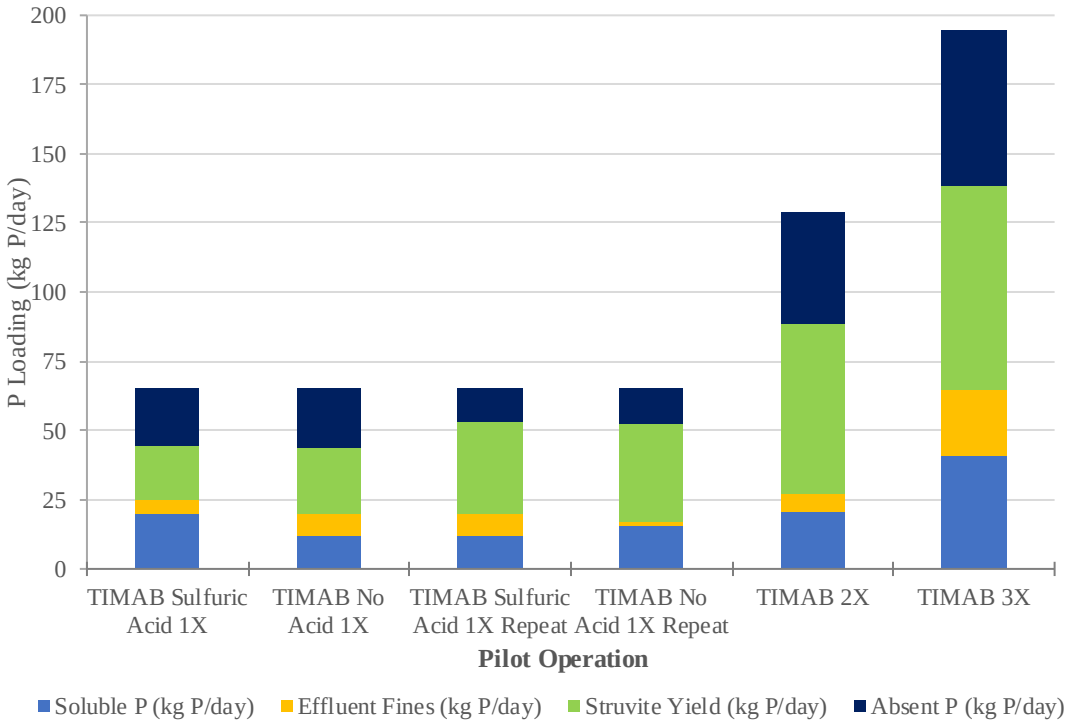

Figure 42: P Allocation of MgO Pilot in 2018

The absent phosphorus calculated missing from reactor 3 pilot tests accounted for 18 – 30% of the average reactor loading in 2018. There does not seem to be any correlation between the % missing phosphorus and reactor loading. For example, for the Timab 2X design load test 46% of phosphorus was unallocated while for the Timab 3X design load test only 29% of phosphorus was absent. Performance of the pilot in 2018 was comparable to baseline performance and the MgO pilot was continued with plans to upgrade the MgO dosing system. The line plugging experienced during the continuous direct dosing of MgO slurry to the reactor showed the limitations of this system, especially when higher slurry concentrations were used when exceeding the design load. Optimal reactor pH and Mg:P were achieved by dosing MgO at a low flow which resulted in line plugging. This system was not expected to work unless the transport of MgO slurry was improved by increasing velocity in the line.

The updated design including an intermittent dosing strategy using a recirculation loop was implemented to eliminate low flow of slurry to the reactor and stop the line plugging. Throughout the Mg:P control trials in 2018 it was noticed that pH strongly influenced the P removals and thus optimization of the MgO pilot reactor. This holds true for normal operation of Pearl reactors which are a pH-controlled process. With high pH (pH > 8.0), the effluent OP removal of the reactor was typically greater than 90%. While with low pH < 7.5, the OP removal in the reactor could decrease below 70% removal which is not considered optimal operation. The limitations of process efficiency due to effluent pH indicated that a new intermittent dosing configuration could be controlled by effluent pH

while achieving the necessary Mg dosing to the reactor. However, before intermittent dosing was tested there was a short test performed with an alternative Mg source, $Mg(OH)_2$ pre-made slurry, and the results are outlined in the following section.

5.4.3. MgO Pilot Operation: Alternative Mg Source – $Mg(OH)_2$

After the initial 2018 trials utilizing Timab MgO, a pre-made 60% $Mg(OH)_2$ slurry was used for 2 weeks in December 2018. This test was initially operated at 3X design load, but poor reactor operation resulted in the loading being lowered. As discussed previously, $Mg(OH)_2$ is cheaper than $MgCl_2$ and more expensive than MgO solid. The benefit of using the pre-made $Mg(OH)_2$ slurry is the avoidable on-site slurry preparation and concern of line plugging due to settling MgO solids. The performance of this short test was comparable to previous tests using MgO, however there was severe beaching in the reactor clarifier that led to its termination. Table 18 outlines the average performance seen from the pilot during the 2-week operation time.

Table 26:Mg(OH)2 Test Performance Summary

Test Name, Reactor Load	Duration	Avg OP Removal (%)	Avg TP Removal (%)	Avg CEL OP Removal (%)	Avg CEL TP Removal (%)	Yield (%)	Avg INF OP Concentration (mg/L)
60% $Mg(OH)_2$, 2X	12/5-12/18/2018	81	65	91	39	31	356

OP removal was optimal however the fines loss issues observed during these 2 weeks was observed with the low TP removal. As for the recovered struvite, only 31% of the TP load to the reactor was recovered as struvite. These results align with historical missing P in the SRF. Figure 29 shows the phosphorus allocation of the pilot influent phosphorus.

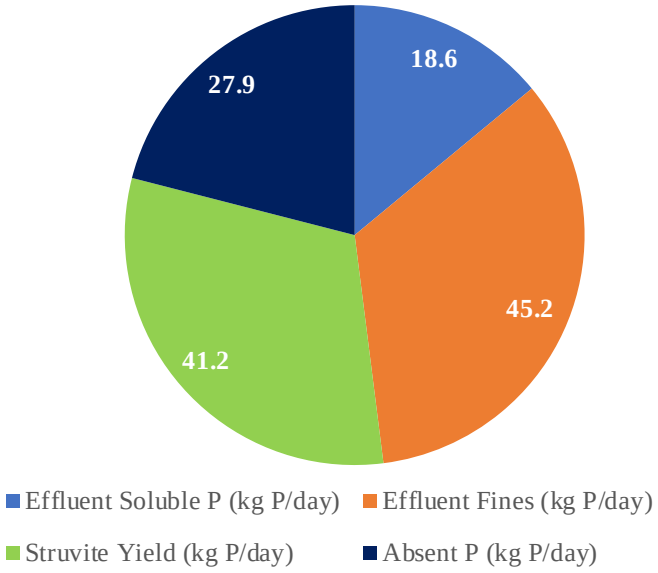

Figure 43: MgO Pilot Trial 2018 - Mg(OH)2 Test P Allocation

Due to comparable results achieved with MgO and $Mg(OH)_2$, it was determined that a slaking system for MgO slurry dosing would be successful at keeping solid MgO suspended while maximizing chemical cost savings with respect to using MgO versus $Mg(OH)_2$. These two factors led to the construction of the slaking system and MgO usage in 2019-2020 trial tests.

5.4.4. MgO Pilot Operation: pH Control

The intermittent dosing system of MgO slurry at an Mg:P between 1:1 – 1.5:1 was controlled off the effluent pH due to the direct effect it had on P removal. Typically, an of 1.2:1 Mg:P was determined g\for the majority of the tests performed under pH control. When restarting the pilot after MgO dosing modifications, were complete a new MgO, Baymag 30 HP (Baymag), was utilized for the next pilot testing at 3X and 2X design load. Table 19 defines the average pilot operation when utilizing Baymag after the slurry dosing configuration update.

Table 27: Pilot Operation under pH Control Utilizing Intermittent Dosing

Trial Test Name	Date	Effluent pH	Avg OP Removal (%)	Avg TP Removal (%)	Avg CEL OP Removal (%)	Avg CEL TP Removal (%)	INF OP Concentration (mg/L)
Baymag 3X	3/5 – 5/1/2019	8.01	90	78	88	67	393

Baymag 2X	5/8 – 7/20/2019	8.16	90	64	90	70	506

Due to the test being operated around an 8 pH on average, OP removal seemed to do especially well when using Baymag. However, in the latter portion of the trial test it is observed that the TP removal seemed to be struggling which was due to fines washout in the form of billowing out of the clarifier. The billowing of fines is not considered optimal operation, so the reactor was emptied and stopped on July 20, 2019 for a reactor inspection and cleaning. It is worth noting that before this cleaning the reactor had not been cleaned since January 2019. Typically, the pilot reactor did not remain in service for more than 3 months without a reactor inspection and cleaning. Disassembly of the reactor revealed substantial scale build up around the injection port and the reactor between the injection port and harvesting zone. While the reactor was down for cleaning, it was also decided to remove the last remaining baffle in the lower vertical portion of the reactor (zone 1) in response to the scaling that was observed. Baffles that existed in zone 2 and zone 3 were removed from reactor 3 prior to the pilot, estimated to have occurred prior to the year 2014.

After the cleaning and baffle removal from R3 had been completed, the pilot was restarted with Baymag MgO at a higher upflow velocity to determine if that influenced the product size in the reactor and limited fines washout. Timab M98 MgO was re-ordered and swapped in as the MgO slurry used for the pilot test due to low Baymag inventory. The Timab MgO slurry was used at high upflow velocities until the test was terminated due to poor TP removal. Phosphorus removal from the high upflow velocity tests can be seen in Table 20.

Table 28:MgO Pilot Trial – High Upflow 2X Test Average Operation

Trial Test Name	Date	Effluent pH	Avg OP Removal (%)	Avg TP Removal (%)	Avg CEL OP Removal (%)	Avg CEL TP Removal (%)	Avg INF OP Concentration (mg/L)
Baymag High Upflow	8/6– 8/27/2019	7.93	94	29	98	65	529
Timab High Upflow	8/27 – 9/9/2019	8.04	66	60	71	59	423

The test results did not show an increase in product size or phosphorus recovery due to the increased upflow velocity in the reactor possibly contributing to fines washout. Reactor operation during the high upflow trials can be seen in Figure 30 with Baymag used during August 13 – 26, 2019 and Timab used August 27, 2019 – September 9, 2019.

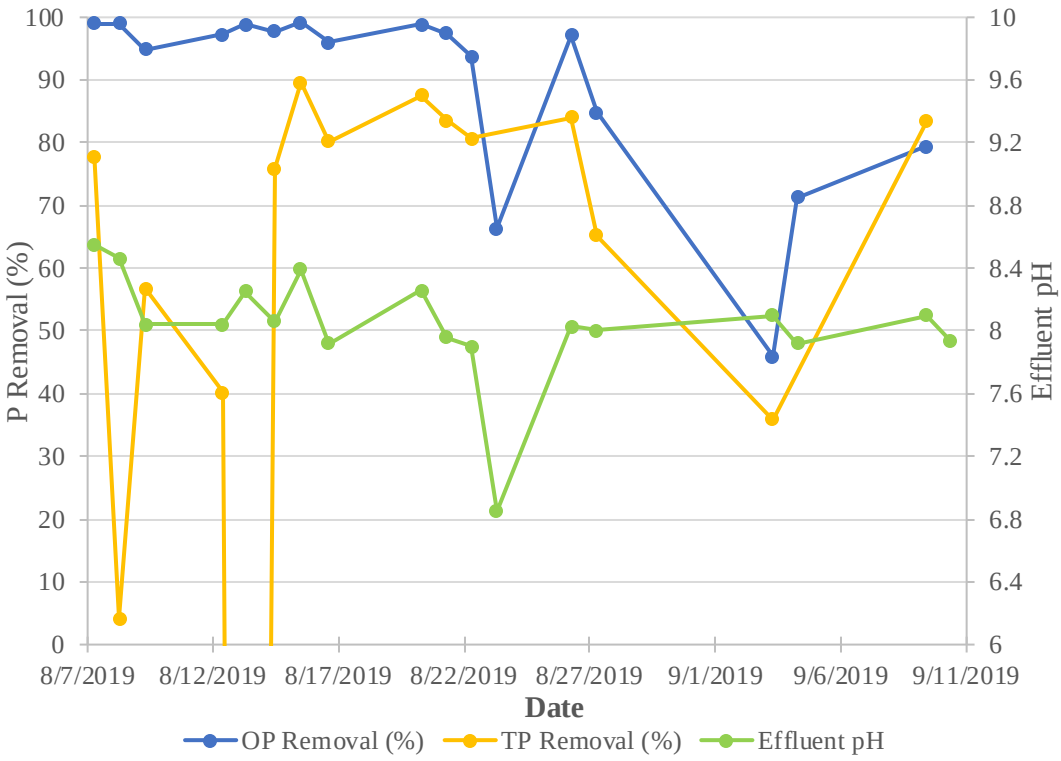

Figure 44:MgO Pilot Trial – 2X Design Load Operated at High Upflow Velocity Utilizing Intermittent Baymag 30 HP (8/7 – 8/26/2019) and Timab M98 Slurry (8/27 – 9/9/2019) Dosing

It can be observed that switching to Timab M98 on August 28, 2019 caused low removal with high upflow velocity even though there was adequate effluent pH. The poor removals observed was the basis of the decision to adjust the reactor upflow velocities to what they were originally operated at. With typical upflow velocity operation the heated Timab slurry test was started on September 11, 2019. Heating of the MgO was performed with a submersible heater in the slurry tote at 55 °C (131 °F). Due the success of the heated Timab trial it was repeated in December 2019. The heated Timab 2X test average operation is observed in Table 21.

Table 29:MgO Pilot Trial – Heated Timab 2X Average Operation

Test Name	Duration	Effluent pH	Avg OP Removal (%)	Avg TP Removal (%)	Avg CEL OP Removal (%)	Avg CEL TP Removal (%)	INF OP Concentration (mg/L)
Heated Timab 2X	9/11–10/3/2019	7.93	84	74	89	79	418
Heated Timab 2X Repeat	12/9/2019–1/13/2020	7.97	90	80	97	86	447

Analysis performed on site and at the CEL agreed in terms of OP and TP removal and the TP removal also comparable to the struvite yield of the pilot reactor, which was 80.4%. Historically the TP removal and yield have never showed much agreement in the pilot reactor or conventional $MgCl_2$ reactors. After the 2019 tests were completed, the yield and removal were compared to the baseline reactor operation with and without baffles. Figure 31 defines the performance of the pilot reactor during each test in terms of P removal and yield and defines the average influent phosphorus concentration. The lower baffle was removed from R3 prior to the Baymag 2X high upflow test. Figure 31 illustrates that the Baymag 2X trial was one of the poorer performing tests seen during the entire trial. The explanation of this performance is likely the excessive scaling that occurred in the bottom of the reactor and injection port causing the observed billowing of fines. The entire injection port of the reactor possessed a thick lining of struvite scale with creating small cross-sectional area for flow to travel through the remaining length of the reactor.

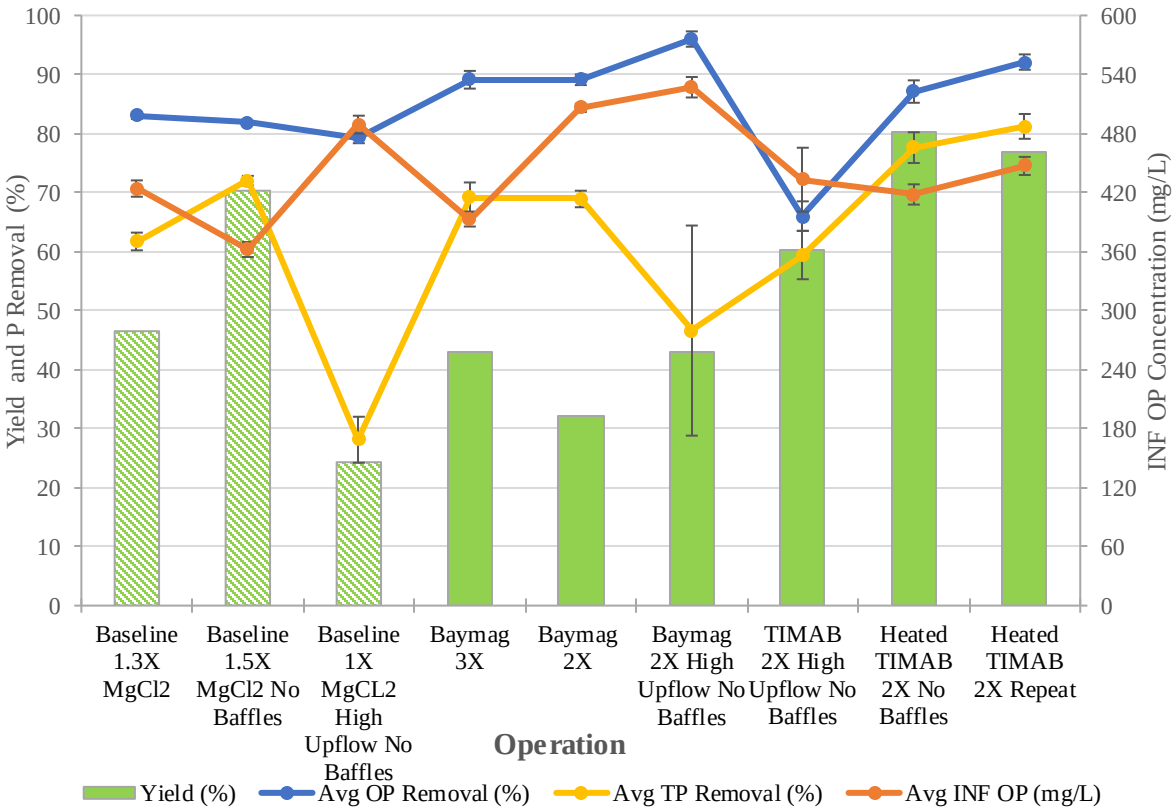

Figure 45:MgO Pilot Trial Summary 2019

It was noticed that the TP removal from the pilot better represents the struvite yielded from the reactor beginning with the Baymag 2X High upflow test. Random Fines billows were observed during the Baymag 2X high upflow test. Fines loss observed during this test was better quantified with the low average TP removal determined from grab samples. Historically, fines loss was unclear, and randomness of fines may have contributed to the mass imbalance observed in the past. As mentioned previously, it is again noticeable around July 2019 that the pilot reactor TP removal and struvite yield were aligning suddenly as was observed with reactor 1. This solidified the hypothesis that the lower baffle was hindering the reactor performance and efficiency, in terms of phosphorus removal, struvite yield, fines washout, and reactor scaling. There are trials where the yield exceeds the removal, and this may have to do with not fully understanding the moisture content of each wet harvest bag from the tests. It is conservatively estimated that the bag weight is 20% moisture content. It has been observed that the struvite product in a bag can dry to <10% moisture content at the top of the bag 2 weeks after the wet harvest, while the material in the bottom can be 20% moisture content 5 months after the wet harvest. Figure 32 represents the phosphorus allocation during 2019 pilot trial tests.

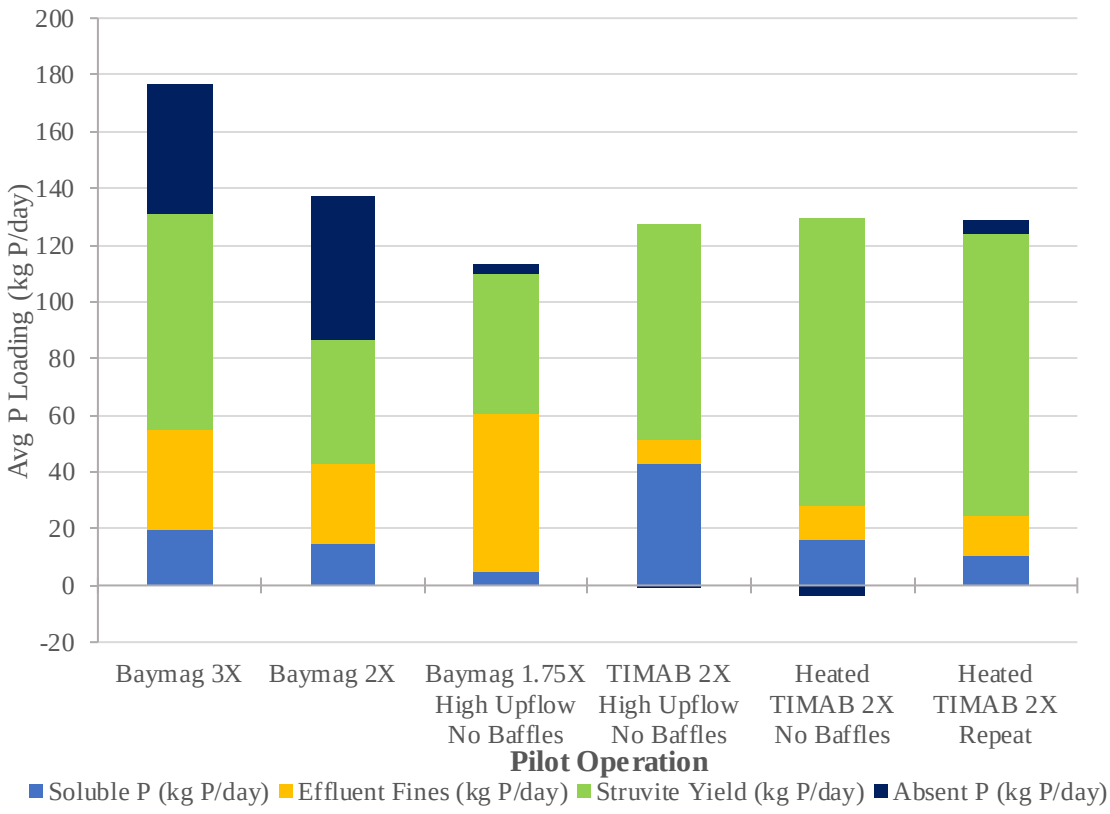

Figure 46:MgO Trial 2019 P Allocation

Throughout 2019, struvite product size became an increasing issue as there did not seem to be a remedy for the small product obtained from the pilot reactor. Table 17 defines the average product sizes for each 2019 trial test based off sieve shaker box results taken from material harvested through the dryer. Unfortunately, many trials involved manually harvesting the material out of the reactor through wet harvesting. In 2019, shaker boxes were not done on material that was wet harvested as it typically looked <70 SGN, or what was commonly called 45 SGN. Due to the increasing wet harvesting of the pilot, the percent of material wet harvested for each trial test is also indicated in Table 22.

Table 30: MgO Pilot 2019 Harvesting Data

Trial Name	Average Struvite Product Size (SGN)	Percent Wet Harvested (%)
Baymag 3X	156	31.2
Baymag 2X	72	47.1
Baymag 2X High Upflow	249	28.2

Timab 2X High Upflow	102	75
Heated Timab 2X	-	87.5
Heated Timab 2X Repeat	80	75

The small product caused beaching in the reactor clarifier and became a common occurrence when consistently operating the pilot reactor above design reactor loading. Beaching in the clarifier prompted a harvesting leg in the upper portion of the reactor to be retrofitted. The upper harvest leg was installed prior to the Heated Timab 2X test to allow for fines to be removed from the upper reactor and attempt to grow product in the lower portion of the reactor. Clarifier beaching and the upper wet harvest leg can be observed in Figure 58 and 59 of Supplemental Information. Pilot reactor yield and percent wet harvested material of each test can be observed in Figure 57 in the Supplemental Information.

5.4.5. MgO Pilot Operation: MgO Slurry Hydration Extent Control

Initial 2019 MgO pilot tests showed a high conversion of MgO to $Mg(OH)_2$ (~98% hydrated for Baymag 2X, 70% hydrated for Timab 2X). As lower hydration extents were not consistently tested for struvite precipitation a new dosing configuration was constructed to limited slurry retention time and hydration extent. After constructing the automated batching MgO dosing system in April 2020 it was possible to test variable hydration extents of MgO. The variable hydration tests were tested with the reactor operating at 2X design load. Both Timab and Baymag were used in these pilot tests.

Initially, Baymag was utilized for three weeks to understand how the hydration extent range changed with respect to %MgO slurry concentration. Desired hydration extent ranges were targeted by adjusting the slurry % MgO w/w concentration and thus altering the average retention time of slurry in the tank prior to batching to the reactor. After the hydration testing with Baymag, it was decided to test Timab at a low hydration extent, targeting 15 – 30% hydrated. Due to the reactivity difference between Baymag and Timab, minimal hydration did not seem as successful with the less reactive Timab product. This low of a hydration with Timab was found to cause MgO beaching in the reactor clarifier and can be observed as the yellow/brown particles under a microscope at 100X magnification in Figure 33. Figure 33 also shows struvite particles which are transparent and seem to have precipitated by heterogenous nucleation on the MgO particles. The local supersaturation experienced at the MgO surface caused by MgO dissolution is thought to have caused the heterogenous nucleation. This product was considered inadequate as previous scaling observed in the reactor during an unhydrated trial (October 2019) was 20.6% Mg, where pure struvite possesses around 10% Mg. The MgO hydrating time was extended to promote further MgO dissolution in response to this beaching/scaling.

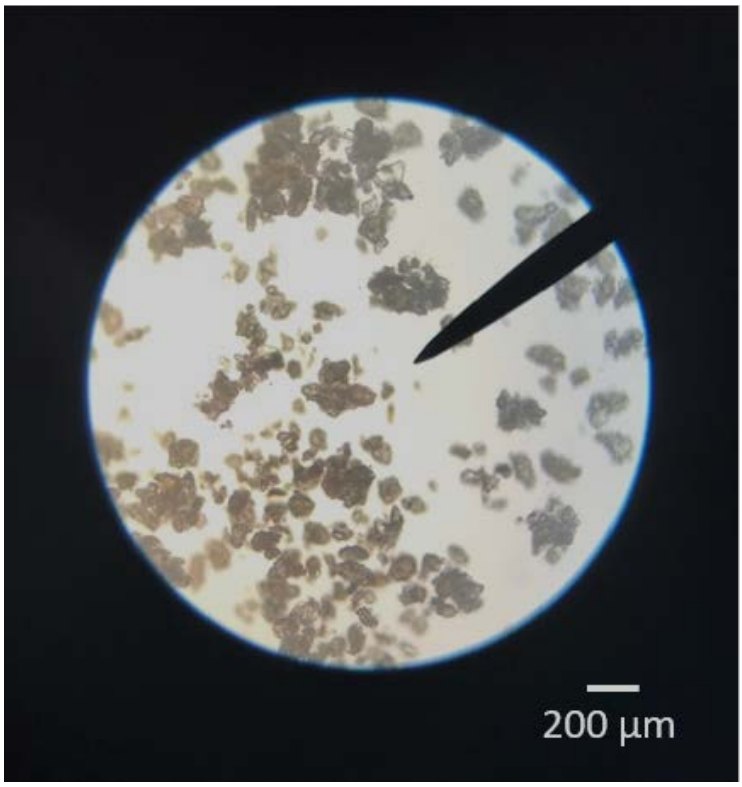

Figure 47: Timab MgO Particles from Reactor Beaching during Unsuccessful Unhydrated MgO Trial (October 2019) under 100X Magnification

The hydration extent of the Timab MgO slurry was extended by increasing the slurry concentration and thus increasing the average slurry retention time in the tank prior to dosing to the reactor. Targeting the new slurry concentration resulted in a hydration extent range of 30 – 50 % hydrated. Lastly, a test with 25-55% hydration extent was performed. The performance of the reactor during these tests was acceptable and analogous to the performance of the reactor utilizing almost fully hydrated MgO slurry. Operationally, the Timab low hydration extent (15 – 30%) test was inadequate due to the scale-like beaching of MgO that occurred in the pilot reactor clarifier. Figure 34 exhibits the overall performance of the pilot during these three tests in 2020.

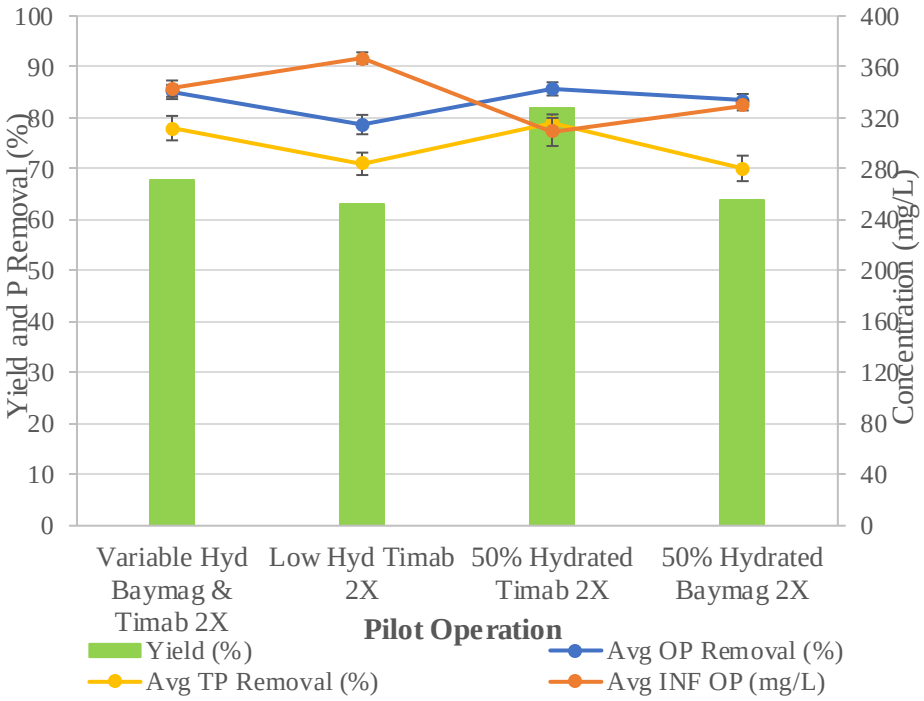

Figure 48: MgO Pilot Trial 2020 Performance Summary

The low hydration Timab test achieved the lowest yield and removal out of the three tests previously described. Even with the poorer performance, the low hydration Timab test still achieved 63% struvite yield. Results of the 2020 pilot trial continue to show reasonable correlation between TP removal and yield of the pilot reactor. Based on these results it seems as if the lack of MgO hydration has little effect on struvite precipitation or reactor performance as every test achieved over 60% yield. However, low hydration of Timab M98, i.e. 15 – 30% hydration extent, is to be avoided as excessive MgO beaching in the clarifier is considered poor operation. Allocation of phosphorus during these 2020 MgO pilot tests was performed and can be seen in Figure 35. The initial variable hydration tests had an average of 12.8 kg P/day that was unaccounted for while the low Timab hydration test had an average of 10.3 kg P/day missing. These average missing phosphorus values account for 9.8% and 7.9% of the average daily reactor loading, respectively. However, the next test as the hydration extent of Timab was increased to 30 – 50% in response to the beaching in the clarifier there was not a large percentage of missing phosphorus from the test. The negative absent phosphorus has been thought to occur due to the uncertainty of the moisture content throughout the length of the wet harvest bags manually filled from the reactor, as previously mentioned. Towards the middle of the trial there were some slight polymer issues upstream of the SRF that led to a couple days of some organic solids being captured in wet harvest bags.

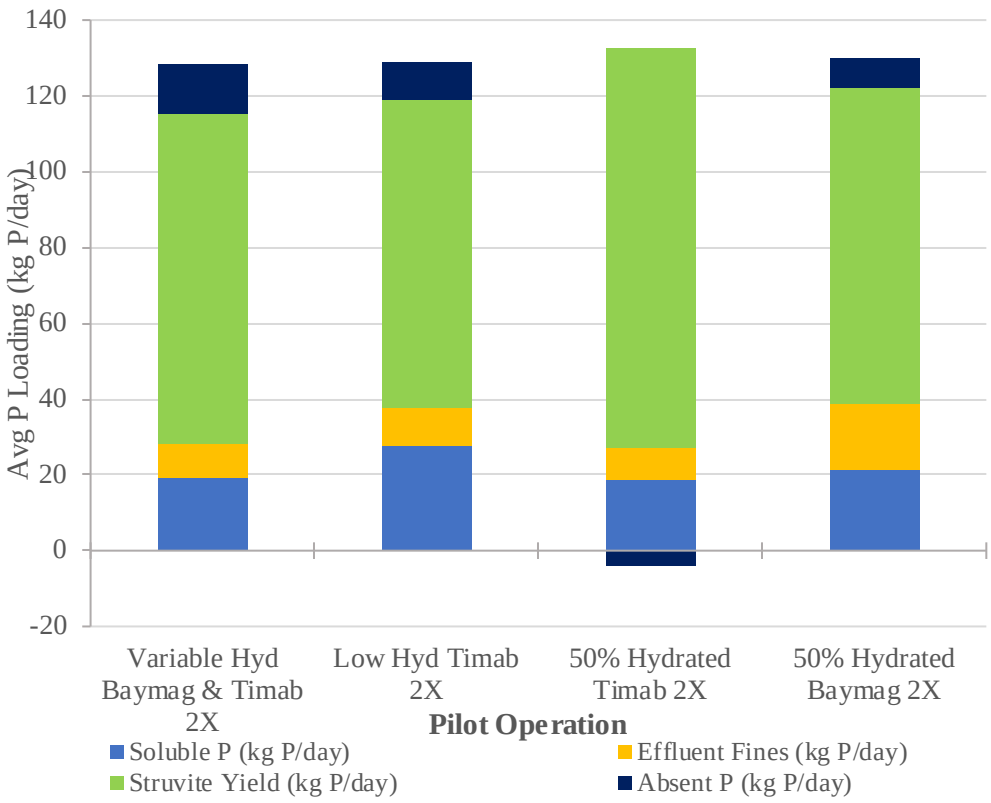

Figure 49: MgO Pilot Trial 2020 Phosphorus Allocation

Operation of the pilot reactor during the lower hydration tests resulted in scale-like beaching that can be observed in Figure 36. This beaching seemed to be a mixture of MgO and struvite and heterogeneous nucleation of struvite on MgO particle which was previously identified in Figure 33. The struvite yield that could have been captured in the clarifier beaching was not easy to account for or clean out of the reactor.

Figure 50: MgO Pilot Reactor Clarifier Scaling (May 28, 2020)

The stratification of scale seen in Figure 36 shows a light brown layer of beaching which seemed to be MgO and non-scaled gray layer of beaching which depicted typical struvite beaching observed in past pilot reactor operation.

The average particle sizes obtained from upper and lower wet harvesting of the reactor through time for each test can be observed in Figure 37. These are results from sieving products through the sieve screen box. Fines are considered as product of 70 SGN or less. It can be observed that partially hydrated Timab M98 did allow for growth of fines observed in the upper portion of the reactor throughout the test duration. Baymag usage observed more growth in product observed in the lower portion of the reactor while average product size in the upper portion of the reactor decreased. Heated Timab (50-80% hydrated) showed an initial decline in product size and little growth throughout time and 75 SGN material harvested at the end of the test.

It is hypothesized that the size, reactivity, and hydration of the MgO products used caused different struvite product sizes throughout time in different regions of the reactor.

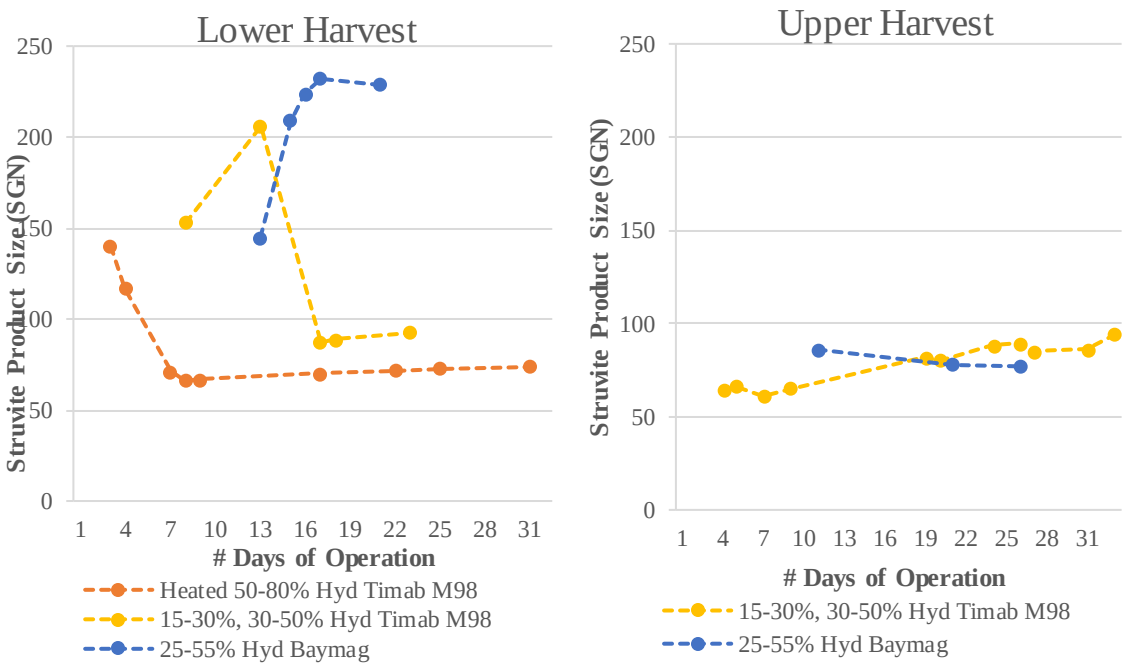

Figure 51: Average Struvite Particle Size Throughout a Test Duration for Different MgO Products and Hydration

5.4.6. MgO Pilot Operation: Effluent OP Cascade Control

Utilizing a continuously monitoring OP analyzer on the pilot reactor effluent it was possible to control the reactor operation by targeting a desired phosphorus removal. A cascade controller was implemented with a primary controller achieving an OP removal setpoint and outputting a pH setpoint to the secondary loop in response to the error between the process and setpoint. The secondary controller of the cascade utilized the setpoint

outputted by the primary controller and manipulated the MgO dosing valve frequency to achieve the setpoint.

Tuning of the cascade PID was done by utilizing the root mean square error (RMSE) method on different P&I parameters. The smaller error achieved by a controller when trying to achieve setpoint, the better. The RMSE tuning method was also used on controller step tests. A step test involved changing the pH setpoint of the controller and observing the response of the pH controlled by the PID output on the manipulated variables, MgO dosing valve frequencies. The secondary controller was tuned first under typical pH control, not using the cascade control. Different proportional (P) and integral (I) gain values were inputted into the secondary controller to determine which P&I values showed the best controller tuning when changing the pH setpoint, or lowest RMSE. Secondary loop results (4-hour test duration) of the RMSE method under various P&I parameter iterations can be seen in the table 23 below.

Table 31: Root Mean Squared Error (RMSE) Results for Various Controller Proportional (P) & Integral (I) Parameters

P&I(seconds) Parameters	RMSE for Controller	RMSE for Step Tests
10&200 seconds	0.079	-
20&100 seconds	0.016	0.052
30&75 seconds	0.058	-
40&100 seconds	-	0.069
30&75 seconds	-	0.115

Utilizing the RMSE results, the P&I parameters chosen for the secondary controller were P = 20 and I = 100 seconds. With the secondary parameters in place, P&I parameters could be tested on the primary controller.

Due to the time required of the continuously monitoring OP analyzer to sample and analyze, it was necessary to accelerate the response observed from the analyzer in order to properly run the system utilizing cascade OP control. Primary controller tuning is still occurring, to have OP removal cascade control implementation in the future for pilot restart in 2021.

5.5.Conclusions

Through the entirety of the MgO pilot trial it became clear that it was feasible to utilize MgO as an alternative MgO source for struvite precipitation in a full-scale Ostara Pearl® 500 reactor. Utilizing MgO in a pilot Pearl reactor:

- Eliminated $MgCl_2$ and NaOH addition as MgO provides alkalinity to the reactor
- Did not require addition of H_2SO_4 during full-scale operation to achieve adequate reactor P removal and yield
- Achieved comparable P removal and yield to that of baseline $MgCl_2$ operation in 2018 and early 2019
- Allowed the pilot reactor outperformed baseline reactor operation with 2X pilot reactor operation was comparable to 1.5X baseline reactor operation

The closing of the P mass imbalance historically observed at the SRF occurred in late 2019 for the conventional $MgCl_2$ reactors and the pilot reactor. The closing of the P imbalance correlates with the removal of the baffle and reduction of irregular flow through the height of the reactor. Though overall SRF yield improved throughout the course of the pilot operation, it is observed that the pilot reactor could operate at a higher reactor loading while achieving high TP removal and yield. Baseline performance at 1.5X resulted in a yield of 70% of theoretical struvite production and TP removal of 73%. The MgO pilot reactor testing at 2X design reactor loading resulted in yields between 63-82% and TP removals of 71-81%.

Other notable pilot reactor operations included:

- MgO hydration extent control did not result in poor reactor operation when limiting the hydration extent to 30-50%
- Partial hydration and high hydration (when heating MgO slurry) both resulted in optimal reactor operation, yielding 80% or more of the theoretical struvite production.
- Hydration extents tested below 30% (15-30%) were shown to achieve optimal performance in terms of OP and TP removal
    - the scaling of excess MgO in the reactor clarifier hindered operation and lower yield values (63%) were observed.

The pilot reactor has alternative control methods that can be utilized to fine-tune the reactor operation– achieve a specific OP removal (%), maintain a desired Mg:P, continuously of intermittently dose the reactor, or operate under pH control. The main limitations of the MgO pilot reactor was the post-processing equipment's inability to manage the small product. This issue is to be further investigated with an upgrade of the struvite dryer intended to achieve higher throughput of material to maintain steady operation with the pilot reactor at 2X design reactor loading.

6. Conclusions and Engineering Significance

The use of MgO for struvite precipitation can have a positive impact on the environment as it is a naturally occurring mineral that can eliminate the need for $MgCl_2$ derived from seawater. The use of NaOH for alkalinity is not needed when using MgO. MgO is also cheaper, NaOH costs \$500-600/ton while $MgCl_2$ costs \$350-700/ton. Switching from $MgCl_2$ to MgO can eliminate over 60% of the costs associated with Mg addition to the reactors, MgO is \$1/kg Mg while $MgCl_2$ is \$2.7/kg Mg (Verigin, M., et al., WEFTEC, 2020). The positive results from the MgO pilot since 2018 have

proved that this process is possible for full-scale struvite precipitation and can achieve a stable operation at loading rates greater than the design load when using an Ostara Pearl® 500 reactor. It has been observed that utilizing MgO for loading the reactor beyond design load produces small struvite particles and harvesting of the small material has shown to be the limiting factor of this alternative Mg source.

The aspects of MgO usage for struvite recovery were especially important for HRSD Nansemond Treatment Plant to understand as it will be acquiring a neighboring treatment plant's wastewater flow in the future. The future of HRSD Nansemond Treatment Plant solids handling is also being discussed, the introduction of WASSTRIP and the continuation of solids handling would increase digested solids dewatering and centrate production. The replacement of $MgCl_2$ and NaOH with MgO shows promise if it were necessary for reactors to operate optimally above design load to process more centrate while reducing expensive operational costs associated with the conventional Pearl process (Verigin, M., et al., 2020). However, it was discovered after the removal of the vertical quadrant baffles in the reactors that the conventional $MgCl_2$ reactors were performing comparably to the pilot reactor and the removal and yield achieved in the reactors were accounting for most of the phosphorus loaded into the SRF. Even with the conventional $MgCl_2$ and MgO pilot reactor performing equally, the costs are a major consideration in the future if load to the SRF increases due to upgrades and additional solids handling.

The further investigation of MgO slurry helped understand what was being dosed to the reactor and if different methods of pretreatment impacted the performance of the reactor once dosed with MgO slurry. The effect of the hydration extent and reactivity of MgO product on struvite precipitation was observed in bench-scale jar testing and full-scale pilot reactor operation. The hydration extent range used for full-scale operation, once exceeding the initially tested 15 – 30% hydrated range, showed little to no effect on the struvite precipitation. The rate of struvite precipitation and OP removal (%) during jar tests was more rapid for more reactive MgO products. Jar tests also showed variation in struvite precipitation with MgO products various hydration extents. Jar testing revealed that the reactivity and hydration extent can cause the "slowly available" Mg2+ reserve to be available for further struvite precipitation through time. Further relating the jar testing results to the time that particles are retained in a full-scale Pearl® 500 reactor can suggest which MgO product could best achieve the level of "slowly available" Mg2+ reserve desired.

References

Adnan, A., Mavinic, D.S., Koch, F.A. (2003) Pilot-scale Study of Phosphorus Recovery Through Struvite Crystallization – Examining the Process Feasibility. NRC Canada J. Environ. Eng. Sci., 2. 315 – 324.

Adnan, A., Koch, F.A., Mavinic, D.S. (2003). Pilot-scale Study of Phosphorus Recovery Through Struvite Crystallization – II. Applying in-reactor Supersaturation Ratio as a Process Control Parameter. NRC Canada J. Environ. Eng. Sci., 2. 473 – 483.

Aphane, M.E., van der Merwe, E.M., Strydom, C.A. (2009). Influence of Hydration Time on the Hydration of MgO in Water and in a Magnesium Acetate Solution. Journal of Thermal Analysis and Calorimetry, 96 (2003) 3. 987 – 992.

Babić – Ivančić, V., Kontrec, J., Kralj, D., Brečević, L. (2002). Precipitation Diagrams of Struvitre and Dissolution Kinetics of Different Struvite Morphologies. Croatian Chemical Society, Zagreb.

Bhuiyan, M.I.H., Mavinic, D.S., and Beckie, R.D. (2007). Nucleation and Growth Kinetics of Struvite in a Fluidized Bed Reactor. J. of Crystal Growth, 310. 1187 – 1194.

Birchal, V.S.S., Rocha, S.D.F., Ciminelli, V.S.T. (2000). The Effect of Magnesite Calcination Conditions on Magnesia Hydration. Minerals Engineering, 2000, 13 (14-15). 1629 – 1633.

Birchal, V.S., Rocha, S.D.F., Mansur, M.B., Ciminelli, V.S.T. (2001). A Simplified Mechanistic Analysis of the Hydration of Magnesia. The Canadian Journal of Chemical Engineering, 79. 507 – 511.

Borgerding, J. (1972). Phosphate Deposits in Digestion Systems. J. Wastewater Pollutant Control Fed. 44. 813 – 819.

Bouropoulos, N.C. and Koutsoukos, P.G. (2000) Spontaneous Precipitation of Struvite from Aqueous Solutions. J. Crystal Growth 213. 381 – 388.

Britton, A., Koch, F.A., Mavinic, D.S., Adnan, A., Oldham, W.K., and Udala, B. (2005). Pilot-Scale Struvite Recovery from Anaerobic Digester Supernatant at an Enhanced Biological Phosphorus Removal Wastewater Treatment Plant. NRC Canada J Environ. Eng. Sci., 4. 265 – 277.

Buchanan, J.R., Mote, C.R. and Robinson, R.B. (1994). Thermodynamics of Struvite Formation. Transactions American Society Agricultural Engineers, 37(2). 617 – 621.

Burns, J.R. and Finlayson, B. (1982). Solubility Product of Magnesium Ammonium Phosphate Hexahydrate at Various Temperatures. J. Urology, 182. 426 – 428.

Canteford, J.H. (1985). Magnesia– An Important Industrial Mineral: A Review of Processing Options and Uses. Mineral Processing and Extractive Review, 2. 57 – 104.

Castro, S.R., Araújo, M.A.C., Lange, L.C. (2015). Evaluation of the Hydration Process of an Industrial Magnesia Compound to Obtain Struvite Crystals: A Technique for Recovering Nutrients. Metallurgy and Materials. R. Esc. Minas, Ouro Preto, 68 (1). 77 – 84.

Capdevielle, A., Sýkorová, E., Biscans, B. Béline, F., Daumer, M.-L. (2013). Optimization of Struvite Precipitation in Synthetic Biologically Treated Swine Wastewater– Determination of the Optimal Process Parameters. J. Hazard. Mater.

Crutchik, D., Garrido, J.M. (2016). Kinetics of the Reversible Reaction of Struvite Crystallization. J. Chemosphere, 154. 567 – 572.

Crutchik, D., Rodrigues, S., Ruddle, D., Garrido, J.M. (2018). Evaluation of a Low-Cost Magnesium Product for Phosphorus Recovery by Struvite Crystallization. J. Chem. Technol. Biotechnol. (2018) 93. 1012 – 1021.

Doyle, J.D. and Parsons, S.A. (2002). Struvite Formation, Control and Recovery. Wat. Res., 36. 3925 – 3940.

Driver, J., Lijmbach, D., Steen, I. (1999) Why Recovery Phosphorus for recycling, and how? Environmental Technology 20(7). 651 – 662.

Dunn, S., Impey, S., Kimpton, C., Parsons, S.A., Doyle, J. and Jefferson, B. (2004). Surface Diagnostics for Scale Analysis. Water Science and Technology, 49. 183 – 190.

Edge, D. (2000) Perspectives for Nutrient Removal from Sewage and Implications for Sludge Strategy. Environ. Technol., 20 ,759.

EPA National Pollutant Discharge Elimination System (NPDES).

Hanum, F., Yuan, L.C., Kamahara, H., Aziz, H.A., Atsuta, Y., Yamada, T. and Daimon, H. (2019) Treatment of Sewage Sludge Using Anaerobic Digestion in Malaysia: Current State and Challenges. Frontiers in Energy Research 7(19).

Harrison, M.L., Johns, M.R., White, E.T., and Mehta, C.M. (2011). Growth Rate Kinetics for Struvite Crystallization. Chemical Engineering Transactions, 25. 309 – 314.

Huang, H., Guo, G., Zheng, P., Zhang, D., Liu, J., Tang, S. (2016). Feasibility of

Physicochemical Recovery of Nutrients from Swine Wastewater: Evaluation of Three Kinds of Magnesium Sources. Journal of Taiwan Institute of Chem. Engineers (2017) 70. 209 – 218.

Jardin, N. and Popel, J.J. (1996). Behaviour of Waste Activated Sludge from Enhanced Biological Phosphorus Removal During Sludge Treatment. Water Env. Research, 68(6). 965 – 973.

Kiani, D., Sheng, Y., Lu, B., Barauskas, D., Honer, K., Jiang, Z., Baltrusaitis, J. (2018). Transient Struvite Formation during Stoichiometric 1:1 NH_4^+ and PO_4^{3-} Adsorption/Reaction on Magnesium Oxide (MgO) Particles. ACS Sustainable Chem. Eng. 2109, 7. 1545 – 1556.

Kirinovic, E., et al. (2017). Spectroscopic and Microscopic Identification of the Reaction Products and Intermediates during the Struvite ($MgNH_4PO_4 \cdot 6H_2O$) Formation from Magnesium Oxide (MgO) and Magnesium Carbonate ($MgCO_3$) Microparticles. ACS Sustainable Chemistry and Engineering.

Le Corre, K.S., Valsami-Jones, E., Hobbs, P., and Parsons, S.A. (2009). Phosphorus Recovery from Wastewater by Struvite Crystallization: A Review. Critical Reviews in Environmental Science and Technology, 39(6). 433 – 477.

Liati, M., Xianqiu, C. (1987) The Microstructural Changing of Magnesite during Calcination. Proc. 2nd International Conference on Refractories, 1. 255 – 266.

Luo, Y., Li, H., Huang, Y.R., Zhao, T.L., Yao, Q.Z., Fu, S.Q., Zhou, G.T. (2018) Bacterial Mineralization of Struvite using MgO as Magnesium Source and its Potential for Nutrient Recovery. J. Chem. Eng. 195 – 202.

Mamais, D., Pitt, P.A., Cheng, Y.W., Loiacono, J. and Jenkins, D. (1994). Determination of Ferric Chloride Dose to Control Struvite Precipitation in Anaerobic Sludge Digesters. Water Env. Research 66(7). 912 – 918.

Matabola, K.P., van der Merwe, E.M., Strydom, C.A., Labuschagne, J.W. (2010). The Influence of Hydrating Agents on the Hydration of Industrial Magnesium Oxide. Journal of Chem. Technol. Biotechnol. (2010) 85. 1569 – 1574.

Mehta, C.M. and Batstone, D.J. (2013). Nucleation and Growth Kinetics of Struvite Crystallization. Water Res., 47. 2890 – 2900.

Metcalf & Eddy | AECOM (2014). Wastewater Engineering Treatment and Resource Recovery,

A. 494 – 498, 1674 – 1683.

Mullin, J.W. (2001) Crystallization. Butterworth-Heinemann.

Münch, E.V. and Barr, K. (2001). Controlled Struvite Crystallization for Removing Phosphorus from Anaerobic Digester Sidestreams. Wat. Res. 35(1). 151 – 159.

Nan, L. (1989). Formation, Compressibility and Sintering of Aggregated MgO Powder. J. of Materials Science, 24(7). 485 – 492.

Ohlinger, K.N., Young, T.M., and Schroeder, E.D. (1998). Predicting Struvite Formation in Digestion. Wat. Res., 32(12). 3607 – 3614.

Ohlinger, K.N., Young, T.M., and Schroeder, E.D. (1999). Kinetics Effects on Preferential Struvite Accumulation in Wastewater. J. of Environ. Eng., 125(8). 730 – 737.

Oster, M., Reyer, H., Ball, E., Fornara, D., McKillen, J., Sorensen, K.U., Poulsen, H.D., Andersson, K., Dbiba, D., Rosemarin, A., Arata, L., Sckokai, P., Magowan, E. and Wimmers, K. (2018). Bridging Gaps in the Agricultural Phosphorus Cycle from an Animal Husbandry Perspective – The Case of Pigs and Poultry. MDPI Sustainability Journal 2018, 10, 1825.

Ovivo Inc. (2017). Phospaq™ Process. Ovivo Worldwide Experts in Water Treatment. Municipal Biosolids Management. oviviwater.com

Park, N., Chang, H., Jang, Y., Lim, H., Jung, J., and Kim, W. (2020). Critical Conditions of Struvite Growth and Recovery using MgO in Pilot Scale Crystallization Plant. Water Science & Technology. IWA 2020.

Quintana, M., Sanchez, E., Colmenarejo, M.F., Barrera, J., Garcia, G., and Borja, R. (2005). Kinetics of Phosphorus Removal and Struvite Formation by the Utilization of By Product of Magnesium Oxide Production. Chem. Eng. Journal 111 (2005). 45 – 52.

Quintana, M., et al. (2007). Removal of Phosphorus through Struvite Precipitation Using a By-Product of Magnesium Oxide Production (BMP): Effect of the Mode of BMP Preparation. Chem. Eng. Journal 136 (2008). 204 – 209.

Quintana, M., et al. (2004). Use of a Byproduct of Magnesium Oxide Production to Precipitate Phosphorus and Nitrogen as Struvite from Wastewater Treatment Liquors. Journal of Agricultural and Food Chemistry 2004, 52. 294 – 299.

Rahaman, M.S., Mavinic, D.S., and Meikleham, A. (2013). Modeling Phosphorus Removal and Recovery from Anaerobic Digester Supernatant Through Struvite Crystallization in a Fluidized Bed Reactor. J. Water Research, 51. 1 – 10.

Rahaman, M.S., Mavinic, D.S., and Ellis. N. (2014) Fluidisation Behaviour of Struvite Recovered from Wastewater. J. of Env. Eng. and Science, 9(2). 137 – 149.

Rahman, M.M., Salleh, M.A.M., Rashid, U., Ahsan, A., Hossain, M.M., and Ra, C.S. (2013). Production of Slow Release Crystal Fertilizer from Wastewaters Through Struvite Crystallization – A Review. Arabian Journal of Chemistry (2014) 7. 139 – 155.

Rocha, S.D.F., Mansur, M.B. and Ciminelli, V.S.T. (2004) Kinetics and Mechanistic Analysis of Caustic Magnesia Hydration. J. of Chem. Biotechnology, 79. 816 – 821.

Ronteltap, M., Maurer, M., and Gujer, W. (2007). Struvite Precipitation Thermodynamics in Source Separated Urine. Water Research, 41(5). 977 – 984.

Romero-Güiza, M.S., Tait, S., Astals, S., del Valle-Zermeño, R., Martínez, M., Mata-Alvarez, J. and Chimenos, J.M. (2015). Reagent Use Efficiency with Removal of Nitrogen from Pig Slurry via Struvite: A Study on Magnesium Oxide and Related By-Products. Water Research 84 (2015). 286 – 294.

Ruzhitskaya, O. and Gogina, E. (2017). Methods for Removing Phosphorus from Wastewater. MATEC Web of Conferences, 106.

Salutsky, M.L., Dunseth, M.G., Ries, K.M., and Shapiro, J.J. (1972). Ultimate Disposal of Phosphate from Wastewater by Recovery as Fertilizer. Effluent Water Treatment Journal, 22. 509 – 519.

Shaddel, S., Ucar, S., Andreassen, J. and Østerhus, S. (2019). Engineering of Struvite Crystals by Regulating Supersaturation – Correlation with Phosphorus Recovery, Crystal Morphology and Process Efficiency. Journal of Env. Chem. Eng., 7.

Smithson, G.L. and Bakhshi, N.N. (1969). The Kinetics and Mechanism of the Hydration of Magnesium Oxide in a Batch Reactor. The Canadian Journal of Chemical Engineering, 47. 508 – 513.

Snoeyink, V. and Jenkins, D. (1980). Water Chemistry. John Wiley & Sons. New York.

Stolzenburg, P., Capdevielle, A., Teychené, S. and Biscans, B. (2015). Struvite Precipitation with MgO as a Precursor: Application to Wastewater Treatment.

Stumm, W. and Morgan, J. (1981). Aquatic Chemistry. Wiley – Interscience, New York.

Tang, X., Guo, L., Chen, C., Liu, Q., Li, T., and Zhu, Y. (2014). The analysis of Magnesium Oxide Hydration in Three-phase Reaction System. J. of Solid-State Chem., 213. 32 – 37.

Tarruya, T., Ueno, Y. and Fujii, M. (2000). Development of Phosphorus Resource Recycling Process from Sewage. IWA World Conf., Paris, Poster Session.

Taylor, A.W., Frazier, A.W., and Gurney, E.L. (1963). Solubility Products of Magnesium Ammonium and Magnesium Potassium Phosphates. Transactions Faraday Society, 59. 1580 – 1584.

USGS (2017). Mineral Commodity Summaries; U.S. Geological Survey.

Van der Merwe, E.M., Strydom, C.A. and Botha, A. (2004). Hydration of Medium Reactive Industrial Magnesium Oxide with Magnesium Acetate – Thermogravimetric Study. J. Thermal Analysis and Calorimetry, 77. 49 – 56.

Verigin, M., Lee. R.M., Seib, M., Lycke, D., Lai, K. (2019). Doubling Down on Phosphorus. WEFTEC 2019

Verigin, M., Goy, S., Prasad, R., Sparks, J., Jones, R. (2020). Reducing Phosphorus Recovery Operating and Capital Costs at Nansemond WWTP by Using Low Solubility Magnesium Sources. WEFTEC 2020.

Webb, K. and Ho, G. (1992). Struvite Solubility and its Application to a Piggery Effluent Problem. Water Science and Technology, 26. 2229 – 2232.

Ye, X., Ye, Z.-L., Lou, Y., Pan, S., Wang, X., Wang, M.K., and Chen, S. (2016). A Comprehensive Understanding of the Saturation Index and Upflow Velocity in a Pilot-scale Fluidized Bed Reactor for Struvite Recovery from Swine Wastewater. Powder Technology, 295 (2016). 16 – 26.

Yuan, Z., Pratt, S. and Batstone, D.J. (2012). Phosphorus Recovery from Wastewater Through Microbial Processes. Current Opinion in Biotechnology, 23. 878 – 883.

Zhang, X., Zheng, Y., Feng, X., Han, X., Bai, Z., and Zhang, Z. (2015). Calcination Termperature Dependent Surface Struvite and Physicochemical Properties of Magnesium Oxide. J. of Rotal Society of Chemistry, 5. 86102 – 86112.

Appendix: Supplemental Information

Jar testing:

Jar testing data collected from 45-minute and 150-minute durations are in the tables and figures in this section.

Table 32: Jar Testing Phosphorus Removal Using Various MgO Products at Different Hydration Extents and Mg:P Molar Ratios

MgO Product	Hydration	Activity (s)	Phosphorus Removal at Mg:P Molar Ratios (%)		
			0.85:1 Mg:P	1:1 Mg:P	1.25:1 Mg:P
Baymag	Hydrated	23	80.8	88	99.2
	Unhydrated		61	69	90
Timab (M98)	Hydrated	47	54.5	63	77.4
	Unhydrated		44	50	61
MX95	Hydrated	35.6	61.3	66	87
	Unhydrated		47	53	58
MX97	Hydrated	28.1	60.9	69.4	86.6
	Unhydrated		49.3	55.9	72
AK98	Hydrated	13	79	94	99
	Unhydrated		71	85	99

Determining the acid volume necessary to change the pH of centrate:

Determine the initial Total Alkalinity (mg/L $CaCO_3$) and pH of the centrate

Determine $C_{T,CO3}$:

$$[Alk]\left(\frac{eq}{L}\right) @\ initial\ pH = (\alpha_1 + 2\alpha_2)c_{T,CO_3} + \frac{Kw}{[H^+]} + [H^+]$$

Input $C_{T,CO3}$ to determine [Alk] at desired pH:

$$[Alk]\ \left(\frac{eq}{L}\right)\ @\ desired\ pH = \ (\alpha_1 + 2\alpha_2)c_{T,CO_3} + \frac{Kw}{[H^+]} + [H^+]$$

$$\alpha_1 = \frac{[H^+]K_{a1}}{[H^+]^2 + [H^+]K_{a1} + K_{a1}K_{a2}}$$

$$\alpha_2 = \frac{K_{a1}K_{a2}}{[H^+]^2 + [H^+]K_{a1} + K_{a1}K_{a2}}$$

Volume of Acid:

$$N_{centrate}V_{centrate} = N_{Acid}V_{acid}$$

$$V_{Acid} = \frac{([Alk]\ @intial\ pH - [Alk]\ @\ desired\ pH)V_{centrate}}{N_{Acid}}$$

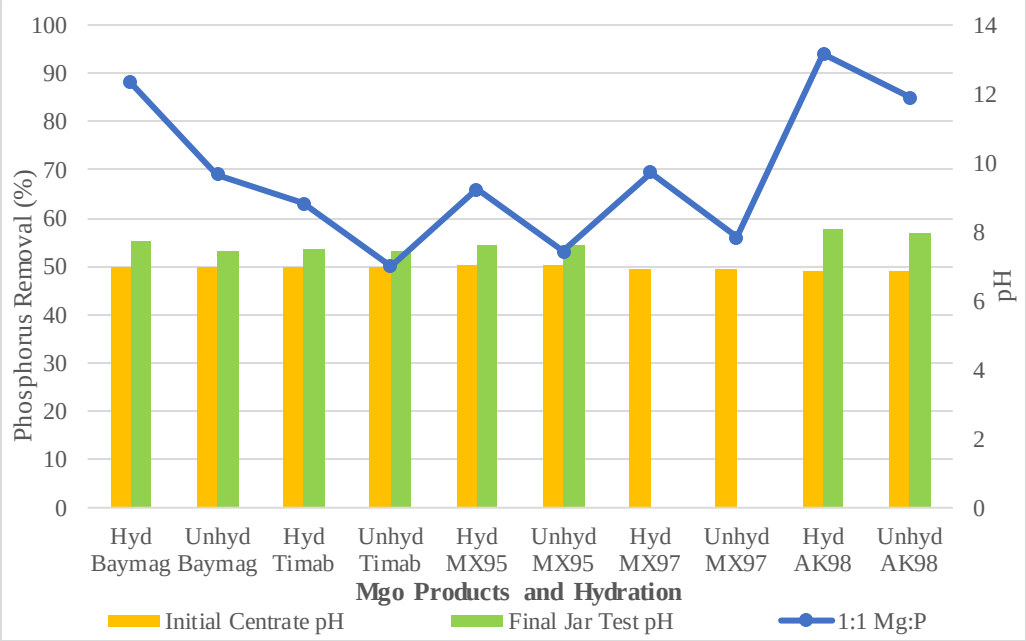

Figure 52: Initial and Final pH during 45-minute 1:1 Mg:P Jar Tests Determining the Effect of Various MgO Products on Phosphorus Removal

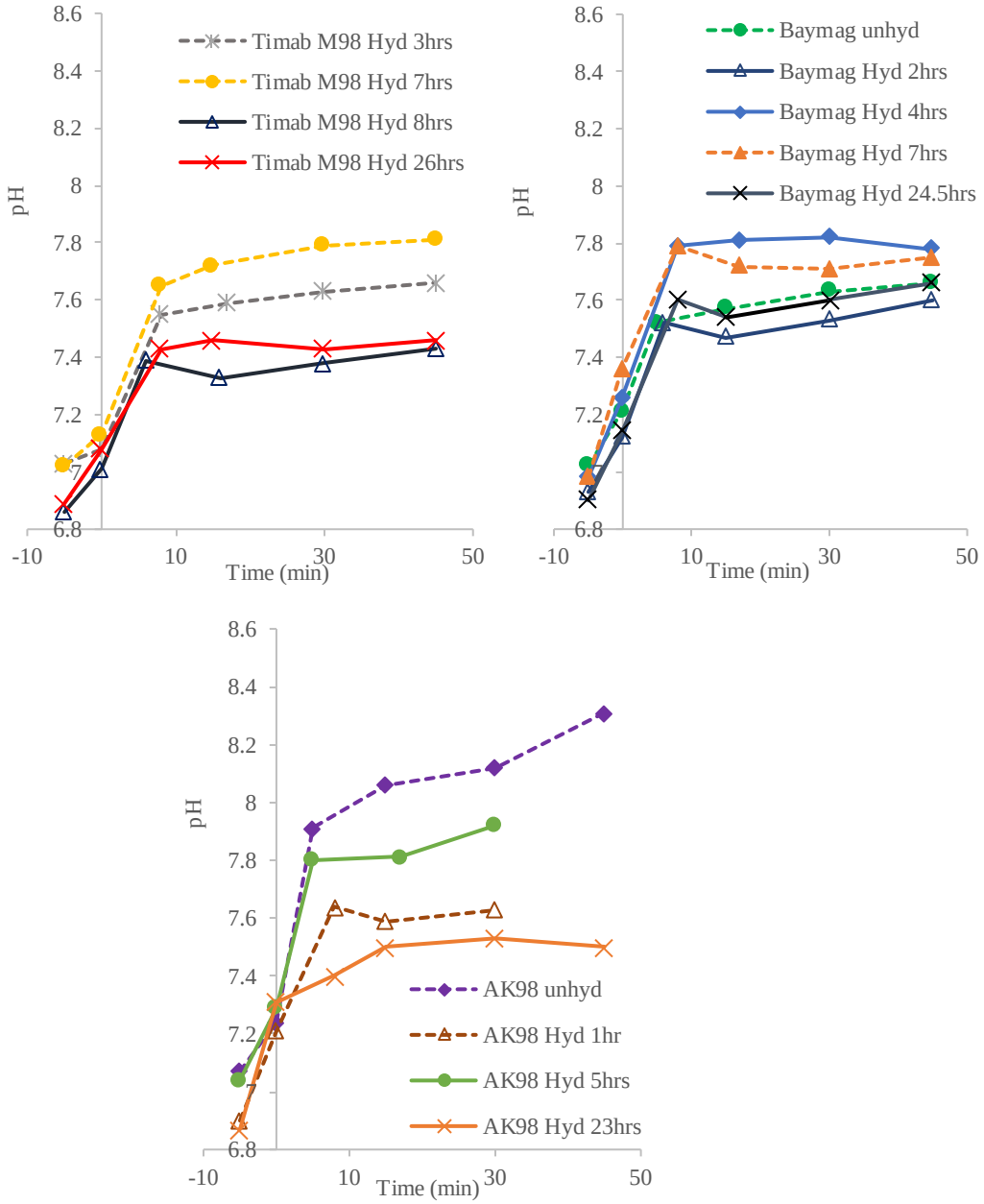

Figure 53: pH throughout 45-miute Struvite Precipitation Jar Tests with MgO Products of Various Hydration Extent

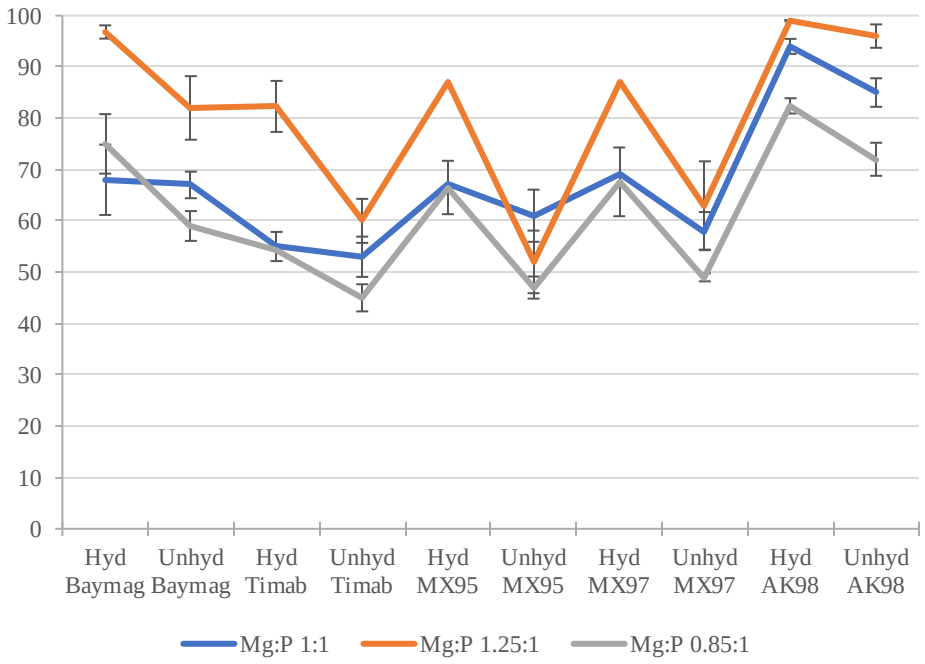

Figure 54: Average OP Removal of Various MgO Products and Hydration Extent at Different Mg:P Ratios

Full-scale MgO Pilot Reactor Operation:

Table 33: Baseline Reactor Operation

Date and Reactor(s) Operation	Average OP Removal (%)		Average TP Removal (%)	
	On-site	CEL	On-site	CEL
4/30-6/17/2015 SRF	-	72.3	-	41.8
8/28-12/3/2017 R1	74.8	79.8	-	70
11/24/2017-3/2/2018 SRF	79.1	83.3	-	55.1
1/11/2019-3/5/2019 R1&R2	-	83.3	-	61.7
7/20-9/13/2019 R1	81	83.8	16	48.5

9/9-9/25/2019 R1	81.2	85.5	31.7	54.6
10/21-11/26/2019 R1&R2	80.7	83.5	72.1	73.3
1/13-3/9/2020 R1&R2	80.6	86.7	73.4	74.7
6/23-7/21/2020	83.5	90.6	-	84.1

MgO Dry Feeder Motor Calibration Curves:

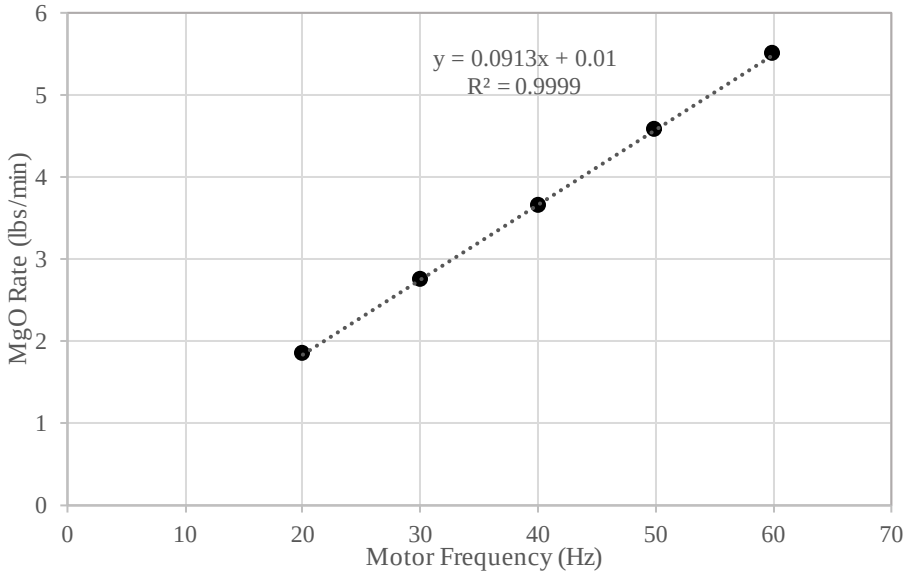

Figure 55: MgO Motor Calibration Curve – Baymag 30 HP

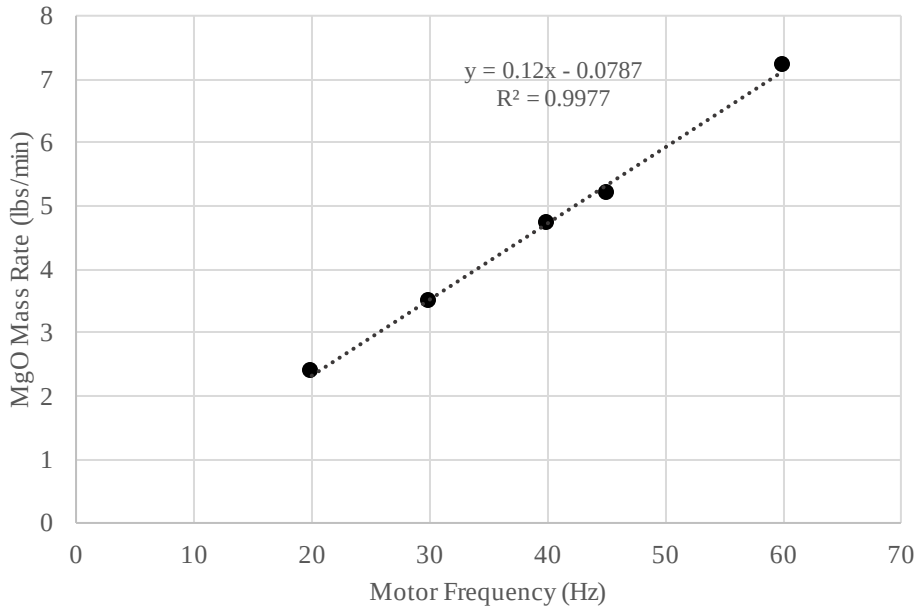

Figure 56: MgO Dry Feed Motor Calibration Curve – Timab M98

To determine the intermittent MgO feed rate to the reactor:

$$\boldsymbol{MgO\ Pulse}\left(\frac{\boldsymbol{L}}{\boldsymbol{pulse}}\right) = \frac{\Delta\, Volume}{\Delta t} \tag{42}$$

$$\boldsymbol{MgO\ Flow\ Required}\left(\frac{\boldsymbol{L}}{\boldsymbol{min}}\right) = \tag{43}$$

$$\frac{Mg{:}\,P\ Ratio \cdot Daily\ P\ Loading\left(\frac{kg}{day}\right)\left(\frac{24.3\ kg\ Mg}{30.97\ kg\ P}\right)\left(\frac{40.3\ kg\ MgO}{24.3\ kg\ Mg}\right)}{\frac{0.08 * 1}{\left(\frac{0.08}{3.58\ kg/L}\right)+\left(\frac{1-0.08}{1\ kg/L}\right)} \cdot \left(\frac{day}{24\ hour}\right) \cdot \left(\frac{hour}{60\ min}\right) \cdot MgO\ Purity\left(\frac{m}{m}\right)}$$

$$MgO\ Dosing\ Frequency\ = \frac{MgO\ Pulse\left(\frac{L}{pulse}\right) \cdot Current\ Dosing\ Frequency}{MgO\ Flow\ Required\left(\frac{L}{min}\right)} \tag{44}$$

MgO Pilot Reactor Operation 2018-2019:

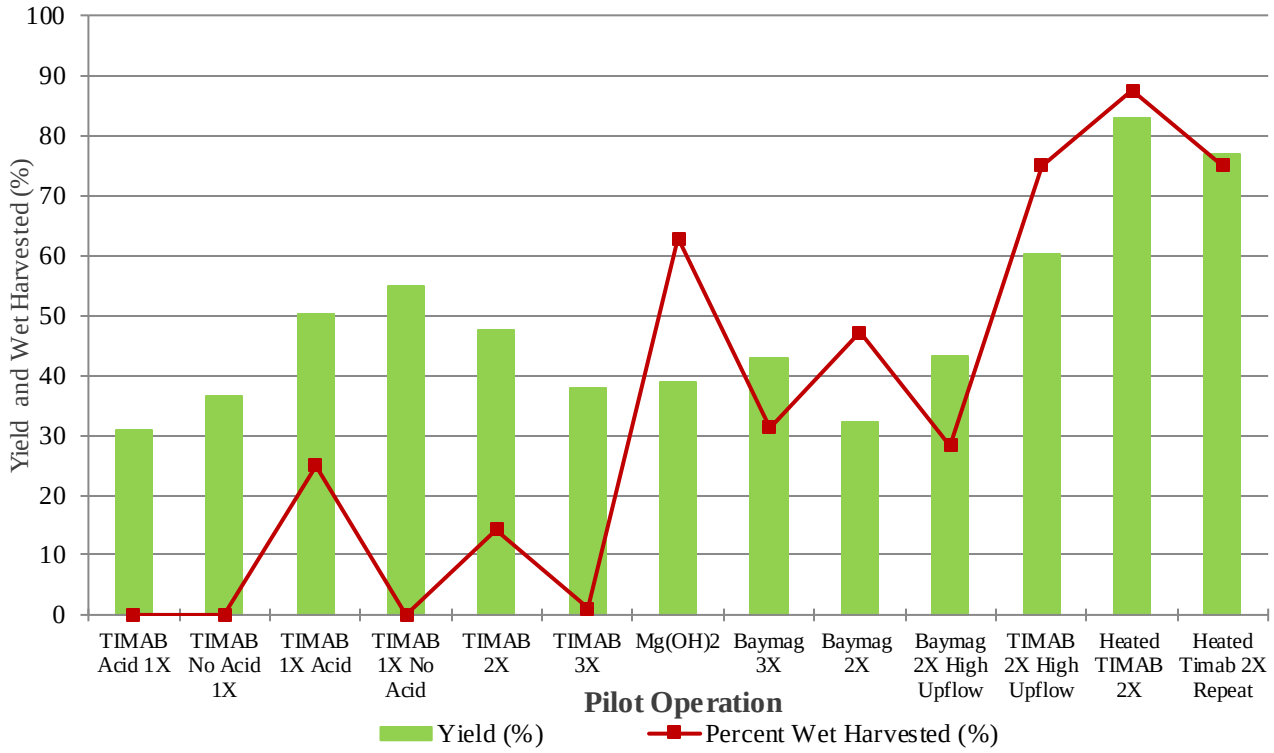

Figure 57: Yield and Percent Wet Harvested Material of the MgO Pilot Tests 2018-2019

Figure 58: Upper Wet Harvest Leg of Pilot Reactor (R3)

Figure 59: Pilot Reactor Clarifier Beaching